nature

SUPPLEMENTARY INFORMATION

https://doi.org/10.1038/s41586-019-1251-y

In the format provided by the authors and unedited.

Palaeo–Eskimo genetic ancestry and the peopling of Chukotka and North America

Pavel Flegontov[1,2,3]*, N. Ezgi Altınışık[1,27], Piya Changmai[1,27], Nadin Rohland[4], Swapan Mallick[4,5,6], Nicole Adamski[4,5], Deborah A. Bolnick[7,8], Nasreen Broomandkhoshbacht[4,5], Francesca Candilio[9,10], Brendan J. Culleton[11], Olga Flegontova[1,2], T. Max Friesen[12], Choongwon Jeong[13], Thomas K. Harper[14], Denise Keating[9], Douglas J. Kennett[11,14,26], Alexander M. Kim[4,15], Thiseas C. Lamnidis[13], Ann Marie Lawson[4,5], Iñigo Olalde[4], Jonas Oppenheimer[4,5], Ben A. Potter[16], Jennifer Raff[17], Robert A. Sattler[18], Pontus Skoglund[4,19], Kristin Stewardson[4,5], Edward J. Vajda[20], Sergey Vasilyev[21], Elizaveta Veselovskaya[21], M. Geoffrey Hayes[22,23,24], Dennis H. O'Rourke[17], Johannes Krause[13], Ron Pinhasi[25], David Reich[4,5,6]* & Stephan Schiffels[13]*

[1]Department of Biology and Ecology, Faculty of Science, University of Ostrava, Ostrava, Czech Republic. [2]Institute of Parasitology, Biology Centre, Czech Academy of Sciences, České Budějovice, Czech Republic. [3]A. A. Kharkevich Institute for Information Transmission Problems, Russian Academy of Sciences, Moscow, Russia. [4]Department of Genetics, Harvard Medical School, Boston, MA, USA. [5]Howard Hughes Medical Institute, Harvard Medical School, Boston, MA, USA. [6]Broad Institute of MIT and Harvard, Cambridge, MA, USA. [7]Department of Anthropology, University of Connecticut, Storrs, CT, USA. [8]Institute for Systems Genomics, University of Connecticut, Storrs, CT, USA. [9]School of Archaeology, University College Dublin, Dublin, Ireland. [10]Soprintendenza Archeologia, Belle Arti e Paesaggio per la città metropolitana di Cagliari e le province di Oristano e Sud Sardegna, Cagliari, Italy. [11]Institutes of Energy and the Environment, Pennsylvania State University, University Park, PA, USA. [12]Department of Anthropology, University of Toronto, Toronto, ON, Canada. [13]Department of Archaeogenetics, Max Planck Institute for the Science of Human History, Jena, Germany. [14]Department of Anthropology, Pennsylvania State University, University Park, PA, USA. [15]Department of Anthropology, Harvard University, Cambridge, MA, USA. [16]Department of Anthropology, University of Alaska Fairbanks, Fairbanks, AK, USA. [17]Department of Anthropology, University of Kansas, Lawrence, KS, USA. [18]Tanana Chiefs Conference, Fairbanks, AK, USA. [19]Francis Crick Institute, London, UK. [20]Department of Modern and Classical Languages, Western Washington University, Bellingham, WA, USA. [21]Institute of Ethnology and Anthropology, Russian Academy of Sciences, Moscow, Russia. [22]Department of Medicine, Northwestern University Feinberg School of Medicine, Chicago, IL, USA. [23]Department of Anthropology, Northwestern University, Evanston, IL, USA. [24]Center for Genetic Medicine, Northwestern University Feinberg School of Medicine, Chicago, IL, USA. [25]Department of Anthropology, University of Vienna, Vienna, Austria. [26]Present address: Department of Anthropology, University of California, Santa Barbara, CA, USA. [27]These authors contributed equally: N. Ezgi Altınışık, Piya Changmai.
*e-mail: pavel.flegontov@osu.cz; reich@genetics.med.harvard.edu; schiffels@shh.mpg.de

Supplementary information

Paleo-Eskimo genetic legacy across North America

Pavel Flegontov, N. Ezgi Altınışık, Piya Changmai, Nadin Rohland, Swapan Mallick, Nicole Adamski, Deborah A. Bolnick, Nasreen Broomandkhoshbacht, Francesca Candilio, Brendan J. Culleton, Olga Flegontova, T. Max Friesen, Choongwon Jeong, Thomas K. Harper, Denise Keating, Douglas J. Kennett, Alexander M. Kim, Thiseas C. Lamnidis, Ann Marie Lawson, Iñigo Olalde, Jonas Oppenheimer, Ben A. Potter, Jennifer Raff, Robert A. Sattler, Pontus Skoglund, Kristin Stewardson, Edward J. Vajda, Sergey Vasilyev, Elizaveta Veselovskaya, M. Geoffrey Hayes, Dennis H. O'Rourke, Johannes Krause, Ron Pinhasi, David Reich, Stephan Schiffels

CONTENTS

Supplementary tables

Supplementary Table 1. Summary of genome-wide data from 48 newly reported ancient individuals.

Notes:

* based on being a father or son of I5319 at the same site who has a calibrated radiocarbon date

** based on being a 2nd to 3rd degree relative of I5319 at the same site who has a calibrated radiocarbon date

*** context from 16 other dates at the same site

Supplementary Table 2. Reservoir-adjusted radiocarbon calibrations and stable isotope data for 46 ancient skeletal samples analyzed in this study. Average calibrated ages (Cal BP, μ) and their 95% confidence intervals are shown (CalBP, 2σ).

Supplementary Table 3. Information on newly genotyped present-day individuals.

Supplementary Table 4. Composition of the genomic and SNP array datasets used in this study. Individual counts correspond to dataset versions after removal of outliers, relatives, and ancient samples with a high percentage of missing data, but prior to a more stringent filtering applied to the datasets used for f_4-statistics, for *qpWave,* and for *qpAdm* analyses (see the Methods). Meta-populations are abbreviated as follows: Paleo-Eskimos (P-E), Eskimo-Aleut speakers and ancient Neo-Eskimos (E-A), Chukotko-Kamchatkan speakers (C-K), proto-Paleo-Eskimos (PPE, i.e. groups having uncertain position within the C-K/E-A/P-E clade), Na-Dene speakers (mostly Athabaskans, ATH), Northern First Peoples (NAM), Southern First Peoples (SAM), Basal First Peoples (BAM), West Siberians (WSIB), East Siberians (ESIB), Southeast Asians (SEA), Europeans (EUR), Africans (AFR). Shotgun sequencing data were generated in this study for one ancient Aleut individual (I0719 or 378620) and one ancient Athabaskan individual (I5319 or MT-1) or taken from three published sources: the Simons Genome Diversity Project (Mallick et al. 2016), Raghavan et al. (2015), and Moreno-Mayar et al. (2018). Two SNP array datasets were used: based on the HumanOrigins array and on Illumina arrays. HumanOrigins data were taken from Mathieson et al. (2015) and Jeong et al. (2019, in press) or generated in this study for Alaskan Iñupiat and West Siberians (Enets, Kets, Nganasans, and Selkups). Illumina data were taken from the following sources: Li et al. 2008, Behar et al. 2010, Rasmussen et al. 2010, Fedorova et al. 2013, Raghavan et al. 2014a, 2014b, 2015, Verdu et al. 2014, Kushniarevich et al. 2015. Genome-wide targeted enrichment data were generated in this study using the 1240K SNP panel (Fu et al. 2015) for 48 ancient individuals (11 Aleuts, 3 Northern Athabaskans, 21 Neo-Eskimos of the Old Bering Sea culture, one Middle Dorset Paleo-Eskimo, and 12 individuals from the Ust'-Belaya site on the Angara river), and merged with both SNP array datasets. Before the merging step, the following low-coverage samples were removed: 5 ancient Aleuts, 2 Neo-Eskimos (one from the Ekven and another from the Uelen site), and 3 Ust'-Belaya Angara individuals. One ancient Athabaskan sample was removed as a first-degree relative of another sample.

Notes:

* The Dakelh population was referred to as Athabaskan in Rasmussen et al. (2010) and as 'Northern Athabaskan 1' or simply Athabaskan in Raghavan et al. (2015).

** The Caucasian (CAU), Middle Eastern (ME), South Asian (SAS), and Australo-Melanesian (OCE) meta-populations were included in the HumanOrigins dataset, but were not used for most analyses except for *ADMIXTURE*.

Supplementary Table 5. Details of datasets used in this study.

Notes:

* transitions were removed in this dataset version

** all individuals had missing rates below the threshold, except for the Middle Dorset individual having the missing rate of 0.89-0.90

*** rare variants occurring from 2 to 5 times in reference populations (AFR, EUR, SEA, SIB, C-K)

^ listing only segregating sites among the 9 populations analyzed with *Rarecoal*. The total number of sites analyzed is 14,740,571, as in the rare allele sharing analysis

^^ analyzed as 9 meta-populations and 3 ancient genomes mapped on the tree

Supplementary Table 6. Z-scores and site counts for f_4-statistics (American$_{i\ \text{Half A}}$, American$_j$; American$_{i\ \text{Half B}}$, Dai). Statistics were calculated for 6 datasets (HumanOrigins, 1240K, Illumina, with or without transitions), and percentage of significantly positive f_4-statistics (Z > 3) is shown for each dataset version.

References (for Supplementary tables)

1000 Genomes Project Consortium. A global reference for human genetic variation. *Nature* 526, 68–74 (2015).

Behar, D. M. *et al*. The genome-wide structure of the Jewish people. *Nature* **466**, 238–242 (2010).

Fedorova, S. A. *et al*. Autosomal and uniparental portraits of the native populations of Sakha (Yakutia): implications for the peopling of Northeast Eurasia. *BMC Evol. Biol*. **13**, 127 (2013).

Fu, Q. *et al*. An early modern human from Romania with a recent Neanderthal ancestor. *Nature* **524**, 216–219 (2015).

Jeong, C. *et al*. Characterizing the genetic history of admixture across inner Eurasia. *Nature Ecology and Evolution*, in press (2019).

Kushniarevich, A. *et al*. Genetic heritage of the Balto-Slavic speaking populations: A synthesis of autosomal, mitochondrial and Y-chromosomal data. *PLoS ONE* **10**, e0135820 (2015).

Li, J. Z. *et al*. Worldwide human relationships inferred from genome-wide patterns of variation. *Science* **319**, 1100–1104 (2008).

Mallick, S. *et al*. The Simons Genome Diversity Project: 300 genomes from 142 diverse populations. *Nature* **538**, 201–206 (2016).

Mathieson, I. *et al*. Genome-wide patterns of selection in 230 ancient Eurasians. *Nature* **528**, 499–503 (2015).

Moreno-Mayar, J. V. *et al*. Terminal Pleistocene Alaskan genome reveals first founding population of Native Americans. *Nature* **553**, 203–207 (2018).

Raghavan, M. *et al*. The genetic prehistory of the New World Arctic. *Science* **345**, 1255832 (2014a).

Raghavan, M. *et al*. Upper Palaeolithic Siberian genome reveals dual ancestry of Native Americans. *Nature* **505**, 87–91 (2014b).

Raghavan, M. *et al*. Genomic evidence for the Pleistocene and recent population history of Native Americans. *Science* **349**, 1–20 (2015).

Rasmussen, M. *et al*. Ancient human genome sequence of an extinct Palaeo-Eskimo. *Nature* **463**, 757–762 (2010).

Verdu, P. *et al*. Patterns of admixture and population structure in native populations of northwest North America. *PLoS Genet*. **10**, e1004530 (2014).

Supplementary Information section 1

Description of archaeological sites

1.1 Ancient Eastern Aleutian Islanders

The skeletal samples from the eastern Aleutians were selected from curated collections at the Smithsonian Institution by M. Geoffrey Hayes, who was gloved, sleeved, and masked at all times to prevent self-contamination of the samples. All samples were small, fragmentary ribs free of pathological lesions and were immediately placed in sterile ziplock bags (Hayes 2002) for transport to the lab for analysis.

The remains were excavated or collected by Aleš Hrdlička in the late 1930s. The geographic locations of the material are burial caves on Shiprock Island (northeast of Umnak Island), and Kagamil, one of the sacred Islands of the Four Mountains, immediately west of Umnak (Extended Data Table 1). The third site providing samples for molecular analysis is Chaluka, a deep midden site on Umnak adjacent to the contemporary village of Nikolski.

For the present study, the samples available for analysis included six individuals from Kagamil, with three osteologically determined to be female, one as probably female (later identified genetically as a male), and two as male. As reported by Brenner Coltrain et al. (2006), these six Kagamil samples exhibit a calibrated age range of 479 – 596 years before present (calBP). The single individual from Shiprock was identified as a male with an age of 749 calBP. Finally, four individuals from the Chaluka site at Nikolski (three males and one female according to genetic data) exhibited an age range of 702 – 2,305 calBP. In this study, the dates were recalibrated (Supplementary Table 1 and 2) using an updated marine reservoir correction as described in Supplementary Information section 2.

Based on cranial metrics, Hrdlička (1945) postulated that the mummified remains from the burial caves on Kagamil and Shiprock represented immediate ancestors of modern Aleut people who had replaced an earlier population of 'Pre-' or 'Paleo-Aleuts' about a millennium ago. He viewed the remains at Chaluka as representatives of this earlier occupation of the Islands.

Although Hrdlička (1945) considered the 'Paleo-Aleuts' to be older than 'Neo-Aleuts', with only the latter ancestral to modern Aleut people following a replacement event around 1,000 years ago, direct dating of the ancient remains (Brenner Coltrain, et al. 2006) clearly established that while all individuals recovered from Chaluka were 'Paleo-Aleuts' by Hrdlička's cranial metric criteria, they coexisted with 'Neo-Aleuts' for several hundred years following the appearance of the latter at about 1,000 calBP. Thus, the strict replacement model of Hrdlička's was untenable and the prehistory of peoples of the Aleutian chain, at least in the east, proved to be more complex than previously thought (Smith et al. 2009).

Molecular characterization of the ancient Aleut individuals was conducted following consultations with and permissions from local communities and authorities, including the Chaluka Corporation, the Aleut Corporation, and the Aleutians Pribilof Islands Association.

References (for this section)

Brenner Coltrain, J. B., Hayes, M.G. & O'Rourke D.H. Hrdlička's Aleutian population-replacement hypothesis. A radiometric evaluation. *Curr. Anthropol.* **47**, 537–548 (2006).

Hayes, M. G. Paleogenetic assessments of human migration and population replacement in North American Arctic prehistory. Doctoral Dissertation, University of Utah (2002).

Hrdlička, A. *The Aleutian and Commander Islands and their inhabitants*. Philadelphia: Wistar Institute of Anatomy and Biology (1945).

Smith, S. *et al*. Inferring population continuity versus replacement with aDNA: A cautionary tale from the Aleutian Islands. *Hum. Biol.* **81**, 19–38 (2009).

1.2 Ancient Northern Athabaskans

The ancient Athabaskan population in this study is derived from three individuals found intermingled in a non-burial context in the riparian zone of the upper Kuskokwim river. Tochak is the Athabaskan place-name for the area around the modern mixed ethnic community of McGrath, southwest Interior Alaska. Known as the Tochak McGrath Discovery, the three individuals were buried in overbank sediments that also feature unassociated buried organic bands with terrestrial and aquatic fauna, hearth matrix, flaked stone and bone artifacts. The human remains could not be linked stratigraphically to the surrounding cultural occupation features. We genetically determined the three individuals to be successive generations of consanguineous relatives: 30-40 year-old male (MT-1), 19-20 year-old male (MT-2), and 2-3 year old female (MT-3) (Extended Data Table 1). The genetic analysis indicates a father-son relationship for MT-1 / MT-2, a grandfather-granddaughter relationship for MT-1 / MT-3, and an uncle-niece relationship for MT-2 / MT-3. To reduce correlation in the genetic sequences, only individuals MT-1 and MT-3 were selected for downstream genetic analyses. Nearly complete skeletal representation and articulation pattern of all three individuals in massive sand deposits suggest that these individuals died together of exposure and were buried by overbank sedimentation.

Soon after the time of discovery, a tripartite agreement was reached for scientific analysis between the McGrath Native Village Council (the federal recognized Alaska Native tribe), MTNT Ltd. (consortium of Alaska Native Claims Settlement Act village corporations) and Tanana Chiefs Conference (the regional non-profit consortium of 37 federally recognized Athabaskan Tribes and Alaskan Native associations in the Yukon and Kuskokwim river basins in Interior Alaska). R.A. Sattler has facilitated community-based research, collaboration with academic institutions, tribal consultation, public outreach and further data recovery at the Tochak discovery locale (Sattler et al. 2013).

References (for this section)

Sattler, R. A. *et al*. Tochak McGrath discovery: Precontact human remains in the Upper Kuskokwim River region of interior Alaska. *Alaska J. Anthropol*. **11**, 185–186 (2013).

1.3 Early Neo-Eskimos (Old Bering Sea culture)

Four and 17 individuals buried at neighboring Uelen and Ekven cemeteries, respectively, were sequenced in this study (Extended Data Table 1). These cemeteries of the Old Bering Sea (Drevneberingomorskaya) culture are located on the Chukotka Peninsula. The Uelen burial ground is separated by only 170 m from the present-day settlement Uelen on the coast of the Chukchi Sea, and the Ekven burial ground is about 40 km away. The site was discovered in 1955 by D. A. Sergeyev, and its further excavation was carried out by the Institute of Ethnography of the Academy of Sciences of the USSR (details are reported in Levin & Sergeyev 1964, Dikov 1967, Arutyunov & Sergeyev 1969).

Both sites represent burial grounds of the Old Bering Sea culture of sea mammal hunters and fishers of the Arctic zone of Siberia and North America. This culture is related to others in the Bering Straits region that partially overlap in time (1,700-1,000 calBP): Okvik, Punuk, and Birnik, collectively (with the later related Thule tradition) termed the Northern Maritime tradition (Collins 1964). The Old Bering Sea stage is the earliest in development of this cultural tradition and is dated to between ~2,300-1,300 calBP (Arutyunov and Sergeyev 1975, Gerlach and Mason 1992) with evidence for continuity with the later Okvik, Punuk, and Birnik cultures (Arutyunov and Sergeyev 1969, Gerlach and Mason 1992, Bronshtein et al. 2016, Mason 2016).

Mortuary behavior at the Ekven burial ground (189 burials) is more variable than that in other cemeteries of this culture. The buried were laid not only in an extended position, but also in a curled position, and there are numerous paired and group burials. Human remains from the Uelen and Ekven burial grounds provide an important source of data for the bioanthropology of Old Bering Sea culture individuals (Levin & Sergeyev 1964, Debets 1975). Odontological materials from the Ekven burial ground, and to a lesser extent from Uelen, are very similar to those of present-day Eskimos (especially from Alaska) (Zubov 1969).

According to all cultural traits studied, the Ekven and Uelen ancient populations were extremely similar. Which is quite natural, since the distance between the two sites does not exceed 35-40 kilometers. Nevertheless, even with such a close neighborhood between the two burial grounds, there are some differences.

This difference is observed, for example, in the ratio of the "x" and "y" harpoon tips. According to the classification principles by H. Collins (Collins 1964), if the tip is equipped with blades located in the same plane with a hole for the line, this is expressed by the letter "x", and if the planes are perpendicular, then the letter "y" is used. In Uelen, "x" harpoon tips prevail; in Ekven, on the contrary, the "y" series is more numerous. It was noted that the type "x" has advantages over the supposedly earlier type "y" (Arutyunov and Sergeev, 1969).

Excavations in 1962-1967 at the Ekven cemetery, along with previously known burials in an elongated position, revealed a new type of burial that had not previously been found in ancient Eskimo burial grounds, namely, the appearance of skeletons in a crooked position. A considerable number of paired and collective burials was found at the Ekven cemetery. Some burials were disturbed by later graves (for example, burial 21). In some tombs scattered bones of other individuals were found in addition to the main skeleton. Presumably, such burials were made on the site of older burials, and the old skeletons were destroyed and fell with a backfill into new burials.

References (for this section)

Arutyunov, S. A. & Sergeyev, D. A. *Drevniye kul'tury aziaskih eskimosov: uelenskiy mogil'nik* [*Ancient cultures of Asian Eskimos: the Uelen burial ground*]. Moscow: Nauka (1969).

Arutyunov, S. A. & Sergeyev, D. A. *Problemy etnicheskoy istorii Beringomorya: ekvenskiy mogil'nik* [*Problems of the ethnic history of the Bering Sea region: the Ekven burial ground*]. Moscow: Nauka (1975).

Bronshtein, M. M., Dneprovsky, K. A. & Savintesky, A. B. Ancient Eskimo cultures of Chukotka. *The Oxford Handbook of the Prehistoric Arctic*, ed. Friesen, T. M., Mason, O. K. New York: Oxford University Press. 469–488 (2016).

Collins, H. B. The Arctic and Subarctic. *Prehistoric Man in the New World*, ed. Jennings, J. D. & Norbeck, E. Chicago: University of Chicago Press. 85–114 (1964).

Debets, G. F. Paleoantropologicheskiye materialy iz drevneberingomorskih mogil'nikov Uelen i Ekven [Paleoantropological materials from the Old Bering Sea burial grounds Uelen and Ekven]. *Problemy etnicheskoy istorii Beringomorya: ekvenskiy mogil'nik* [*Problems of the ethnic history of the Bering Sea region: the Ekven burial ground*], ed. Arutyunov, S. A. & Sergeyev, D. A. Moscow: Nauka. 198 (1975).

Dikov, N. N. Uelenskiy mogil'nik po dannym raskopok 1956, 1958 i 1963 gg [The Uelen burial ground according to excavations in 1956, 1958 and 1963]. *Istoriya i kul'tura narodov Severa Dal'nego Vostoka* [*History and culture of the peoples of the northern Far East], Trudy SVKNII SO AN SSSR, vol. 17*. Moscow: Nauka (1967).

Gerlach, C. & Mason, O. K. Calibrated radiocarbon dates and cultural interaction in the Western Arctic. *Arctic Anthropol.* **29**, 54–81 (1992).

Levin, M. G. & Sergeyev, D. A. Drevniye mogil'niki Chukotki i nekotorye aspekty eskimosskoy problemy [Ancient burial grounds in Chukotka and some aspects of the Eskimo problem]. *Doklady na VII Mezhdunarodnom kongresse antropologicheskih i etnograficheskih nauk*. Moscow (1964).

Mason, O. K. The Old Bering Sea florescence about Bering Strait. *The Oxford Handbook of the Prehistoric Arctic*, ed. Friesen, T. M., Mason, O. K. New York: Oxford University Press. 417–442 (2016).

Zubov, A. A. Antropologicheskiy analiz cherepnyh seriy iz Ekvenskogo i Uelenskogo mogil'nikov [Anthropological analysis of cranial series from the Ekven and Uelen burial grounds]. *Drevniye kul'tury aziatskih eskimosov: uelenskiy mogil'nik* [*Ancient cultures of Asian Eskimos: the Uelen burial ground*], ed. Arutyunov, S. A. & Sergeyev, D. A. Moscow: Nauka (1969).

1.4 The Ust'-Belaya site on the Angara river

The Ust'-Belaya burial ground (Ust-Belaya II - Shumilikha) is located on the right bank of the Belaya River at the confluence with the Angara River. This is burial ground is unique not only for the Angara basin and the Baikal region, but also for Eastern Siberia because of burials in a sitting position. Separate burials of such a type and small clusters of them are found throughout Eastern Siberia, particularly in Transbaikalia and Mongolia, but such a large necropolis has not been found anywhere. In addition, in an eroded floodplain burials of another type were found: lying, in birch bark, and with partial cremation (Gerasimova 1981).

References (for this section)

Gerasimova, M. M. Cherepa iz II Ust'-Bel'skogo mogil'nika (Shumilikha) [Skulls from Ust'-Belaya II (Shumilikha) burial ground]. *Bronzovy vek Priangarya [The Bronze Age in the Angara basin]*. Irkutsk (1981).

1.5 The Dorset Period of the Paleo-Eskimo tradition

The Dorset period of the Paleo-Inuit (Paleo-Eskimo) tradition in the Eastern North American Arctic is represented by a sample (I10427, NiNg-1) from the Buchanan site near Cambridge Bay, Victoria Island, Nunavut, Canada. Buchanan was originally excavated by Taylor (1967); renewed excavation by Friesen in 2007 yielded the sample described here. It is an adult left lower 3rd molar with heavy wear. This tooth was recovered from a depth of 15 cm below surface level in a warm-season dwelling. Artifacts from this tent ring are consistent with the Middle Dorset period, with no evidence of mixing or intrusive artifacts. The seven diagnostic harpoon heads are all of the Middle Dorset Frobisher Grooved type. The sample was previously subjected to shallow shotgun sequencing (0.004x coverage) and radiocarbon dating (Raghavan et al. 2014). The radiocarbon date has been recalibrated in this study to 1,900 – 1,610 calBP using a different marine reservoir correction (see section 2). The previously published calibrated date was older: 2,182 – 2,123 calBP (Raghavan et al. 2014).

The Middle Dorset specimen was recovered as part of a collaborative project initiated by the Kitikmeot Heritage Society (KHS)of Cambridge Bay, Nunavut. Sampling of the specimen for DNA, AMS dating, and isotopic analysis was discussed with the KHS before the research occurred, and specific permission for this analysis was received from the Nunavut Government via a destructive analysis request. This latter permission involved consultation with the Inuit Heritage Trust, a Nunavut-wide body dedicated to the preservation, enrichment, and protection of Inuit Cultural Heritage.

References (for this section)

Raghavan, M. *et al*. The genetic prehistory of the New World Arctic. *Science* **345**, 1255832 (2014).

Taylor, W. E. Summary of archaeological field work on Banks and Victoria Islands, Arctic Canada, 1965. *Arctic Anth.* **4**, 221–243 (1967).

1.6 Alaskan Iñupiat

Iñupiat samples in this study were collected, along with genealogical records and participant surveys, by M. Geoffrey Hayes and Jennifer A. Raff from the communities of Atqasuk, Anaktuvuk Pass, Utqiaġvik (formerly known as Barrow), Kaktovik, Nuiqsut, Point Hope, Point Lay, and Wainwright between 2008-2010 as described in Raff et al. (2015). This project was begun at the suggestion of an Elder in Utqiaġvik to complement ancient DNA work on burial

populations in the region, and was approved by Northwestern University's Institutional Review Board, after consultation with the Ukpeagvik Iñupiat Corporation, the Native Village of Barrow, and Senior Advisory Council of Barrow (Elders). Of the 181 samples collected, 35 individuals who consented to have their DNA used for ancestry research were selected for inclusion in this study to represent a diversity of mitochondrial haplogroups and geographic origins (reported in Raff et al. 2015) and to represent both sexes in as close to equal proportions as possible. During the outlier removal procedure described in the Methods section, 20 individuals with minimal admixture from outside populations were selected for downstream analyses.

References (for this section)

Raff, J. A. *et al*. Mitochondrial diversity of Iñupiat people from the Alaskan North Slope provides evidence for the origins of the Paleo- and Neo-Eskimo peoples. *Am. J. Phys. Anthropol*. **157**, 603–614 (2015).

Supplementary Information section 2

Radiocarbon dating

We report 11 new direct AMS ^{14}C bone dates from the Penn State Accelerator Mass Spectrometer laboratory (PSUAMS) and recalibrate 13 previously published radiocarbon dates from three other AMS radiocarbon laboratories (Arizona [AA]: 11; Beta Analytic [Beta]: 1; UC Irvine [UCIAMS]: 1; see Supplementary Table 2 and Fig. S2.1). Bone preparation and quality control methods for the AA and Beta samples are described elsewhere (Brenner Coltrain et al. 2006, Halffman et al. 2015).

2.1 Old Bering Sea and Ust'-Belaya Angara samples

At PSUAMS and UCIAMS, bone collagen for ^{14}C and stable isotope analyses and was extracted and purified using a modified Longin method with ultrafiltration (Kennett et al. 2017). Bones were initially cleaned of adhering sediment and the exposed surfaces were removed with an X-acto blade. Samples (200–400 mg) were demineralized for 24–36 h in 0.5N HCl at 5 °C followed by a brief (<1 h) alkali bath in 0.1N NaOH at room temperature to remove humates. The residue was rinsed to neutrality in multiple changes of Nanopure H_2O, and then gelatinized for 12 h at 60 °C in 0.01N HCl. The resulting gelatin was lyophilized and weighed to determine percent yield as a first evaluation of the degree of bone collagen preservation. Rehydrated gelatin solution was pipetted into pre-cleaned Centriprep (McClure et al. 2010) ultrafilters (retaining 430 kDa molecular weight gelatin) and centrifuged 3 times for 20 min, diluted with Nanopure H_2O and centrifuged 3 more times for 20 min to desalt the solution. Carbon and nitrogen concentrations and stable isotope ratios were measured at the Yale Analytical and Stable Isotope Center with a Costech elemental analyzer (ECS 4010) and Thermo DeltaPlus analyzer. Sample quality was evaluated by % crude gelatin yield, %C, %N and C/N ratios before AMS ^{14}C dating. C/N ratios for all 11 samples fell between 3.14 and 3.32, indicating good collagen preservation (Van Klinken 1999).

Collagen samples (~2.1 mg) were combusted for 3 h at 900 °C in vacuum-sealed quartz tubes with CuO and Ag wires. Sample CO_2 was reduced to graphite at 550 °C using H_2 and a Fe catalyst, with reaction water drawn off with $Mg(ClO_4)_2$ (Santos et al. 2004). Graphite samples were pressed into targets in Al cathodes and loaded on the target wheel for AMS analysis. The ^{14}C ages were corrected for mass-dependent fractionation with measured $\delta^{13}C$ values (Stuiver and Polach 1977) and compared with samples of Pleistocene whale bone (backgrounds, 48,000 ^{14}C BP), late Holocene bison bone (~1,850 ^{14}C BP), late AD 1800s cow bone and OX-2 oxalic acid standards for calibration.

2.2 Northern Athabaskan (Tochak McGrath) samples

Collagen removed from the femur of MT-1 (I5319; the eldest individual) yielded a radiocarbon age of 1170 ± 30 BP (AMS lab code Beta-337194). This age estimate provides an older limiting age on the time of death of the Tochak family. Isotopic analysis has determined relatively high carbon and nitrogen values on all three individuals that suggest a strong marine component to their diet (i.e., anadromous salmon) (Halffman et al. 2015).

The isotopic values suggest that the radiocarbon age on human collagen may over-estimate the actual time of death, and the date was calibrated as described below. Given the direct age on MT-1 as a maximum limiting age, charcoal dates from matrix of two spatially separate hearths at the Tochak site provide a younger limiting age of around 350 years before present: 320 ± 30 BP (465-300 calBP; AMS lab code Beta-333837) and 380 ± 30 BP (505-320 calBP; AMS lab code Beta-343499).

2.3 Middle Dorset sample

The Middle Dorset tooth from the Buchanan site yielded a direct AMS date of 2,325 ± 15 BP (UCIAMS 86237). When assuming 90% marine contribution to diet, and using the geographically closest ΔR of 232 ± 30, from Bathurst Inlet (Coulthard et al 2010), the date calibrates to 1,900-1,610 calBP (95.4% confidence). Two radiocarbon dates have also been obtained for caribou bone from the same feature: 1,790 ± 15 BP (1,809-1,627 calBP, 95.4% confidence, UCIAMS 76625), and 1,725 ± 15 BP (1,696-1,568 calBP, 95.4% confidence, UCIAMS 76626). These radiocarbon dates are consistent with the direct tooth date, and with other Middle Dorset dates from the region (Friesen 2016).

2.4 Calibration of radiocarbon dates

All 14C ages were calibrated with OxCal version 4.2.3 (Bronk Ramsey 2013) using mixtures of the northern hemisphere terrestrial calibration curve (IntCal13) and the marine curve (Marine13; Reimer et al. 2013). Marine contribution was estimated using stable carbon and nitrogen isotopes and was assigned values of 0% for far inland contexts (Ust'-Belaya Angara), 50% for inland samples influenced by anadromous salmon (Tochak McGrath), and 90% for coastal samples (all other sites). The geographical context of sites is reflected in the reported δ15N measurements, which range from 11.0 to 15.7‰ (Ust'-Belaya), 15.2‰ (Tochak McGrath), and 18.3 to 22.3‰ (coastal sites).

For dates from Alaska and Chukotka we used a ΔR of 455 ± 81 (Misarti and Maschner 2015), which is based on an average for this region (Reimer and Reimer 2001). For a single date from Victoria Island in Nunavut (UCIAMS-86237) the nearest ΔR value (Bathurst Inlet, 232 ± 30) was used (Coulthard et al. 2010). The reservoir-corrected dates are presented in Supplementary Table 2 and Fig. S2.1.

References (for this section)

Brenner Coltrain, J., *et al*. Hrdlička's Aleutian population-replacement hypothesis. A radiometric evaluation. *Curr. Anthropol*. **47**, 537–548 (2006).

Bronk Ramsey, C. OxCal 4.23 Online Manual https://c14.arch.ox.ac.uk/oxcalhelp/hlp_contents.html (2013).

Byers D. A. *et al*. 2011. Stable isotope chemistry, population histories and Late Prehistoric subsistence change in the Aleutian Islands. *J. Archaeol. Sci.* **38**, 183–196 (2011).

Coulthard, R. D. *et al*. New marine ΔR values for Arctic Canada. *Quat. Geochronol.* **5**, 419–434 (2010).

Friesen, T. M. Middle Dorset communal structures on Victoria Island. *Open Arch*. **2**, 194–208 (2016).

Kennett, D. J. *et al*. Archaeogenomic evidence reveals prehistoric matrilineal dynasty. *Nat. Commun.* **8**, 14115 (2017).

Halffman, C. M., Sattler, R. & Clark, J. L. Bone collagen stable isotope analysis of three late Holocene humans from Interior Alaska. *Am. J. Phys. Anthropol*. **156 (S60)**, 157 (2015).

McClure, S .B., García Puchol, O. & Culleton, B. J. AMS Dating of Human Bone from Cova De La Pastora: New Evidence of Ritual Continuity in the Prehistory of Eastern Spain. *Radiocarbon* **52**, 25–32 (2010).

Misarti, N. & Maschner, H. D. G. The Paleo-Aleut to Neo-Aleut transition revisited. *J. Anthropol. Archaeol*. **37**, 67–84 (2015).

Raghavan, M. *et al*. The genetic prehistory of the New World Arctic. *Science* **345**, 1255832 (2014).

Reimer, P. J. *et al*. Intcal13 and Marine13 radiocarbon age calibration curves 0-50,000 years Cal Bp. *Radiocarbon* **55**, 1869–1887 (2013).

Reimer, P. J. & Reimer, R. W. A marine reservoir correction database and on-line interface. *Radiocarbon* **43**, 461–463 (2001).

Santos, G. M. *et al*. Magnesium perchlorate as an alternative water trap in AMS graphite sample preparation: A report on sample preparation at KCCAMS at the University of California, Irvine. *Radiocarbon* **46**, 165–173 (2004).

Stuiver, M. & Polach, H. A. Reporting of C-14 Data-Discussion. *Radiocarbon* **19**, 355–363 (1977).

Van Klinken, G. J. Bone collagen quality indicators for palaeodietary and radiocarbon measurements. *J. Archaeol. Sci*. **26**, 687–695 (1999).

Fig. S2.1. Plot of probability distributions for new AMS ^{14}C dates (PSUAMS results) and previously published regional radiocarbon data (Brenner Coltrain et al. 2006; Byers et al. 2011; Halffman et al. 2015; Raghavan et al. 2014) with marine reservoir correction. Alaska and Chukotka ΔR = 455 ± 81 (Misarti and Maschner 2015); Victoria Island ΔR = 232 ± 30 (Coulthard et al. 2010). No marine reservoir correction was applied to the Ust'-Belaya Angara samples located in the Baikal region. The brackets below the calibrated distributions are the 68.2% (upper bracket) and 95.4% (lower bracket) credible intervals of the calibrated range.

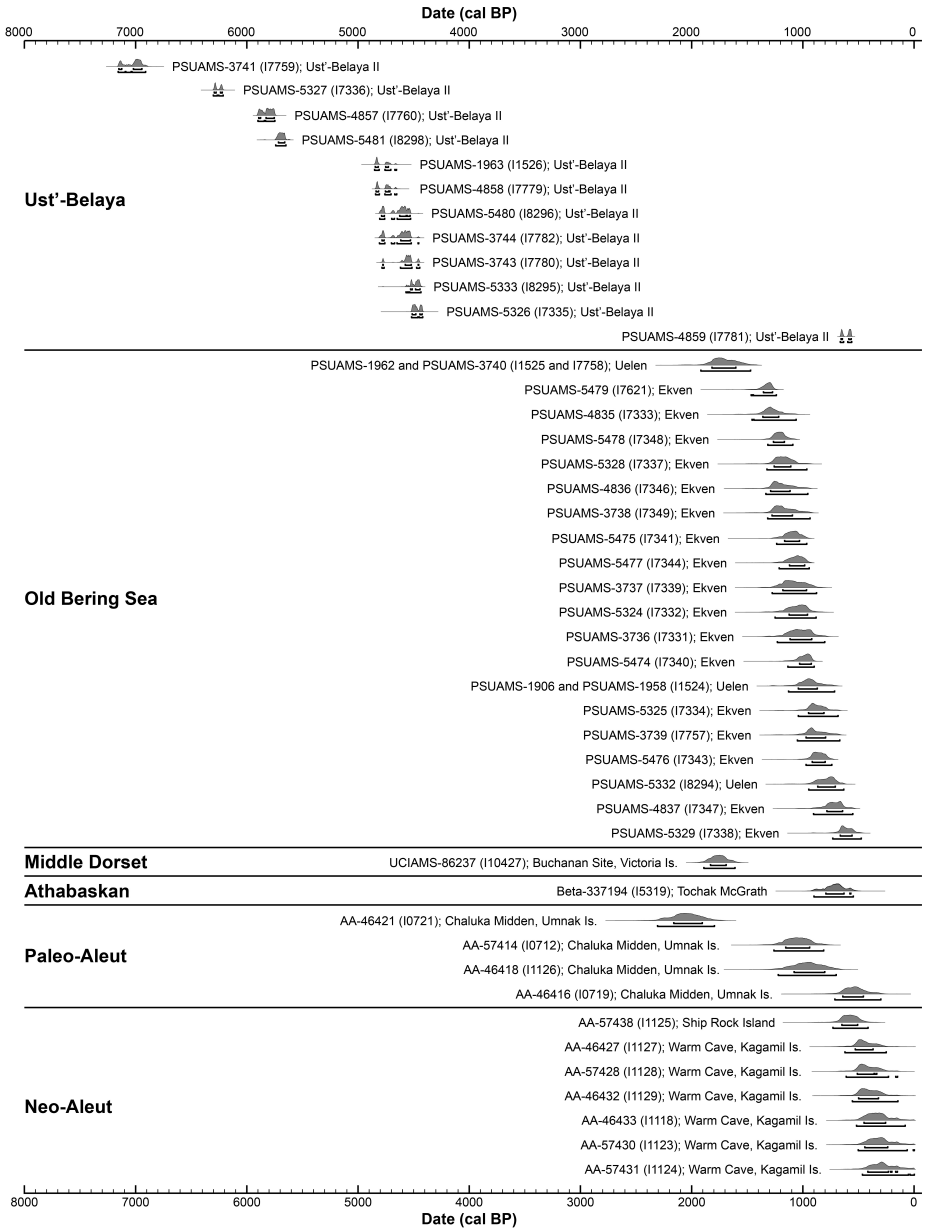

Supplementary Information section 3

Ancient DNA isolation and sequencing

3.1 Ancient DNA isolation

Powder from skeletal remains was prepared in dedicated clean room facilities either at University College Dublin in Dublin Ireland (the samples from Siberia), or Harvard Medical School in Boston USA (the samples from North America). All subsequent DNA extraction, library preparation, target capture enrichment and Illumina sequencing was performed at Harvard Medical School in Boston (USA) (Table S3.1).

For tooth samples, after surface cleaning by fine sandblasting, the dentine area of roots and crowns was milled to obtain fine powder. For petrous samples or the cochlear region of the inner ear was extracted by sandblasting and subsequently milled into fine powder, respectively. In the case of the rib bones from the Aleutian Islanders, bones were cleaned at the surface with a sanding disk and fine powder was collected for DNA extraction by drilling into the cleaned area.

About 75 mg (+/- 9 mg) of powder was then used for DNA extraction following an established protocol by Dabney *et al*. (2013), with modifications as in Korlević *et al*. (2015); that is, the MinElute/Zymo funnel assembly was replaced by the funnel-column assembly from the Roche High Pure Viral Nucleic Acid Large Volume Kit. The final volume of DNA extract was 90 µl.

A double-stranded barcoded Illumina library was prepared for each sample using the 'partial UDG treatment' protocol (Rohland et al. 2015). For 3 libraries the settings were identical to the original publication, and for the remaining 55 libraries updated setting were used (see notes to Table S3.1).

After cleanup of the amplified libraries, we performed a screening step: a capture enrichment targeting the mitochondrial genome and additional nuclear loci (manuscript in preparation) following the procedure described in Maricic *et al*. (2010). After unique identification indices were added to each enriched library, we then sequenced the enrichment product together with the original libraries (also after addition of a unique index pair to each library) – shotgun, on an Illumina NextSeq 500 instrument for 2x 76 cycles and 2x 7cycles.

Nuclear data were produced by enriching the original short libraries for 1.24 million SNP loci following the protocol by Fu et al. 2015 (SNP information in Haak *et al*. 2015, Mathieson *et al*. 2015). For 3 libraries, enrichment reactions were performed on two separate bait pools with 390 thousand and 840 thousand targeted SNPs each. For the rest of the libraries, the two arrays were combined into a single pool targeting 1.24 million SNPs. Sequencing was performed on an Illumina NextSeq 500 instrument for 2x 76 cycles and 2x 7cycles.

Samples I0719 (an ancient Aleutian Islander) and I5319 (an ancient Athabaskan) were both shotgun sequenced on a NextSeq 500 instrument for 2x76 cycles.

References (for this section)

Dabney, J. *et al*. Complete mitochondrial genome sequence of a Middle Pleistocene cave bear reconstructed from ultrashort DNA fragments. *Proc. Natl. Acad. Sci. U. S. A*. **110**, 15758–15763 (2013).

Fu, Q. An early modern human from Romania with a recent Neanderthal ancestor. *Nature* **524**, 216–219 (2015).

Haak, W. *et al*. Massive migration from the steppe was a source for Indo-European languages in Europe. *Nature* **522**, 207–211 (2015).

Korlević, P. *et al*. Reducing microbial and human contamination in DNA extractions from ancient bones and teeth. *Biotechniques* **59**, 87–93 (2015).

Maricic, T., Whitten, M. & Pääbo, S. Multiplexed DNA sequence capture of mitochondrial genomes using PCR products. *PLoS One* **5**, e14004 (2010).

Mathieson, I. *et al*. Genome-wide patterns of selection in 230 ancient Eurasians. *Nature* **528**, 499–503 (2015).
Rohland, N. *et al*. Partial uracil-DNA-glycosylase treatment for screening of ancient DNA. *Philos. Trans. R. Soc. Lond. B Biol. Sci*. **370**, 20130624 (2015).

Table S3.1. DNA extraction, library preparation and nuclear targeted enrichment. For most individuals, one library per individuals was prepared and we here use the individual ID to identify the library as well.

[a] Dabney *et al*. 2013 with the addition of the funnel-column assembly from the Roche kit as in Korlević *et al*. (2015), elution in 2x 45 µl.

[b] Dabney *et al*. 2013 using a smaller portion of lysate with a silica bead cleanup instead of silica based columns, elution in 2x 15 µl.

[1] Rohland *et al*. (2015) with the following modifications: 1) the elution volume after the MinElute cleanup of the ligation reaction was reduced from 20 µl to 16 µl; 2) the Fill-in reaction volume was reduced from 40 µl to 25 µl; 3) the ThermoPol buffer was replaced by the Isothermal amplification buffer; 4) *Bst* polymerase, large fragment (New England Biolabs), was replaced by *Bst* 2.0 Polymerase, large fragment (New England Biolabs); 5) PCR volume was reduced from 400 µl to 100 µl.

[2] Rohland *et al*. (2015) with the following modifications: 1) the elution volume after the ligation reaction cleanup was reduced from 20 µl to 16 µl; 2) the Fill-in reaction volume was reduced from 40 µl to 25 µl; 3) the ThermoPol buffer was replaced by the Isothermal amplification buffer; 4) *Bst* polymerase, large fragment (New England Biolabs), was replaced by *Bst* 2.0 Polymerase, large fragment (New England Biolabs); 5) PCR volume was reduced from 400 µl to 100 µl; 5) the MinElute column cleanups were replaced with silica bead cleanups.

Analysis ID	library components	sample type	powder produced in	powder used for extraction, mg	extraction protocol	extract used for library preparation, µl	library preparation	damage rate in the final nucleotide	nuclear capture protocol
I0712	S0712.E1.L1	bone (rib)	Boston	74	Dabney *et al*. 2013 [a]	30	Rohland et al. 2015	1.5%	390k + 840k
I0719	S0719.E1.L1	bone (rib)	Boston	68	Dabney *et al*. 2013 [a]	30	Rohland *et al*. 2015	1.4%	390k + 840k
I0721	S0721.E1.L1	bone (rib)	Boston	74	Dabney *et al*. 2013 [a]	30	Rohland *et al*. 2015	2.5%	390k + 840k
I1118	S1118.E1.L1	bone (rib)	Boston	67	Dabney *et al*. 2013 [a]	30	Rohland *et al*. 2015 [1]	0.7%	1240k
I1123	S1123.E1.L1	bone (rib)	Boston	76	Dabney *et al*. 2013 [a]	30	Rohland *et al*. 2015 [1]	2.7%	1240k
I1124	S1124.E1.L1	bone (rib)	Boston	75	Dabney *et al*. 2013 [a]	30	Rohland *et al*. 2015 [1]	4.3%	1240k
I1125	S1125.E1.L1	bone (rib)	Boston	74	Dabney *et al*. 2013 [a]	30	Rohland *et al*. 2015 [1]	2.0%	1240k
I1126	S1126.E1.L2	bone (rib)	Boston	74	Dabney *et al*. 2013 [a]	3	Rohland *et al*. 2015 [2]	2.4%	1240k
I1127	S1127.E1.L1	bone (rib)	Boston	73	Dabney *et al*. 2013 [a]	30	Rohland *et al*. 2015 [1]	1.5%	1240k
I1128	S1128.E1.L1	bone (rib)	Boston	73	Dabney *et al*. 2013 [a]	30	Rohland *et al*. 2015 [1]	2.7%	1240k
I1129	S1129.E1.L1	bone (rib)	Boston	73	Dabney *et al*. 2013 [a]	30	Rohland *et al*. 2015 [1]	2.1%	1240k
I1524	S1524.E1.L1	molar	Dublin	68	Dabney *et al*. 2013 [a]	30	Rohland *et al*. 2015 [1]	1.9%	1240k
I1525	S1525.E1.L1	molar	Dublin	72	Dabney *et al*. 2013 [a]	30	Rohland *et al*. 2015 [1]	2.2%	1240k
	S7758.E1.L1	tooth	Dublin	67	Dabney *et al*. 2013 [a]	10	Rohland *et al*. 2015 [2]	1.6%	1240k
I1526	S1526.E1.L1	molar	Dublin	71	Dabney *et al*. 2013 [a]	30	Rohland *et al*. 2015 [1]	3.8%	1240k
	S7778.E1.L1	tooth	Dublin	71	Dabney *et al*. 2013 [a]	10	Rohland *et al*. 2015 [2]	2.4%	1240k
I5319	S5319.E1.L1	petrous	Boston	83	Dabney *et al*. 2013 [a]	10	Rohland *et al*. 2015 [2]	6.4%	1240k
	S5319.E2.L1	petrous	Boston	28	Dabney *et al*. 2013 [b]	10	Rohland *et al*. 2015 [2]	7.3%	1240k
	S5319.E2.L2	petrous	Boston	28	Dabney *et al*. 2013 [b]	30	Rohland *et al*. 2015 [2]	8.0%	1240k
I5320	S5320.E1.L1	petrous	Boston	75	Dabney *et al*. 2013 [a]	10	Rohland *et al*. 2015 [2]	4.0%	1240k
	S5320.E2.L1	petrous	Boston	16	Dabney *et al*. 2013 [b]	10	Rohland *et al*. 2015 [2]	4.6%	1240k
	S5320.E2.L2	petrous	Boston	16	Dabney *et al*. 2013 [b]	30	Rohland *et al*. 2015 [2]	5.0%	1240k
I5321	S5321.E1.L1	petrous	Boston	66	Dabney *et al*. 2013 [a]	10	Rohland *et al*. 2015 [2]	1.0%	1240k
	S5321.E2.L1	petrous	Boston	22	Dabney *et al*. 2013 [b]	10	Rohland *et al*. 2015 [2]	1.2%	1240k
	S5321.E2.L2	petrous	Boston	22	Dabney *et al*. 2013 [b]	30	Rohland *et al*. 2015 [2]	1.5%	1240k

I7331	S7331.E1.L1	molar	Dublin	75	Dabney *et al*. 2013 [a]	10	Rohland *et al*. 2015 [2]	1.5%	1240k
I7332	S7332.E1.L1	molar	Dublin	75	Dabney *et al*. 2013 [a]	10	Rohland *et al*. 2015 [2]	2.1%	1240k
I7333	S7333.E1.L1	molar	Dublin	75	Dabney *et al*. 2013 [a]	10	Rohland *et al*. 2015 [2]	1.4%	1240k
I7334	S7334.E1.L1	molar	Dublin	68	Dabney *et al*. 2013 [a]	10	Rohland *et al*. 2015 [2]	0.9%	1240k
I7335	S7335.E1.L1	molar	Dublin	64	Dabney *et al*. 2013 [a]	10	Rohland *et al*. 2015 [2]	3.2%	1240k
I7336	S7336.E1.L1	molar	Dublin	57	Dabney *et al*. 2013 [a]	10	Rohland *et al*. 2015 [2]	3.4%	1240k
I7337	S7337.E1.L1	molar	Dublin	58	Dabney *et al*. 2013 [a]	10	Rohland *et al*. 2015 [2]	1.2%	1240k
I7338	S7338.E1.L1	molar	Dublin	74	Dabney *et al*. 2013 [a]	10	Rohland *et al*. 2015 [2]	0.6%	1240k
I7339	S7339.E1.L1	molar	Dublin	75	Dabney *et al*. 2013 [a]	10	Rohland *et al*. 2015 [2]	1.6%	1240k
I7340	S7340.E1.L1	molar	Dublin	75	Dabney *et al*. 2013 [a]	10	Rohland *et al*. 2015 [2]	1.1%	1240k
I7341	S7341.E1.L1	molar	Dublin	75	Dabney *et al*. 2013 [a]	10	Rohland *et al*. 2015 [2]	1.8%	1240k
I7342_d	S7342.E1.L1	molar	Dublin	70	Dabney *et al*. 2013 [a]	10	Rohland *et al*. 2015 [2]	1.3%	1240k
I7343	S7343.E1.L1	molar	Dublin	70	Dabney *et al*. 2013 [a]	10	Rohland *et al*. 2015 [2]	1.5%	1240k
I7344	S7344.E1.L1	molar	Dublin	72	Dabney *et al*. 2013 [a]	10	Rohland *et al*. 2015 [2]	1.2%	1240k
I7346	S7346.E1.L1	molar	Dublin	80	Dabney *et al*. 2013 [a]	10	Rohland *et al*. 2015 [2]	1.8%	1240k
I7347	S7347.E1.L1	molar	Dublin	55	Dabney *et al*. 2013 [a]	10	Rohland *et al*. 2015 [2]	1.7%	1240k
I7348	S7348.E1.L1	molar	Dublin	57	Dabney *et al*. 2013 [a]	10	Rohland *et al*. 2015 [2]	1.9%	1240k
I7349	S7349.E1.L1	molar	Dublin	70	Dabney *et al*. 2013 [a]	10	Rohland *et al*. 2015 [2]	1.5%	1240k
I7621	S7621.E1.L1	bone	Dublin	63	Dabney *et al*. 2013 [a]	10	Rohland *et al*. 2015 [2]	3.5%	1240k
I7757	S7757.E1.L1	molar	Dublin	62	Dabney *et al*. 2013 [a]	10	Rohland *et al*. 2015 [2]	1.4%	1240k
I7759	S7759.E1.L1	molar	Dublin	82	Dabney *et al*. 2013 [a]	10	Rohland *et al*. 2015 [2]	3.0%	1240k
I7760	S7760.E1.L1	molar	Dublin	70	Dabney *et al*. 2013 [a]	10	Rohland *et al*. 2015 [2]	2.6%	1240k
I7779	S7779.E1.L1	bone (cranial)	Dublin	63	Dabney *et al*. 2013 [a]	10	Rohland *et al*. 2015 [2]	2.3%	1240k
I7780	S7780.E1.L1	molar	Dublin	67	Dabney *et al*. 2013 [a]	10	Rohland *et al*. 2015 [2]	1.8%	1240k
I7781	S7781.E1.L1	molar	Dublin	66	Dabney *et al*. 2013 [a]	10	Rohland *et al*. 2015 [2]	3.0%	1240k
I7782	S7782.E1.L1	molar	Dublin	62	Dabney *et al*. 2013 [a]	10	Rohland *et al*. 2015 [2]	3.3%	1240k
I8294	S8294.E1.L1	bone (phalanx)	Dublin	75	Dabney *et al*. 2013 [a]	10	Rohland *et al*. 2015 [2]	2.6%	1240k
I8295	S8295.E1.L1	bone (cranial)	Dublin	71	Dabney *et al*. 2013 [a]	10	Rohland *et al*. 2015 [2]	3.5%	1240k
I8296	S8296.E1.L1	bone (cranial)	Dublin	68	Dabney *et al*. 2013 [a]	10	Rohland *et al*. 2015 [2]	4.8%	1240k
	S8297.E1.L1	bone (cranial)	Dublin	68	Dabney *et al*. 2013 [a]	10	Rohland *et al*. 2015 [2]	3.7%	1240k
I8298	S8298.E1.L1	bone (cranial)	Dublin	75	Dabney *et al*. 2013 [a]	10	Rohland *et al*. 2015 [2]	6.5%	1240k
	S8300.E1.L1	bone (cranial)	Dublin	75	Dabney *et al*. 2013 [a]	10	Rohland *et al*. 2015 [2]	5.9%	1240k
I10427	S10427.E1.L2	molar	Boston	73	Dabney *et al*. 2013 [a]	10	Rohland *et al*. 2015 [2]	3.1%	1240k

3.2 Bioinformatic processing

Raw sequencing data was generated on an Illumina NextSeq 500 instrument. For libraries captured against the set of 1.24 million nuclear SNPs, sample-identifying sequences (barcodes) were trimmed. Adapters were stripped and read pairs with at least 15 bp overlap were merged into a single sequence (allowing for 1 mismatch) at least 30 bp in length, using a modified form of the SeqPrep tool (https://github.com/jstjohn/SeqPrep) which retains the highest quality base in the overlap region. Autosomal sequences were aligned to the human reference genome hg19 (1000 genomes version, downloaded at http://ftp.1000genomes.ebi.ac.uk/vol1/ftp/technical/reference/human_g1k_v37.fasta.gz) using *bwa* v.0.6.1 with the *samse* command (Li and Durbin 2009). Following alignment, clusters of duplicate reads were identified based on start and end position, and orientation; for each cluster of reads, the highest quality representative was used.

For libraries with mitochondrial DNA enrichment, the same procedure was used, except that the mitochondrial sequences were treated separately and aligned to the RSRS reference genome (Behar et al. 2012) rather than hg19. We measured damage rates on both ends of mapped reads to assess their authenticity, as summarized in Table S3.1 and in Fig. S3.1.

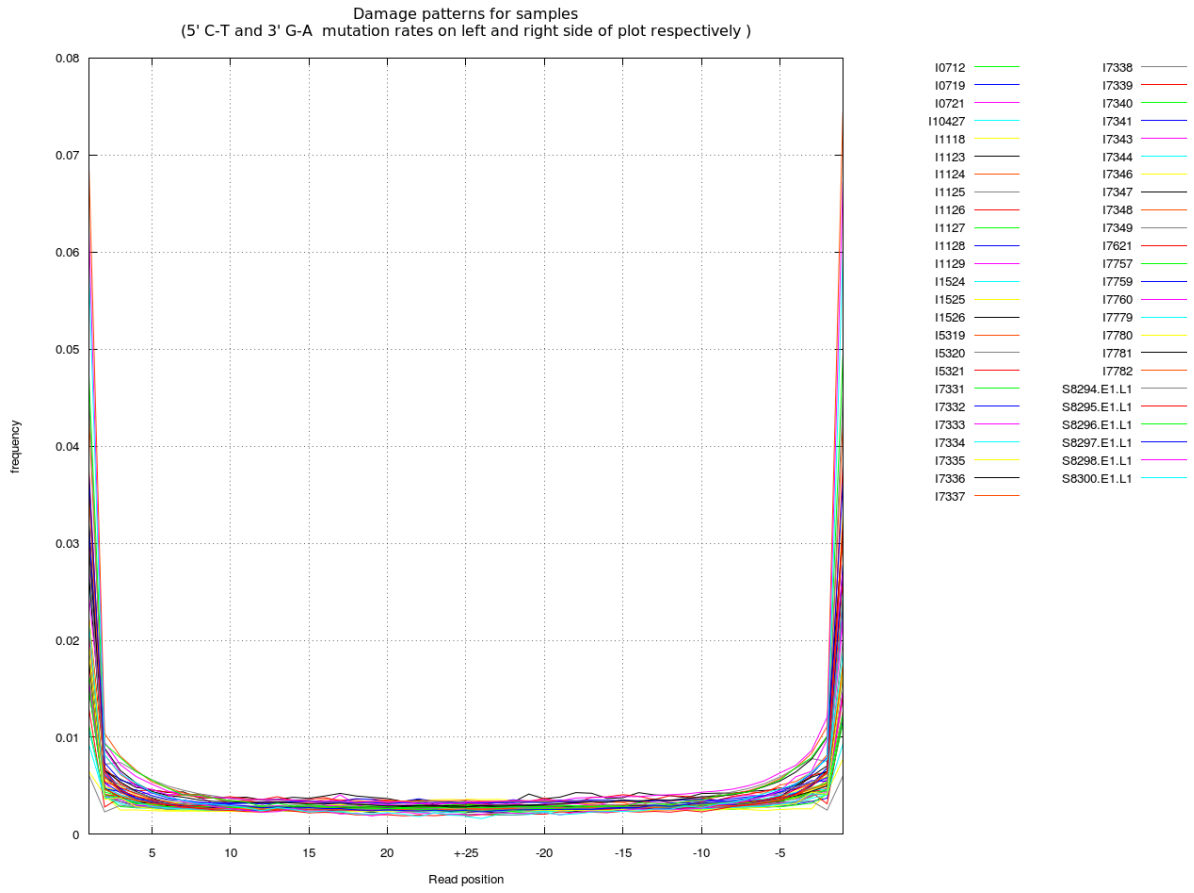

Fig. S3.1: Damage rates (5' C->T, 3' A->G) obtained from mapped reads of all samples.

References (for this section)

Behar, D. M. *et al.* A 'Copernican' reassessment of the human mitochondrial DNA tree from its root. *Am. J. Hum. Genet.* **90**, 675–684 (2012).

Li, H. & Durbin, R. Fast and accurate short read alignment with Burrows-Wheeler Transform. *Bioinformatics* **25**, 1754–1760 (2009).

Supplementary Information section 4

Principal component analysis and outlier removal

The first round of outlier removal (prior to *ChromoPainter v.1* and *v.2*, *fineSTRUCTURE*, HSS, *GLOBETROTTER* analyses and the *ADMIXTURE* analyses presented in Extended Data Fig. 8) is illustrated in Tables S4.1 and S4.2. These spreadsheets display unsupervised *ADMIXTURE* results (K=14 and K=11 in the case of the HumanOrigins and Illumina datasets, respectively), average weighted Euclidean distances, PC1 vs. PC2 plots, and outcomes of the outlier removal procedure for each American and Siberian population composed of 3 or more individuals and having at least one outlier. We note that outliers were removed from all populations, and the above-mentioned populations were selected to illustrate our approach and at the same time to keep the size of the spreadsheets reasonably small. The procedure itself is explained in the Methods section.

Individuals having outlying average weighted Euclidean distances (vs. all other individuals in a population) were identified using the established definition of an outlier: > [3rd quartile + 1.5 × (3rd quartile – 1st quartile)]. Manual removal of outliers based on *ADMIXTURE* profiles, i.e. on outstanding proportions of European and other non-typical ancestry components, was prioritized, and some individuals identified as outliers based on average weighted Euclidean distances were kept if they had a typical *ADMIXTURE* profile (see examples for the Ket, Nganasan, Tubalar, and Yup'ik Chaplin/Sireniki populations in the HumanOrigins dataset, Table S4.1). If a majority of individuals in a population had colonial admixture, we removed only those having the most extreme admixture proportions, in order to keep the final population size reasonably large (see examples for the Splatsin, Stswecem'c, Tlingit and other groups in the Illumina dataset, Table S4.2). Removal of outliers based on average weighted Euclidean distances was prioritized if all individuals had a uniform *ADMIXTURE* profile (see examples for the Karitiana, Mansi, Surui, Xavante, and Zapotec populations in the HumanOrigins dataset, Table S4.1).

To illustrate the effects of the second round of outlier removal (prior to *qpWave*, *qpAdm*, *qpGraph*, *ALDER*, and f_4-statistic analyses), we performed principal component analysis (PCA) on the datasets without transitions used for the above-listed analyses (Fig. S4.1). Native American individuals (i.e. those belonging to the First Peoples, Na-Dene, and Eskimo-Aleut meta-populations) having >1% European, African, or Southeast Asian ancestry according to *ADMIXTURE* were removed, as well as Chukotkan and Kamchatkan individuals with >1% European ancestry. PCA plots for original datasets prior to any outlier removal are shown in Fig. 1a and Extended Data Fig. 2.

We dated 12 burials at the Ust'-Belaya site at the confluence of the Belaya and Angara Rivers: seven burials were dated to ca. 4,500 – 4,800 calBP, four burials were dated to an earlier period between ca. 5,700 and 7,000 calBP, and a medieval burial was dated to ca. 600 calBP (Supplementary Table 2). We generated genome-wide data for all 12 individuals (Supplementary Table 1). Among these samples, 3 were removed due to a high percentage of missing data (Supplementary Table 1), and all but one remaining samples form a tight cluster positioned between the C-K/P-E and Siberian clusters in the space of two principal components (PC1 and PC2, Fig. 1a, Extended Data Fig. 2). Remarkably, an individual I7760 (Mos85) buried at Ust'-Belaya and dated to 5740 – 5900 calBP (Supplementary Table 2) is a genetic outlier demonstrating the typical West Siberian genetic profile (Fig. 1a, Extended Data Fig. 2).

Fig. S4.1. PCA based on the HumanOrigins (**a**) and Illumina (**b**) datasets without transitions used for the

qpWave/apAdm and *ALDER* analyses. The datasets have undergone a stringent outlier removal procedure, as described in the Methods section. The analyses are based on 649 (**a**) or 472 (**b**) individuals and 111,147 (**a**) or 96,155 (**b**) loci. Plots of two principal components (PC1 vs. PC2) are shown (linkage disequilibrium pruning was not applied). The following meta-populations most relevant for our study are plotted: present-day Eskimo-Aleut and Chukotko-Kamchatkan speakers, ancient Chukotkan Neo-Eskimos (Ekven and Uelen sites), ancient Aleuts, Paleo-Eskimos (the Saqqaq, Middle Dorset and Late Dorset individuals), ancient Northern Athabaskans, present-day Na-Dene speakers, Northern and Southern First Peoples, West and East Siberians, the Ust'-Belaya Angara ancient Siberian population, Southeast Asians, and Europeans. Calibrated radiocarbon dates in years before present are shown for ancient samples. For individuals, 95% confidence intervals are shown, and for populations, minimal and maximal median dates among individuals are shown.

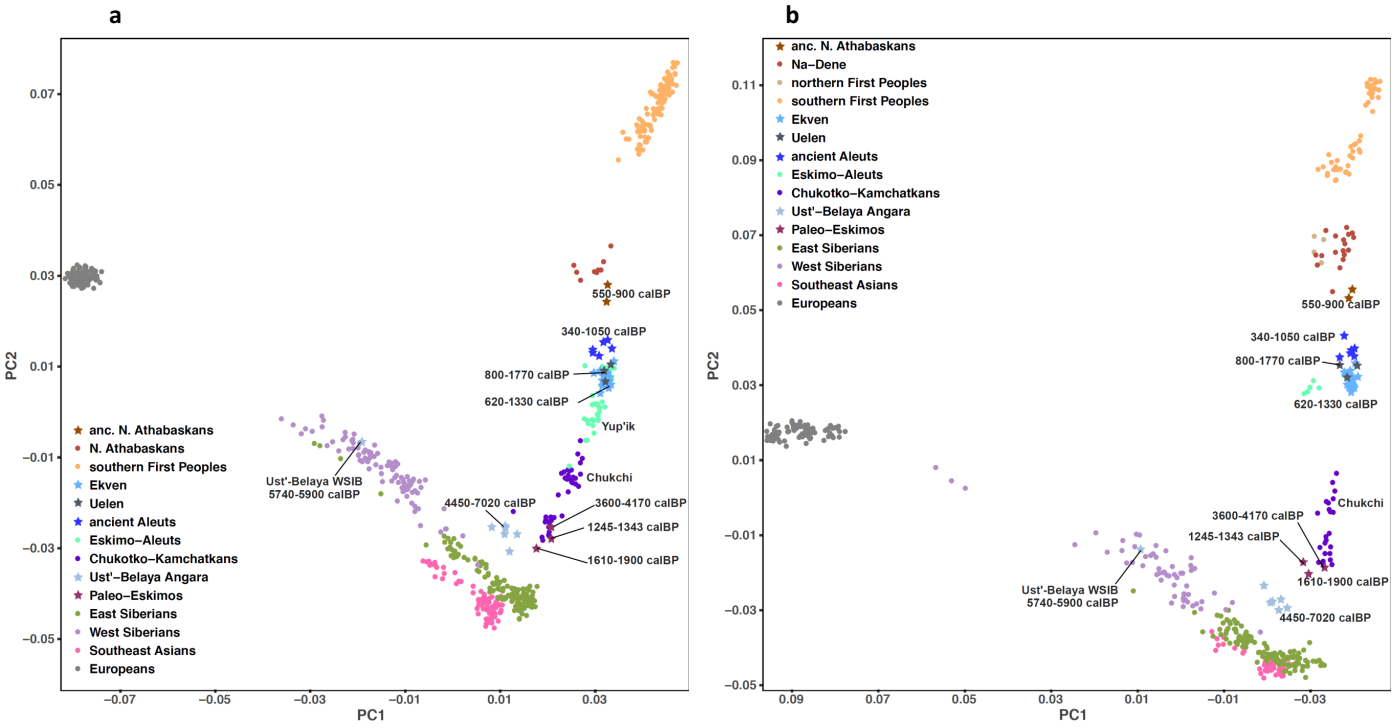

Supplementary Information section 5

Exhaustive analysis of ancestry streams in small population sets

We performed testing of two- and three-way admixture models in groups of three and four populations (triplets and quadruplets) using *qpAdm* (Haak et al. 2015) and *qpWave* (Reich et al. 2012): closely related tools that in conjunction allow testing whether two- or multi-component admixture models fit the data, and allow inferring admixture proportions (*qpAdm*) without assuming a particular tree topology. This class of methods relies on allele frequencies in populations, and thus requires careful definition of population groups and outlier pruning. The *qpWave* tool is used to infer how many independent lines of ancestry relate a set of test populations to a set of outgroups. *qpWave* relies on a matrix of statistics f_4(test$_1$, test$_i$; outgroup$_1$, outgroup$_x$). Usually, few test populations from a certain region and a diverse worldwide set of outgroups (having no recent gene flow from the region of interest) are co-analyzed (Haak et al. 2015, Lazaridis et al. 2016, Skoglund et al. 2015), and a statistical test is performed to determine whether allele frequencies in the test populations can be explained by one, two, or more streams of ancestry derived from the outgroups. If a group of three populations, a triplet, is derived from two ancestry streams according to a *qpWave* test, and any pair of the constituent populations shows the same result, it follows that one of the populations can be modelled as having ancestry from the other two using *qpAdm*. If a set of outgroups includes populations closely related to at least one of the admixture partners, the power to distinguish alternative admixture models is increased.

The following sets of outgroup populations were used for analyses on the HumanOrigins dataset: 1) “OG19”, 19 outgroups from five broad geographical regions: Mbuti, Taa, Yoruba (Africans), Nganasan, Tuvinian, Ulchi, Yakut (East Siberians), Altaian, Ket, Selkup, Tubalar (West Siberians), Czech, English, French, North Italian (Europeans), Dai, Miao, She, Thai (Southeast Asians); 2) “OG19_UB1526”, OG19 and an ancient Siberian individual I1526 (the highest-coverage individual at the Ust’-Belaya Angara site) that is distinct from the other Siberians according to our PCA analyses (section 4) and thus might increase the diversity of Siberian outgroups and the resolution of the method; 3) “OGA”, 8 diverse Siberian populations (Nganasan, Tuvinian, Ulchi, Yakut, Even, Ket, Selkup, Tubalar) and a Southeast Asian population (Dai); 4) “OGA_Koryak”, OGA and Koryak, a C-K group that supposedly provides higher resolution since it is closely related to the putative PPE admixture partners (section 10); 5) “OGA_UB1526”, OGA and the Ust’-Belaya Angara individual I1526.

Similar sets of outgroup populations were used for analyses based on the Illumina dataset: 1) “OG20”: Bantu (Kenya), Mandenka, Mbuti, Yoruba (Africans), Buryat, Evenk, Nganasan, Tuvinian, Yakut (East Siberians), Altaian, Khakas, Selkup (West Siberians), Basque, Sardinian, Slovak, Spanish (Europeans), Dai, Lahu, Miao, She (Southeast Asians); 2) “OG20_UB1526”, OG20 and the highest-coverage Ust’-Belaya Angara individual I1526; 3) “OGA”, 9 Siberian populations (Buryat, Dolgan, Evenk, Nganasan, Tuvinian, Yakut, Altaian, Khakas, Selkup) and Dai; 4) ”OGA_Koryak”, OGA and Koryak; 5) “OGA_UB1526”, OGA and the Ust’-Belaya Angara individual I1526. Population triplets and quadruplets were tested using both the HumanOrigins and Illumina SNP array datasets, with or without transition polymorphisms, and using these five alternative outgroup sets. Paleo-Eskimos (P-E) were represented by the Saqqaq (ca. 3,900 calBP), or Middle Dorset (ca. 1,750 calBP), or Late Dorset individuals (ca. 750 calBP), widely separated in space and time, and two types of SNP calls were tested for the Saqqaq individual: published diploid calls (Raghavan et al. 2014) with 50-58% missing rates in various dataset versions, and pseudo-haploid calls with much lower missing rates of 4-11% (in various dataset versions) generated by us and also used for *qpGraph* model

fitting (section 10). Missing rates for the Middle and Late Dorset samples were as follows: 89-90% and 70-75% in various dataset versions, respectively. Chukotko-Kamchatkan speakers (C-K) served as an alternative PPE source, and were represented by Chukchi, Koryak, and Itelmen (the HumanOrigins dataset), and by Chukchi and Koryak in the case of the Illumina dataset.

For the *qpWave/qpAdm* analyses, any American individuals with >1% European, African, or Southeast Asian ancestry according to the *ADMIXTURE* analysis (Extended Data Fig. 8) were removed, as well as Chukotkan and Kamchatkan individuals with >1% European ancestry. Some additional Chipewyan and West Greenlandic Inuit individuals were removed since European ancestry undetectable with *ADMIXTURE* was revealed in them using *D*-statistics (Yoruba or Dai, Icelander; Chipewyan individual, Karitiana) and (Yoruba or Dai, Slovak; West Greenlandic Inuit individual, Karitiana). Any individual with any of the two absolute Z-scores >3 was removed.

First, we tested if essentially all present-day and ancient American and Chukotkan populations can be modelled as a mixture of two sources: selected First Peoples (FAM) and mostly unadmixed representatives of the PPE clade: P-E or C-K. To this end, we exhaustively tested the following population triplets using *qpAdm*, for four dataset versions and five outgroup sets: 1/ C-K, FAM, PPE; 2/ E-A, FAM, PPE; 3/ Na-Dene (N-D), FAM, PPE; 4/ P-E, FAM, PPE; 5/ SAM, FAM, PPE; 6/ NAM, FAM, PPE. The FAM group was represented by three alternative sources in the case of the HumanOrigins dataset: relatively large SAM populations with no signs of colonial admixture (Guarani, 17 ind.; Karitiana, 12 ind.; Mixe, 10 ind.). In the case of the Illumina dataset, a NAM source with no signs of P-E admixture (Extended Data Figs. 3 and 4) was also added, and the full list of alternative FAM sources was as follows: Pima (SAM, 13 ind.), Karitiana (SAM, 13 ind.), Mixtec (SAM, 7 ind.), Nisga'a (NAM, 3 ind.). A C-K outgroup (Koryak in the "OGA_Koryak" outgroup sets) was not tested for population triplets/quadruplets including a C-K group since such models are expected to be non-fitting by default.

Here we summarize the results for the HumanOrigins transversion-only dataset (Table S5.1). First, C-K (represented by Koryak or Itelmen) does not make a good PPE source for E-A populations since most 2-way admixture models "E-A = FAM + C-K" are non-fitting even at the 0.01 *p*-value threshold (5 or 6 of 18 models fit). This result holds for all outgroup sets tested. However, models including Chukchi as a PPE source fit much better, probably because of an elevated E-A admixture in Chukchi (see Fig. 1a, Extended Data Figs. 2 and 8, sections 5, 8). Notably, the models generally work for ancient Aleuts and the Old Bering Sea group from Uelen, and the former group has no C-K admixture according to our *qpGraph*, *Rarecoal*, and RASS analyses (sections 8, 9, 10). This result can be interpreted in the following way: two-way admixture models "FAM + C-K" do not fit for ancient Neo-Eskimos (Ekven) and for present-day Iñupiat and Yup'ik since two distinct PPE sources contributed to these groups, i.e. the original PPE source and C-K during the later bidirectional gene flow event. Moreover, according to all fitting *qpGraph* models (Fig. S10.3), C-K groups are rather distant from the PPE source in E-A (here named "PPE_{E-A}"), which is much closer to the Saqqaq Paleo-Eskimo.

In line with these phylogenetic models, P-E make a perfect source for ancient and present-day E-A: 332 of 360 models "E-A = FAM + P-E" are fitting at the 0.05 *p*-value threshold. Here we counted all five alternative outgroup sets and four alternative P-E sources (Saqqaq diploid calls, Saqqaq pseudo-haploid calls, the Middle Dorset individual and the Late Dorset individual). Most non-fitting models are of the following type: "Yup'ik = FAM + P-E", with the "OGA_Koryak" outgroup set. Due to a high level of C-K admixture in Yup'ik (see Extended Data Fig. 8, sections 5, 8), an assumption of the method, i.e. absence of gene flow from ingroups to outgroups, is violated, and the models become non-fitting.

Second, both P-E and C-K make good proxies for PPE ancestry in ancient and present-day N-D (Table S5.1): 72 of 108 models "N-D = FAM + C-K" (or 67% of models) are fitting at the 0.05 *p*-value threshold; 126 of 144 models "N-D = FAM + P-E" (or 88% of models) are fitting at the 0.05 *p*-value threshold (here we counted four alternative outgroup sets, three alternative C-K sources, and four alternative P-E sources). These results agree with the best-fitting admixture graph (Fig. S10.5) since PPE_{C-K} and PPE_{P-E} split points are approximately equidistant from the PPE_{N-D} split point, and thus C-K and P-E may serve equally well as proxies for PPE_{N-D}.

Third, most admixture models for 19 SAM populations are consistent with 0% PPE ancestry (Extended Data Fig. 3a-e, Table S5.1. We observe that estimates of PPE ancestry proportions in other populations are highly dependent on the PPE proxies used (Table S5.1): the lowest for the Late Dorset individual, and the highest for Saqqaq pseudo-haploid calls. We refrain from judging which estimates are closer to reality, although ranking of populations according to the PPE ancestry proportion remains relatively stable across various proxies and outgroup sets (Fig. 1b, Extended Data Figs. 3 and 4). Here we ranked populations according to increasing percentage of PPE ancestry (Fig. 1b): 1/ SAM, 2/ Chipewyans and Dakelh, 3/ ancient Athabaskans, 4/ ancient Aleuts, 5/ Iñupiat, Ekven, and Uelen having almost equal percentages, 6/ Yup'ik Naukan, 7/ Yup'ik Chaplin/Sireniki, 8/ C-K and P-E. This ranking is in line with our migration model (see the Discussion and Fig. 3). Gene flow from neighboring NAM groups most likely continued after the initial NAM/P-E admixture event in Na-Dene ancestors, so the percentage of PPE ancestry went down gradually over time. Ancient Aleuts remained in Alaska and never experienced the later pulse of C-K admixture (section 10), which is shared by Ekven, Uelen (ancient Chukotkan Neo-Eskimos of the Old Bering Sea culture), and Iñupiat (present-day Alaskans whose ancestors migrated from Chukotka according to archaeological evidence, Jensen 2016, Mason 2016). Unlike Iñupiat and other Inuit, Yup'ik have remained in Chukotka since their initial backward migration from Alaska (Fig. 3), and had much more time for interacting with local C-K; thus the elevated PPE ancestry proportion in Yup'ik is not unexpected. The C-K/E-A admixture was bidirectional (section 10), and E-A ancestry proportion is also non-uniform among C-K.

The results remain virtually the same for the full HumanOrigins dataset (Table S5.2). Even fewer models "E-A = FAM + Koryak/Itelmen" fit the data: 8 models of 144 at the *p*-value threshold of 0.05, namely the models "ancient Aleuts = FAM + Koryak/Itelmen" with the OGA and OG19 outgroup sets. In contrast, most models "E-A = FAM + P-E" remain fitting: 284 of 360 models at the 0.05 *p*-value threshold. Here we counted all five alternative outgroup sets and four alternative P-E sources. Most non-fitting models are those with the "OGA_Koryak" outgroup, and that result reflects C-K admixture in the ancestors of Yup'ik/Inuit. The results also remain unchanged for Na-Dene speakers: both P-E and C-K make good proxies for PPE ancestry in ancient and present-day N-D (Table S5.2): 71 of 108 models "N-D = FAM + C-K" (or 66% of models) are fitting at the 0.05 *p*-value threshold; 107 of 144 models "N-D = FAM + P-E" (or 74% of models) are fitting at the 0.05 *p*-value threshold (here we counted four alternative outgroup sets, three alternative C-K sources, and four alternative P-E sources). The ranking of populations by PPE ancestry proportions also remains unchanged (Extended Data Fig. 4a-e, Table S5.2).

Next, we repeated the same analyses for the Illumina dataset. An advantage of this dataset is that it includes a wider diversity of Na-Dene speakers (Tlingit and Southern Athabaskans, in addition to Northern Athabaskans) and FAM populations (NAM in addition to SAM). The results of admixture model testing with *qpAdm* are generally similar for the Illumina and HumanOrigins datasets, with the following notable differences. First, for both the transversions-only (Table S5.3) and full datasets (Table S5.4), C-K and P-E represent equally fitting ancestry sources for E-A: 1/ models "E-A = FAM + C-K", 138 (72%, Table S5.3) or 126

(66%, Table S5.4) of 192 models fit the data at the *p*-value threshold of 0.05; 2/ models "E-A = FAM + P-E", 330 (86%, Table S5.3) or 244 (64%, Table S5.4) of 384 models fit the data at the *p*-value threshold of 0.05. Here we counted four alternative outgroup sets and four alternative P-E sources (Saqqaq diploid calls, Saqqaq pseudo-haploid calls, Middle Dorset, and Late Dorset). As expected, the models "E-A = FAM + P-E" with the "OGA_Koryak" outgroup set are non-fitting for all E-A except for ancient Aleuts (Table S5.3). This result reflects C-K admixture in the ancestors of Yup'ik/Inuit.

Another important finding is that PPE ancestry, with a proportion comparable to that found in Na-Dene speakers, was detected in one NAM population, Splatsin, while in Nisga'a, Haida, and in SAM populations it was consistent with 0% (Extended Data Figs. 3f-j and 4f-j, Tables S5.3, S5.4). Here we ranked populations according to increasing percentage of PPE ancestry (Extended Data Figs 3, 4): 1/ SAM, Nisga'a, and Haida, 2/ Southern Athabaskans, 3/ Tlingit, 4/ three Northern Athabaskan groups and Splatsin (NAM), 5/ West Greenlandic Inuit, 6/ ancient Athabaskans, 7/ Alaskan and East Greenlandic Inuit, ancient Aleuts, 8/ Ekven, and Uelen, 9/ C-K and P-E.

We also analyzed other types of population triplets and quadruplets using *qpWave*. To keep the number of tests reasonably low, here we excluded the lowest-coverage Paleo-Eskimo individual, i.e. Middle Dorset. In total, we ran 54,948 *qpWave* tests. The quadruplets tested had the following composition: SAM or NAM + N-D + E-A + P-E or C-K. The triplets tested had the following composition: SAM or NAM or N-D + E-A + P-E or C-K. Below we summarize results for the HumanOrigins dataset: the full and transversion-only versions, with the 0.01 and 0.05 *p*-value thresholds (Tables S5.5 – S5.8). Quadruplets "SAM + N-D + E-A + P-E" and triplets "SAM or N-D + E-A + P-E" were generally consistent with two migration waves (Table S5.5), except for models "SAM + N-D + Yup'ik + P-E" and "SAM or N-D + Yup'ik + P-E" with the "OGA_Koryak" outgroup set. As discussed above, this result reflects the third genetic stream, i.e. the C-K admixture, easily detectable in Yup'ik having a high proportion of C-K ancestry (Extended Data Fig. 8, section 8). Overall, the results are consistent with P-E contributing genetically to both N-D and E-A, and the picture remains the same for the full dataset at both *p*-value thresholds, although it becomes noisier (Tables S5.7, S5.8). When P-E groups in the triplets and quadruplets were replaced by C-K groups, three or rarely even four, but not two migration streams fitted the data in most cases (3,290 vs. 1,270 triplets and quadruplets including Ekven, Inupiat, and Yup'ik), except for population sets including ancient Aleuts (Tables S5.5 – S5.8) and Uelen Neo-Eskimos (Tables S5.5 – S5.7). This pattern was observed for all outgroup sets, except for "OGA_Koryak", which is expected to increase the f_4 matrix rank for any C-K-containing population set: data for 211 vs. 929 triplets and quadruplets fitted 2-stream vs. 3- or 4-stream models, respectively (Table S5.5). Taken together, these results are again consistent with two PPE gene flow events in the E-A history: the first event in Alaska, and another gene flow from C-K to Yup'ik/Inuit ancestors in Chukotka. Ancient Aleuts had remained in Alaska and were not influenced by the latter event. The result observed for Uelen is more difficult to interpret, but it is possibly explained by the fact that Uelen is the smallest E-A group composed of just 3 pseudo-haploid individuals (cf. 6 ancient Aleuts, 16 Ekven Neo-Eskimos, 9 Yup'ik Naukan, 15 Yup'ik Chaplin/Sireniki, 20 Iñupiat, see Supplementary Table 4).

The Illumina dataset allowed us to explore population sets including NAM groups. In the case of the transversion-only dataset and the *p*-value threshold of 0.01 (Table S5.9), *qpWave* results were not influenced by the PPE proxy used: almost all triplets "SAM or NAM or N-D + E-A + P-E or C-K" and quadruplets "SAM or NAM + N-D + E-A + P-E or C-K" were consistent with two migration streams derived from the outgroups. The results were similar for NAM- and SAM-containing population sets (Table S5.9). The C-K admixture in E-A becomes apparent only if an outgroup very close to C-K is used, i.e. Koryak in the "OGA_Koryak"

outgroup set. In this case most quadruplets and triplets including P-E were consistent with three migration streams, except for those including ancient Aleuts, as expected (Table S5.9).

However, most triplets and quadruplets including C-K instead of P-E with the "OGA_Koryak" outgroup set were consistent with two migration streams (344 vs. 36 models, Table S5.9), except for those including ancient Aleuts. The latter sets were mostly consistent with three migration streams (18 models consistent with two streams vs. 58 models consistent with three streams, Table S5.9). This somewhat unexpected result may be interpreted in the following way. If the method cannot easily resolve the PPE_{C-K} and PPE_{P-E} ancestry sources, any population having ancestry from both sources (e.g., Yup'ik and Inuit) might fit the two-stream model due to an apparent lack of resolution, as well as any population having a low-level contribution from any of these sources (e.g., Na-Dene speakers). However, (ancient) Aleuts under our model have a substantial ancestry proportion (ca. 40-50%) derived from PPE_{P-E} only, thus a population group "SAM or NAM or N-D + ancient Aleuts + C-K" is not expected to fit the two-stream model. Overall, the *qpWave* results are noisier for the Illumina dataset (Tables S5.9 – S5.12), as compared to the HumanOrigins dataset (Tables S5.5 – S5.8).

References (for this section)

Haak, W. *et al*. Massive migration from the steppe was a source for Indo-European languages in Europe. *Nature* **522**, 207–211 (2015).

Jensen, A. M. Archaeology of the Late Western Thule/Iñupiat in North Alaska (A.D. 1300–1750). *The Oxford Handbook of the Prehistoric Arctic*, ed. Friesen, T. M., Mason, O. K. New York: Oxford University Press. 513–536 (2016).

Lazaridis, I. *et al*. Genomic insights into the origin of farming in the ancient Near East. *Nature* **536**, 419–424 (2016).

Mason, O. K. Thule Origins in the Old Bering Sea Culture: The Interrelationship of Punuk and Birnirk Cultures. *The Oxford Handbook of the Prehistoric Arctic*, ed. Friesen, T. M., Mason, O. K. New York: Oxford University Press. 489–512 (2016).

Raghavan, M. *et al*. The genetic prehistory of the New World Arctic. *Science* **345**, 1255832 (2014).

Reich, D. *et al*. Reconstructing Native American population history. *Nature* **488**, 370–374 (2012).

Skoglund, P. *et al*. Genetic evidence for two founding populations of the Americas. *Nature* **525**, 104–108 (2015).

Supplementary Information section 6

Haplotype sharing statistics

To investigate Paleo-Eskimo ancestry in Native Americans in a hypothesis-free way, we considered haplotypes shared between Native Americans and the ancient Saqqaq individual. Cumulative lengths of shared autosomal haplotypes were produced with *ChromoPainter v.1* for pairs of individuals, in the form of all vs. all "coancestry matrices" (Lawson et al. 2012). First, for each American individual we considered the length of haplotypes shared with Saqqaq in both the donor-to-recipient and recipient-to-donor directions (in cM), which we refer to as Saqqaq haplotype sharing statistic or HSS. In the same way we estimated haplotype sharing between each American individual and Africans, Europeans, Siberians, and Arctic (Chukotko-Kamchatkan- and Eskimo-Aleut-speaking) groups by averaging HSS across individuals of a given meta-population. To normalize for coverage differences and other biases, we divided the Saqqaq HSS by the African HSS, and termed the resulting statistic "relative HSS." Alternatively, we used Siberian HSS as a normalizer. To visually assess correlation of haplotype sharing with Saqqaq and with closely related Chukotko-Kamchatkan- and Eskimo-Aleut-speaking populations, here collectively termed Arctic, we combined relative Saqqaq HSSs and relative Arctic HSS on two-dimensional plots. We analyzed both the HumanOrigins (Fig. S6.1) and the Illumina (Fig. S6.2) datasets with a more diverse collection of Na-Dene-speaking individuals.

Since the ancient Saqqaq individual has demonstrable genetic affinities to both Arctic and Siberian meta-populations (Rasmussen et al. 2010, Raghavan et al. 2014, 2015, Flegontov et al. 2016, see also ADMIXTURE profiles in Extended Data Fig. 8), we also scrutinized relative Arctic and Siberian HSSs (Figs. S6.3, S6.4). We observe that each meta-population is scattered along a line on the Arctic vs. Siberian two-dimensional HSS plot, which reflects similar ratios of the Siberian and Arctic haplotype sharing among its members. The position of a population along the line depends on the presence of other ancestry components. For example, Aleuts, who have a high level of European admixture (Raghavan et al. 2014, 2015) (see also Extended Data Fig. 8), lie much closer to zero on both axes as compared to other Eskimo-Aleut-speaking groups (Fig. S6.3a,c). While First Peoples form a tight cluster, the Athabaskan-speaking Dakelh and some Chipewyans are shifted considerably towards the Saqqaq individual (Fig. S6.3a,c). Since haplotype sharing statistics behave linearly under recent admixture, we used linear combinations to calculate expected HSSs for mixtures of First Peoples with Saqqaq or with Eskimo-Aleut-speaking populations. We find that HSSs for two Dakelh (Fig. S6.3b,d) and for several Northern Athabaskan, Southern Athabaskan, and Tlingit individuals (Fig. S6.4b,d) are inconsistent with a recent Inuit or Yup'ik admixture event, but consistent with Saqqaq admixture. However, these simple simulations do not rule out an ancient admixture event with a Neo-Eskimo group since subsequent drift in Siberians or Arctic groups could have skewed the HSSs.

Fig. S6.1. Two-dimensional plots of Arctic and Saqqaq haplotype sharing statistics normalized using the African (**a, b**) or Siberian (**c, d**) meta-populations and based on the HumanOrigins SNP array dataset. **a, c,** Plots showing statistics for individuals of all relevant populations and meta-populations (color-coded according to the legend). **b, d,** Enlarged plots showing statistics for individuals of primarily First Peoples ancestry. The highest Saqqaq haplotype sharing statistics among Southern First Peoples is marked by the horizontal line. Northern Athabaskan-speaking individuals (outliers on the Arctic and/or Saqqaq axes) selected for the GLOBETROTTER analysis are marked with circles in panel **d**.

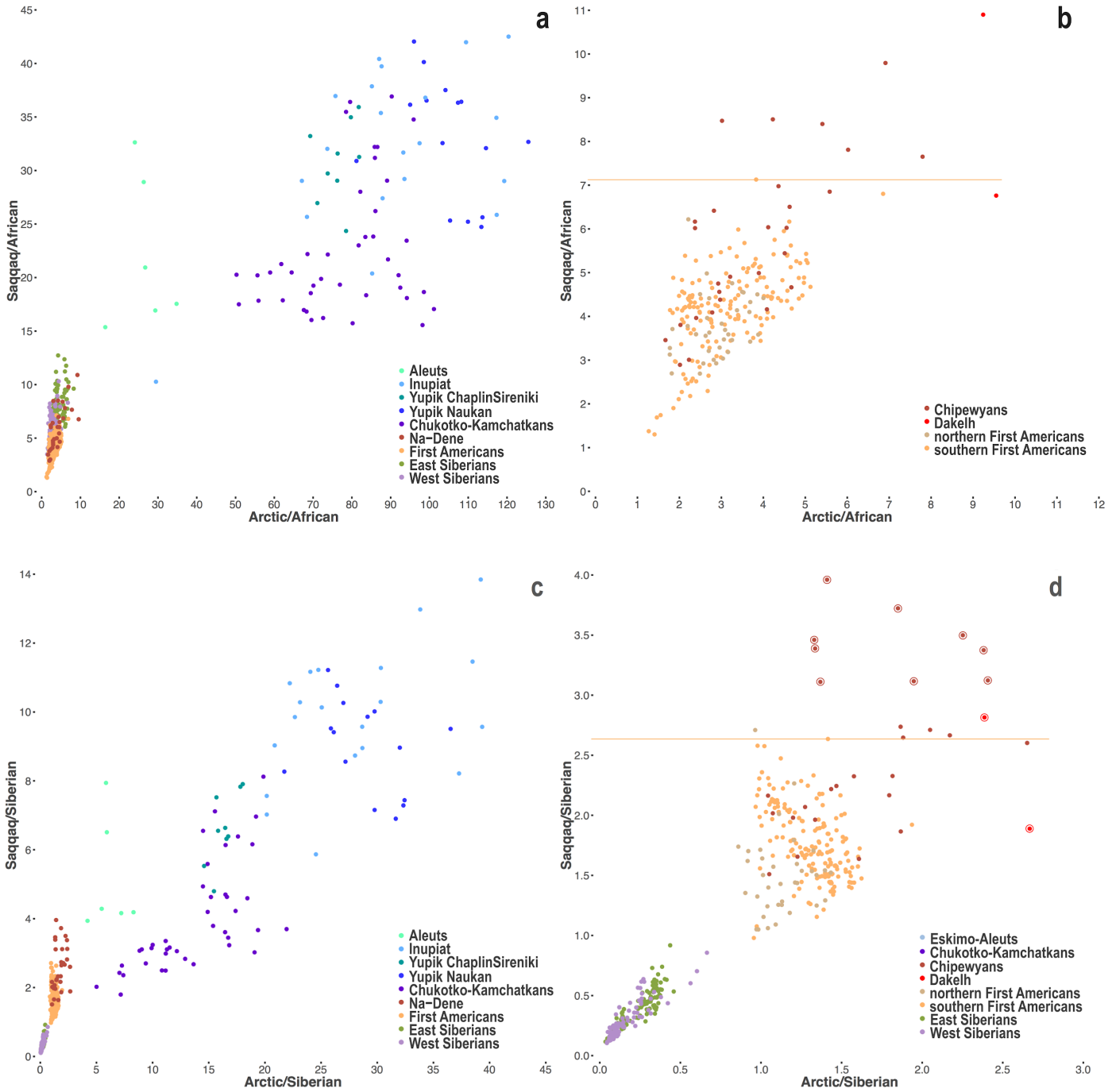

Fig. S6.2. The same results as in Fig. S6.1, but based on the Illumina SNP array dataset. Northern Athabaskan- and Tlingit-speaking individuals (outliers on the Arctic and/or Saqqaq axes) selected for the *GLOBETROTTER* analysis are marked with circles in panel **d**. Two Athabaskan-speaking Dakelh individuals with shotgun sequencing data, also included into the HumanOrigins and whole genome datasets, are marked with callouts.

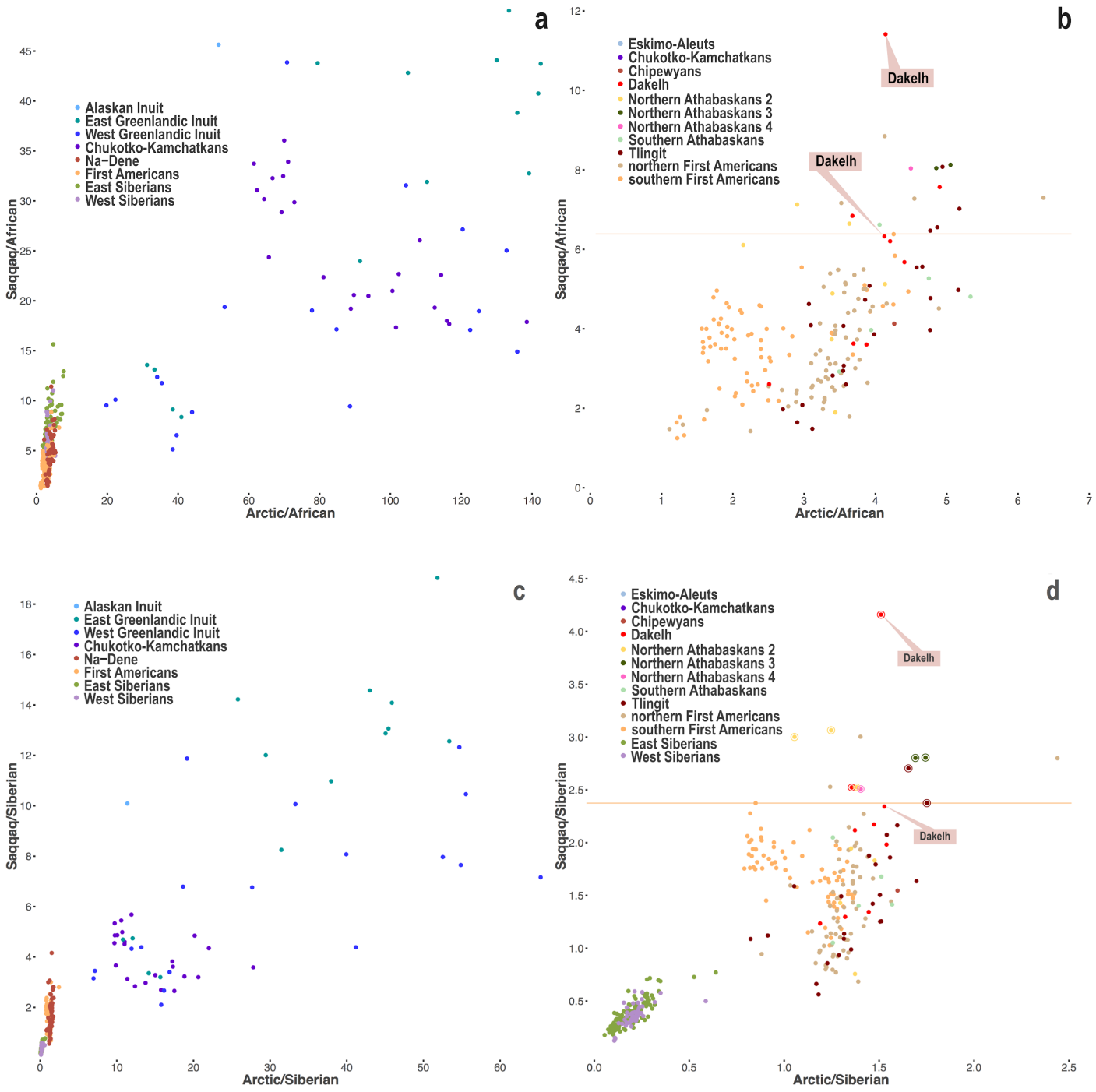

Fig. S6.3. Two-dimensional plots of Arctic and Siberian haplotype sharing statistics normalized using the European (**a, b**) or African (**c, d**) meta-populations and based on the HumanOrigins SNP array dataset. **a, c,** Plots showing statistics for individuals of all relevant populations and meta-populations (color-coded according to the legend). **b, d,** Enlarged areas of the plots showing statistics for First Peoples individuals and simulated mixtures of any present-day southern First Peoples population and the Saqqaq individual (from 5% to 70%, with 5% increments), and similar mixtures with Eskimo-Aleut-speaking populations (>5% of Iñupiat or Yup'ik ancestry). Average values of the statistics in populations were used to calculate the simulated statistics.

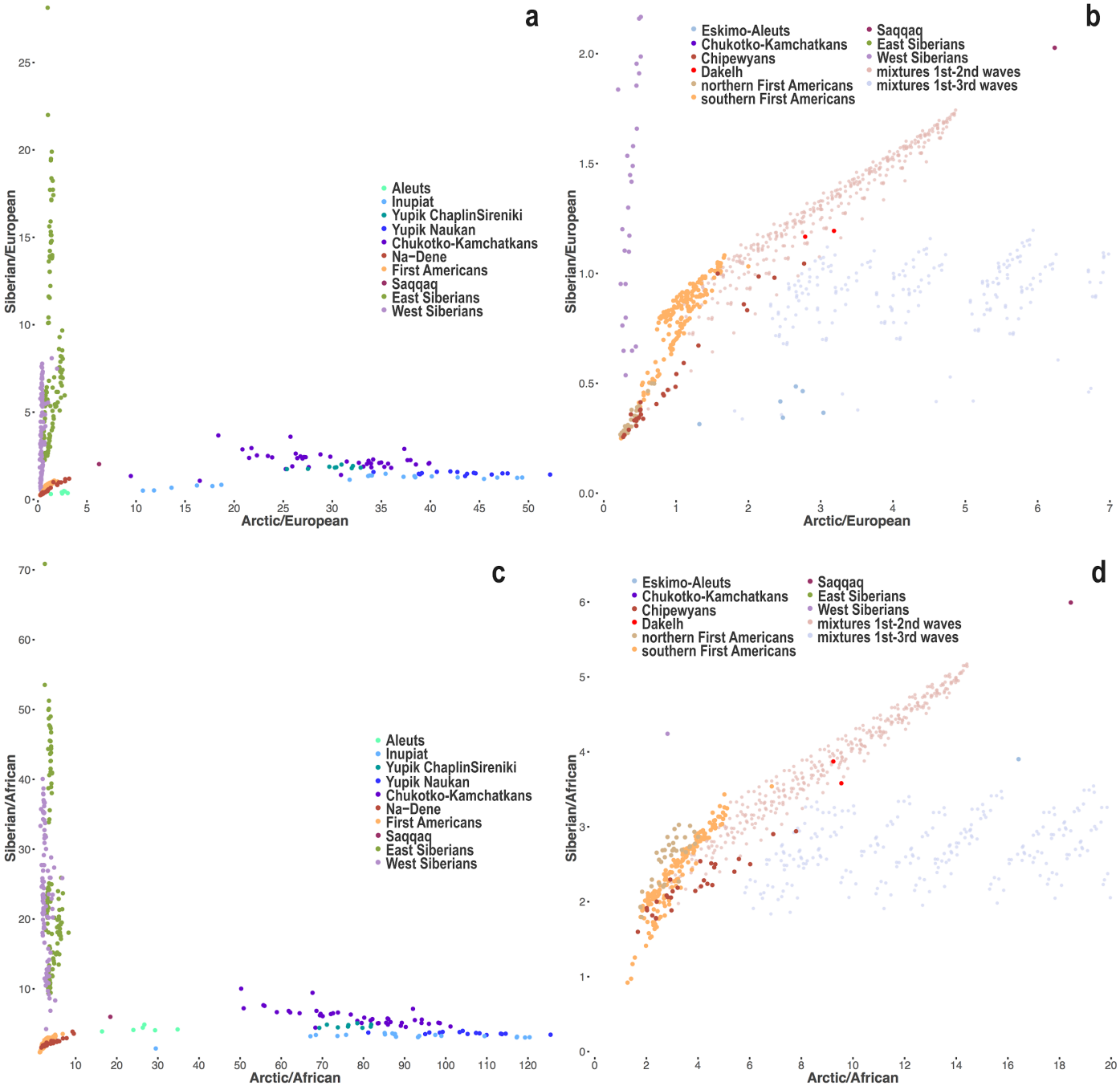

Fig. S6.4. The same results as in Fig. S6.3, but based on the Illumina SNP array dataset. For calculating simulated mixtures, the following Eskimo-Aleut-speaking populations were used: Alaskan Inuit, East or West Greenlandic Inuit. Various Na-Dene-speaking populations are color-coded, and two Athabaskan-speaking Dakelh individuals with shotgun sequencing data, also included into the HumanOrigins and whole genome datasets, are marked with callouts.

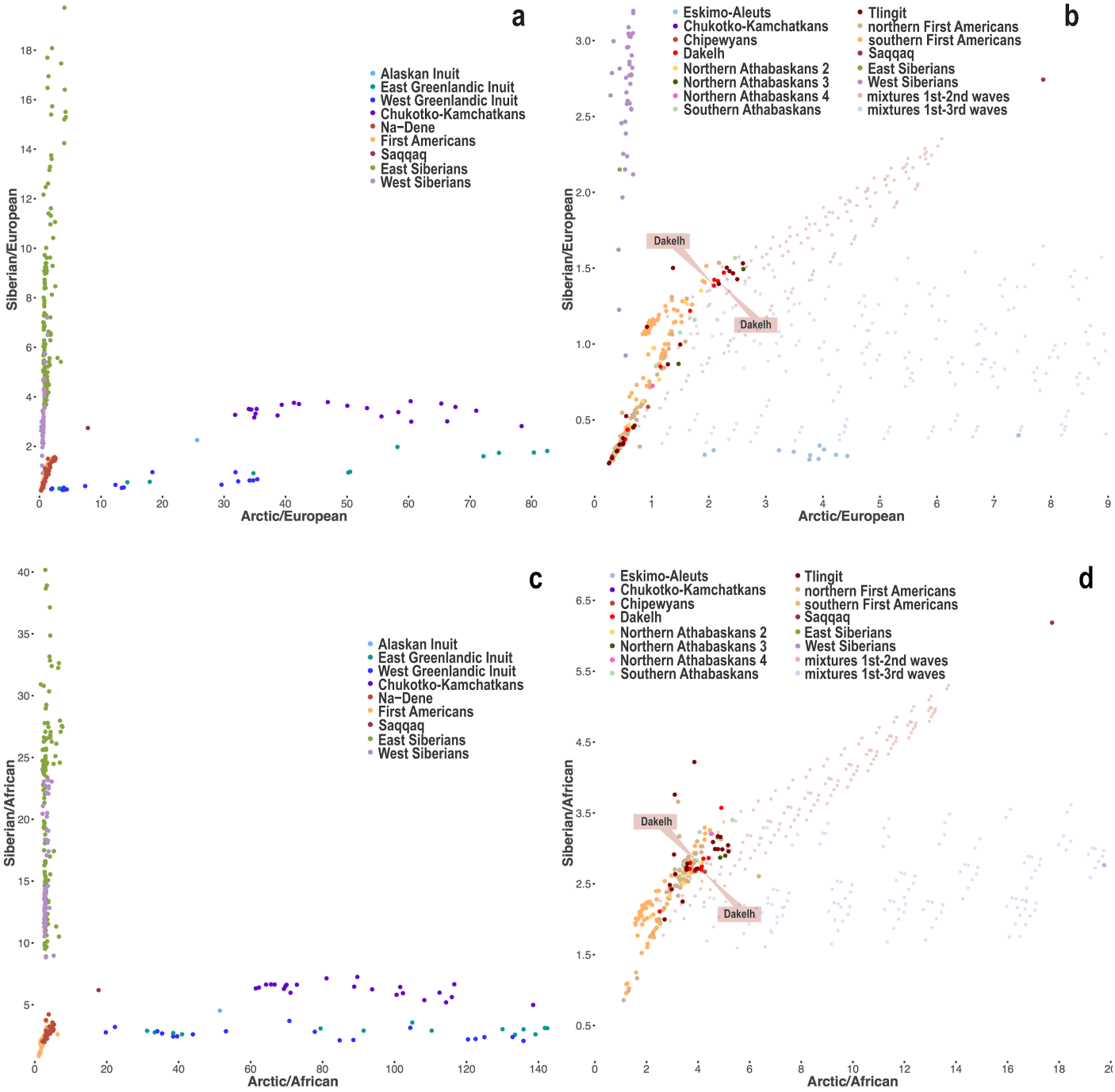

References (for this section)

Flegontov, P. *et al*. Genomic study of the Ket: A Paleo-Eskimo-related ethnic group with significant ancient North Eurasian ancestry. *Sci. Rep*. **6**, 20768 (2016).

Lawson, D. J *et al*. Inference of population structure using dense haplotype data. *PLoS Genet*. **8**, 11–17 (2012).

Raghavan, M. *et al*. The genetic prehistory of the New World Arctic. *Science* **345**, 1255832 (2014).

Raghavan, M. *et al*. Genomic evidence for the Pleistocene and recent population history of Native Americans. *Science* **349**, 1–20 (2015).

Rasmussen, M. *et al*. Ancient human genome sequence of an extinct Palaeo-Eskimo. *Nature* **463**, 757–762 (2010).

Supplementary Information section 7

Admixture inference with *GLOBETROTTER*

To interpret haplotype sharing in a more quantitative way, we analyzed putative admixture events in Na-Dene using *GLOBETROTTER* (Hellenthal et al. 2014). *GLOBETROTTER* operates on coancestry curves, generated from *ChromoPainter v.2* results (Hellenthal et al. 2014), finds the best proxies of admixture partners in a dataset, determines admixture ratios and dates up to two distinct admixture events. To make a complex mixture history of Na-Dene amenable to *GLOBETROTTER* analysis, we pre-selected individuals based on low European admixture and high Saqqaq HSS (selected individuals are marked on two-dimensional HSS plots in Figs. S6.1d and S6.2d). Meta-populations or separate populations were alternatively used as haplotype donors in the *ChromoPainter* v.2 analyses. Substantiating our preliminary conclusions, Saqqaq and First Peoples were determined to be the most likely admixture partners for Na-Dene speakers, with the Saqqaq contribution ranging from 7% to 51%, depending on the dataset and *GLOBETROTTER* set-up. Admixture dates were estimated as follows: 479 – 1,534 ya (95% confidence interval), if meta-populations were used as haplotype donors, and 1,073 – 2,202 ya, if populations were used as haplotype donors (Table S7.1, Fig. S7.1). Although the Paleo-Eskimo admixture in Na-Dene speakers was revealed by *GLOBETROTTER*, in line with other methods used in this study, the admixture dates estimated by *GLOBETROTTER* are much later than those estimated by *Rarecoal* (~4,400 – ~5,000 ya, Table S9.2).

	dataset	HumanOrigins	Illumina	HumanOrigins	HumanOrigins
	haplotype donors	9 meta-populations [a)]	9 meta-populations [a,b)]	67 populations [c)]	67 populations [c,d)]
	target population	Northern Athabaskans (2 Dakelh, 9 Chipewyans) [e)]	2 Tlingit, 8 Northern Athabaskans [e)]	Northern Athabaskans (2 Dakelh, 9 Chipewyans) [e)]	Northern Athabaskans (2 Dakelh, 9 Chipewyans) [e)]
***p*-value for any admixture event**		0	0	0.005	0.005
GLOBETROTTER conclusion		multiple dates	one-date multiway	uncertain	uncertain
coancestry curves	**max. goodness-of-fit** [f)]	0.987	0.503	0.908	0.695
	max. fit improvement for two-date curves [f)]	0.297	0.148	0.276	0.186
two dates, admixture event 1	**inferred date, ya**	144	522	139	67
	95% confidence interval, ya	92 – 178	315 – 898	29 – 249	29 – 153
	source 1	27% NAM	47% NAM	32% Cree (NAM)	36% Ojibwa (NAM)
	source 2	73% SAM	53% NAM	68% Nahua (SAM)	64% Nahua (SAM)
two dates, admixture event 2	**inferred date, ya**	916	522	1,335	1,574
	95% confidence interval, ya	479 – 1,534	N/A	739 – 3,487	1,073 – 2,202
	source 1	28% Saqqaq	7% Saqqaq	39% Iñupiat (E-A)	51% Saqqaq
	source 2	72% SAM	93% NAM	61% Cree (NAM)	49% Cree (NAM)

Table S7.1. The table shows fit statistics for *GLOBETROTTER* coancestry curves, as well as inferred mixture partners, mixture proportions, dates and their 95% confidence intervals. The following abbreviations are used for meta-populations: Eskimo-Aleut speakers, E-A; Northern First Peoples, NAM; Southern First Peoples, SAM.

[a)] The following non-overlapping meta-populations were used: 1/ the Saqqaq ancient genome and 2/ related

Chukotko-Kamchatkan-speaking groups (abbreviated as C-K); 3/ Eskimo-Aleut speakers (Aleuts, Inuit, Iñupiat, Yup'ik, abbreviated as E-A); 4/ Northern First Peoples (NAM); 5/ Southern First Peoples (SAM); 6/ West Siberians (WSIB); 7/ East Siberians (ESIB); 8/ Southeast Asians (SEA); 9/ Europeans (EUR).

[b)] Individuals with >15% West Eurasian admixture components (Extended Data Fig. 8) were removed from the NAM meta-population.

[c)] Individuals with >15% West Eurasian admixture components (Extended Data Fig. 8) were removed from NAM populations, and the remaining NAM individuals were merged into one population.

[d)] Standardizing by a "null" individual was performed to test for consistency, as recommended by the *GLOBETROTTER* manual. This setting might be appropriate if the target population has undergone a bottleneck.

[e)] To make admixture history of the target population less complex and amenable to *GLOBETROTTER* analysis, only Na-Dene-speaking individuals with prior evidence of elevated Paleo-Eskimo ancestry (Figs. S6.1d, S6.2d) and with <10% West Eurasian ancestry estimated with *ADMIXTURE* (Extended Data Fig. 8) were used.

[f)] A maximal fit value across all curves is shown: two-date curves were considered if the overall conclusion was "multiple dates", and one-date curves were considered in other cases. Most relevant coancestry curves illustrating the inferred admixture events are shown in Fig. S7.1.

Fig. S7.1. Coancestry curves: relative probability of jointly copying two genomic chunks from a pair of donors (y-axis) vs. genetic distance between the chunks in cM (x-axis). Several representative curves are shown for each model: those with the best fit and those involving admixture partners inferred with *GLOBETROTTER* or their closest proxies. Only curves reflecting the older Paleo-Eskimo/First Peoples admixture event are shown. Here is a list of *GLOBETROTTER* set-ups we explored: Northern Athabaskan speakers with meta-populations (**a**) or populations (**c**) as haplotype donors (the HumanOrigins dataset); Na-Dene speakers with meta-populations as haplotype donors (the Illumina dataset) (**b**). Results under an alternative setting (normalization by a 'null individual') are also shown for populations as haplotype donors (**d**). Original data are shown in black, and curves approximating two admixture events with different dates – in red, two events with a single date – in green, and one event – in blue. Composition of target Na-Dene populations is given in Table S7.1, and Figs. S6.1d, S6.2d. The following meta-populations were used as haplotype donors: 1/ Saqqaq, 2/ related Chukotko-Kamchatkan speakers (abbreviated as C-K); 3/ Eskimo-Aleut speakers (E-A); 4/ Northern First Peoples (NAM); 5/ Southern First Peoples (SAM); 6/ West Siberians (WSIB); 7/ East Siberians (ESIB), 8/ Southeast Asians (SEA); 9/ Europeans (EUR).

A

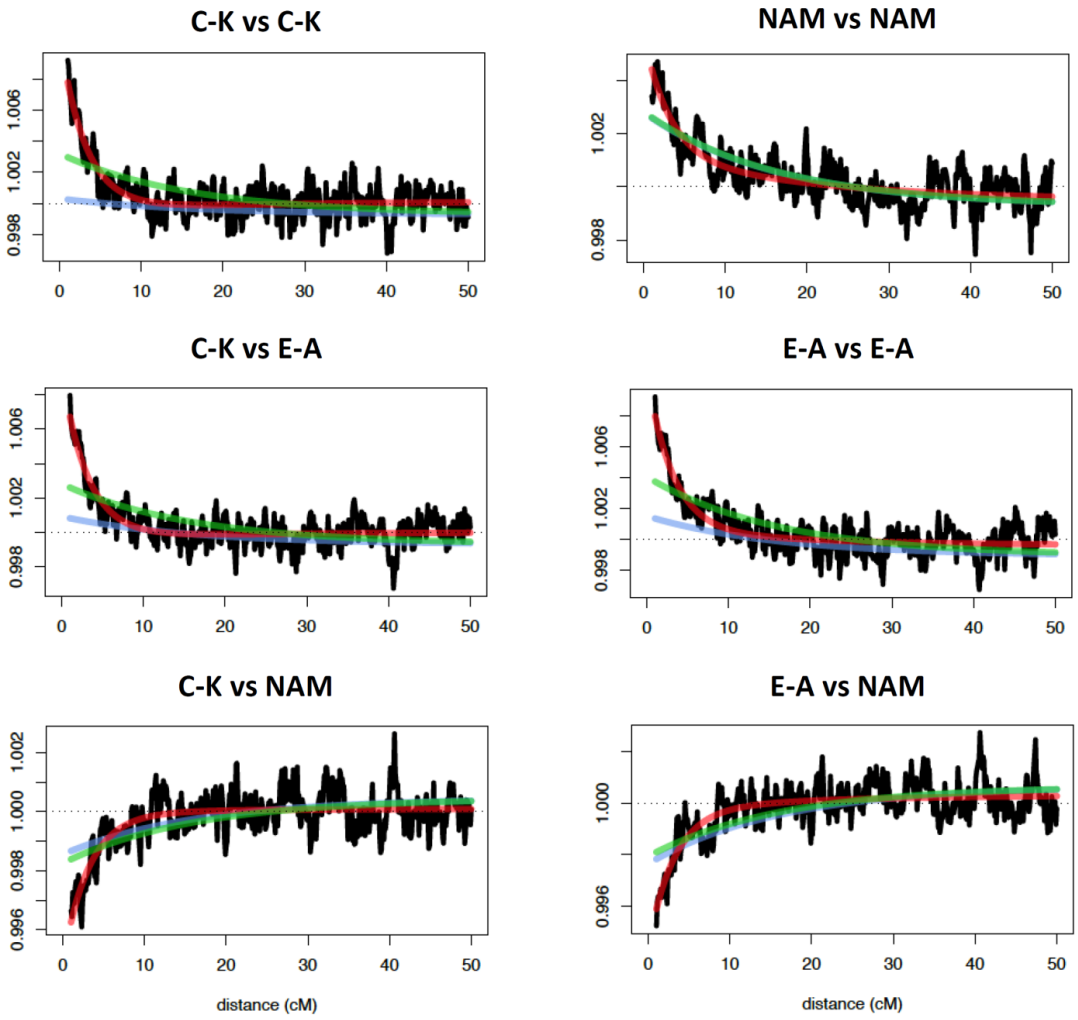
C-K vs C-K
NAM vs NAM
C-K vs E-A
E-A vs E-A
C-K vs NAM
E-A vs NAM
distance (cM)
distance (cM)

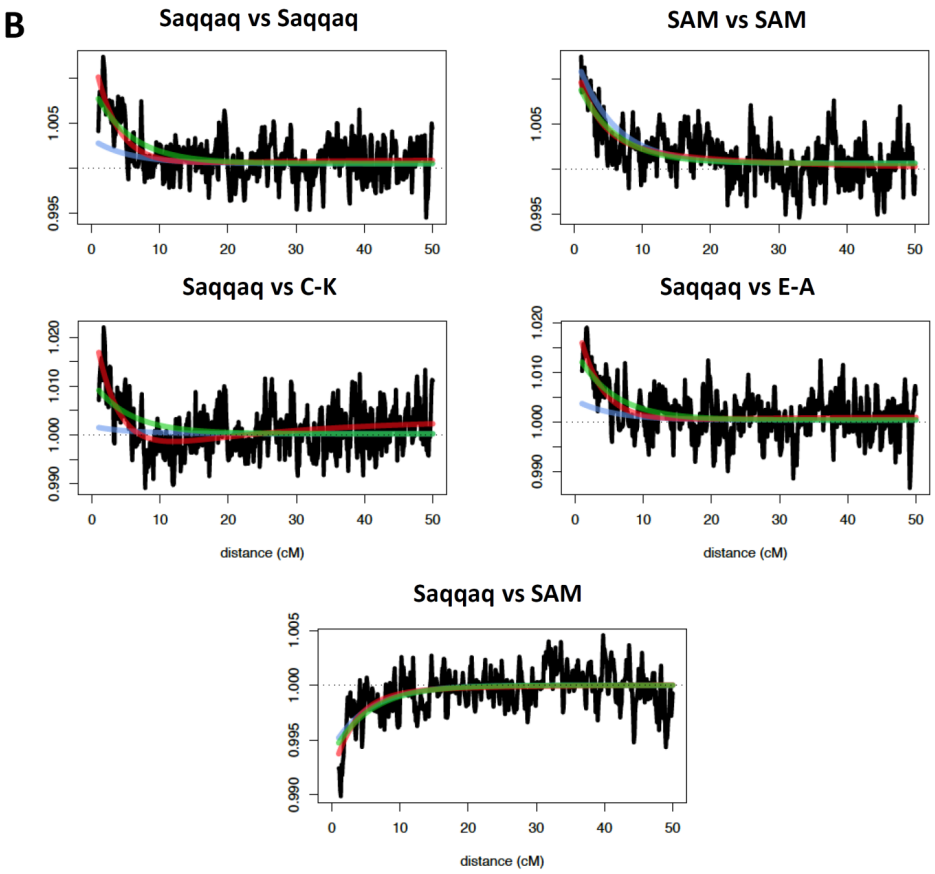
B
Saqqaq vs Saqqaq
SAM vs SAM
Saqqaq vs C-K
Saqqaq vs E-A
Saqqaq vs SAM
distance (cM)

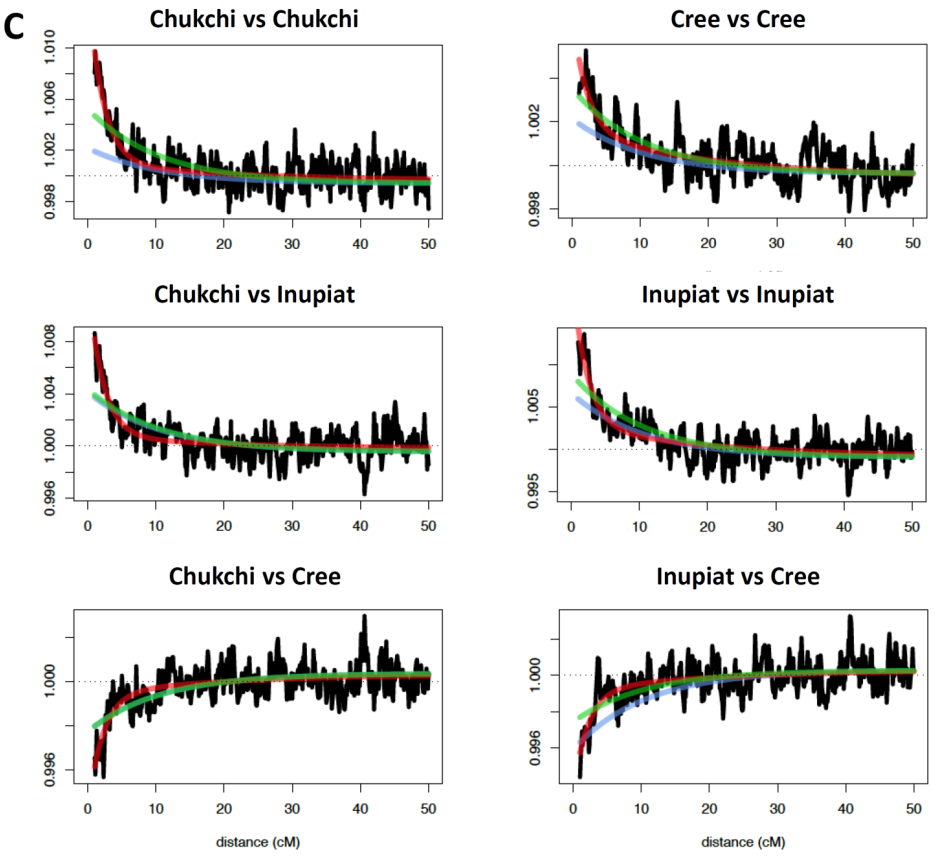
C
Chukchi vs Chukchi
Cree vs Cree
Chukchi vs Inupiat
Inupiat vs Inupiat
Chukchi vs Cree
Inupiat vs Cree
distance (cM)

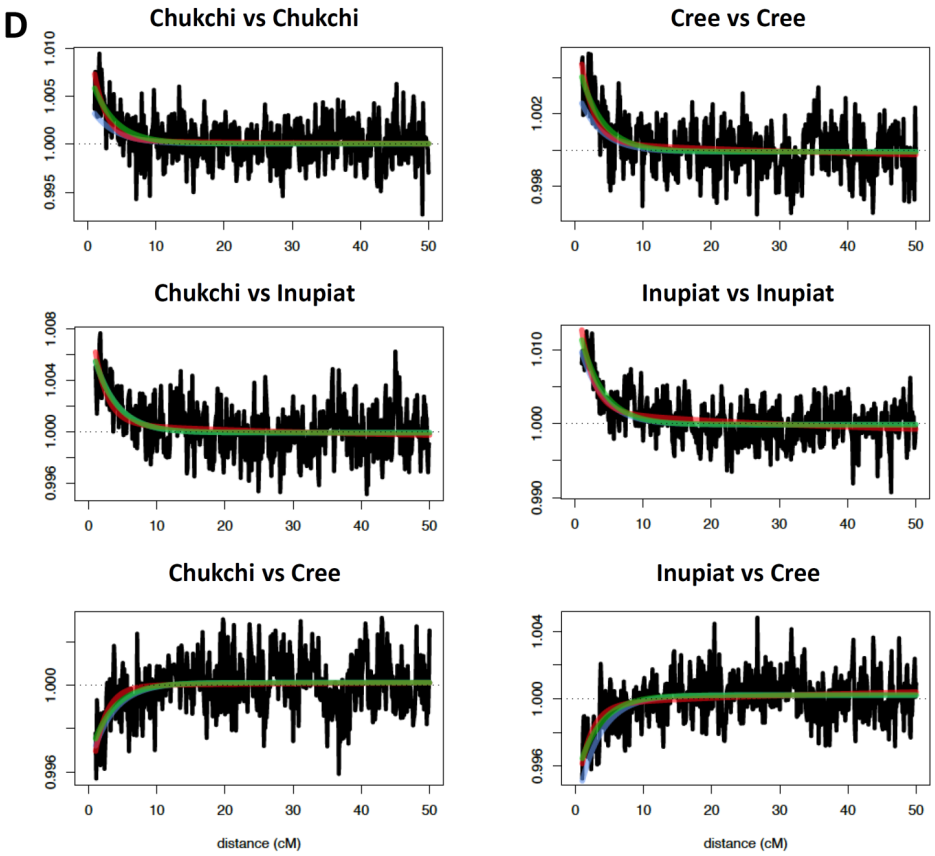

References (for this section)

Hellenthal, G. *et al*. A genetic atlas of human admixture. *Science* **343**, 747–751 (2014).

Supplementary Information section 8

Rare allele sharing statistics

To explore PPE ancestry in American and Beringian populations in a model-free way, we used rare allele sharing statistics. For this analysis, we used all segregating sites in the Simons Genome Diversity panel (Mallick et al. 2016) as well as in the present-day data from Raghavan et al. (2015), restricting to those sites at which at least 90% of individuals in both datasets independently have non-missing data. We also filtered out sites based on genome mappability, as defined in the PSMC pipeline (Li and Durbin 2011). This resulted in a dataset of 14,740,572 segregating sites in the combined dataset. The population composition of the dataset is summarized in Table S8.1.

Abb.	Full Name	Populations[1)]	Nr of samples
AFR	Africans	Bantu Herero, Bantu Kenya, Bantu Tswana, Biaka, Dinka, Esan, Gambian, Ju|'hoan North, Khomani San, Luhya, Luo, Mandenka, Masai, Mbuti, Mende, Somali, Yoruba	39
EUR	Europeans	Basque, Bergamo, Bulgarian, Crete, Czech, English, Estonian, French, Greek, Hungarian, Norwegian, Orcadian, Polish, Sardinian, Spanish, Tuscan	33
SEA	Southeast Asians	Ami, Atayal, Burmese, Cambodian, Dai, Kinh, Lahu, Miao, She, Thai	21
SIB	Core Siberians	Nivkh, Altaian, Buryat, Even, Ket, Mansi, Tubalar, Ulchi, Yakut	22
C-K	Chukotko-Kamchatkan speakers	Itelmen, Koryak, Chukchi	4
P-E	Paleo-Eskimo	Saqqaq	1
ALE	ancient Aleut	ancient Aleut	1
ESK	Eskimo speakers	Yup'ik from Chukotka, East and West Greenlandic Inuit	9
ATH	Northern Athabaskan speakers	Dakelh, Chipewyan, ancient Athabaskan	5
SAM	Southern First Peoples	Aymara, Chane, Huichol, Karitiana, Mayan, Mixe, Mixtec, Piapoco, Pima, Quechua, Surui, Yukpa, Zapotec	29
Total			**164**

Table S8.1: A table listing all modern samples and groups used in the rare allele sharing analysis. Data is from the two sources: Raghavan et al. (2015) and the Simons Genome Diversity Project data set (Mallick et al. 2016), as indicated in Supplementary Table 4.

We then sampled pseudo-haploid genotypes on three ancient shotgun genomes (Saqqaq, I0719 called “Ancient Aleut” and I5319 called “Ancient Athabaskan”), the latter two of which are described in this study for the first time. Here, we used a pseudo-haploid calling method and i) required a minimum of 3 reads at each site, ii) restricted to biallelic sites, iii) called the allele that was supported by the majority of reads at that site. Since this method is subtly dependent on coverage (high-coverage positions will have a stronger reference bias than low-coverage positions), we first downsampled all query positions to the required minimum coverage of 3, respectively.

To quantify rare allele sharing, we developed the rare allele sharing statistics (RASS). Essentially, RASS is similar to an outgroup-f_3-statistic, but ascertained on rare derived alleles in a set of reference populations. Specifically, we define

$$RASS(x, y;\ \{\text{References, Outgroup}\}) = \frac{1}{L}\sum_i x_i\, y_i$$

where the sum runs over all sites with derived allele count below some cutoff (say 5 or less)

within the *Reference* and *Outgroup* populations, x_i is the derived allele frequency in the test individual, y_i is the derived allele frequency in the reference population, and L is the number of sites in the sum (excluding missing data). Here, the *Outgroup* (Africans) is used to polarize derived vs. ancestral alleles – that is, we look at the outgroup population, and take the majority allele in that outgroup population to specify which should be the majority allele for the ascertainment. If the majority of outgroup chromosomes have the non-reference allele, then the ascertainment is done on the reference allele being rare (instead of the non-reference allele).

The following outgroup and reference meta-populations were used (Table S8.1): Africans (39 ind.), Europeans (33 ind.), Southeast Asians (21 ind.), Siberians (22 ind.), Chukotko-Kamchatkan (C-K) speakers (4 ind. including one Chukchi ind.). Importantly, the ascertainment on allele frequency is done only within the reference and outgroup populations, not within the test individuals. Here, reference populations included non-American populations only, while test populations included American populations and Chukotkan Yup'ik, closely related to American Inuit. Because of this ascertainment rule, RASS between test individuals and reference populations is not affected by genetic drift within the test individuals since putative admixture events, and we can therefore formally test for admixture models within the test samples based on RASS (see below). For present-day and ancient First Peoples, Athabaskan speakers, Paleo-Eskimos (P-E), and Eskimo-Aleut (E-A) speakers we estimated RASS vs. Siberian and C-K reference meta-populations. Since among C-K groups Chukchi demonstrate the highest level of E-A admixture (Fig. 1a, Extended Data Figs. 2 and 8, sections 5, 10), for some analyses we excluded the Chukchi individual.

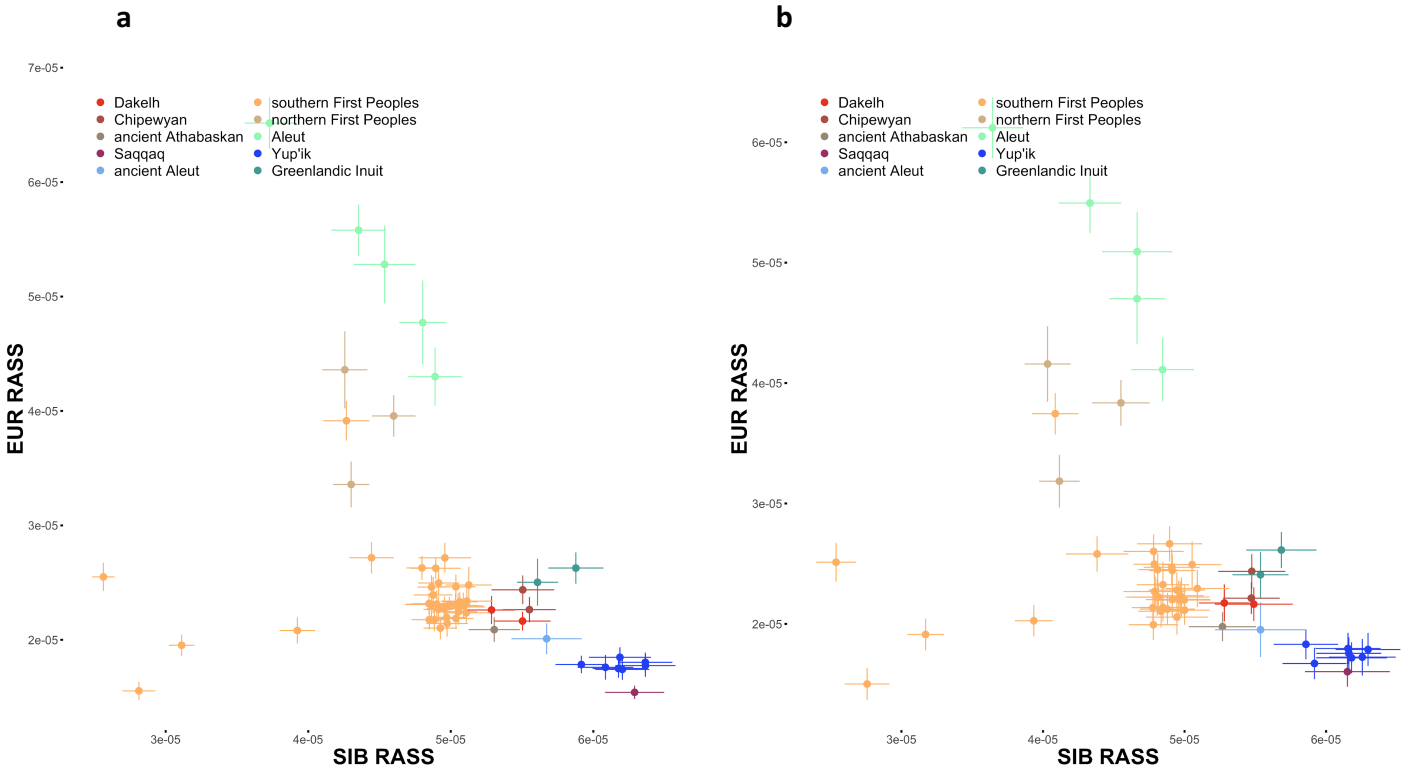

Fig. S8.1. Two-dimensional plots of European (EUR) and Siberian (SIB) rare allele sharing statistics (RASS). Rare alleles occurring from 2 to 10 times in the reference set of 238 haploid genomes (0.8-4.2% frequency) contributed to the statistics; the full (**a**) and transversion-only (**b**) datasets were used. The sample size for this analysis equals 238 + 2 haploid genomes in a target individual since individuals were analyzed separately. Standard deviations were calculated using a jackknife approach with chromosomes used as resampling blocks. Single standard error intervals and means are plotted. Populations and meta-populations are color-coded according to the legend.

We first removed all test individuals with substantial European admixture. To this end, we looked at RASS with SIB vs. EUR (see Fig. S8.1) and identified individuals with higher than expected EUR RASS, as compared to the bulk of Native American individuals. After inspection of Fig. S8.1, we used $>3\times10^{-5}$ as the RASS cutoff to mark individuals as admixed. In addition, we removed Native American individuals that were outliers according to the SIB RASS as they might have a low degree of African admixture (we used $<4.5\times10^{-5}$ as the cutoff to mark individuals as admixed). Since the African meta-population was used as an outgroup for RASS calculation, we could not measure African RASS directly.

We then investigated RASS with C-K vs. RASS with SIB for the transversion-only dataset, as shown in Fig. S8.2. First, we observe that all Athabaskans (four present-day and one ancient individual), are shifted away from the cluster of First Peoples, towards the ancient Saqqaq individual. To explicitly test admixture scenarios, we simulated admixture points of 5%, 10%,...,75% Saqqaq admixture in Native Americans. The simulated points are simply linear combinations of the positions on the plot of various First Peoples individuals and Saqqaq. Importantly, RASS of Athabaskans matches admixture points between 29% and 38%. The ancient Athabaskan is consistent with a slightly higher level of Saqqaq admixture of 42%, in agreement with other analyses (Fig. 1, Extended Data Figs. 2-4). Both C-K and Siberian RASS for the ancient Aleut individual I0719 sequenced by the shotgun approach (2.3x average coverage, Extended Data Table 1) are also perfectly consistent with a First Peoples/Paleo-Eskimo admixture (~65% Saqqaq admixture). In contrast, Inuit and especially Yup'ik individuals are shifted to the right on the x-axis, i.e. they demonstrate elevated C-K RASS not expected under the simple First Peoples/Paleo-Eskimo admixture scenario.

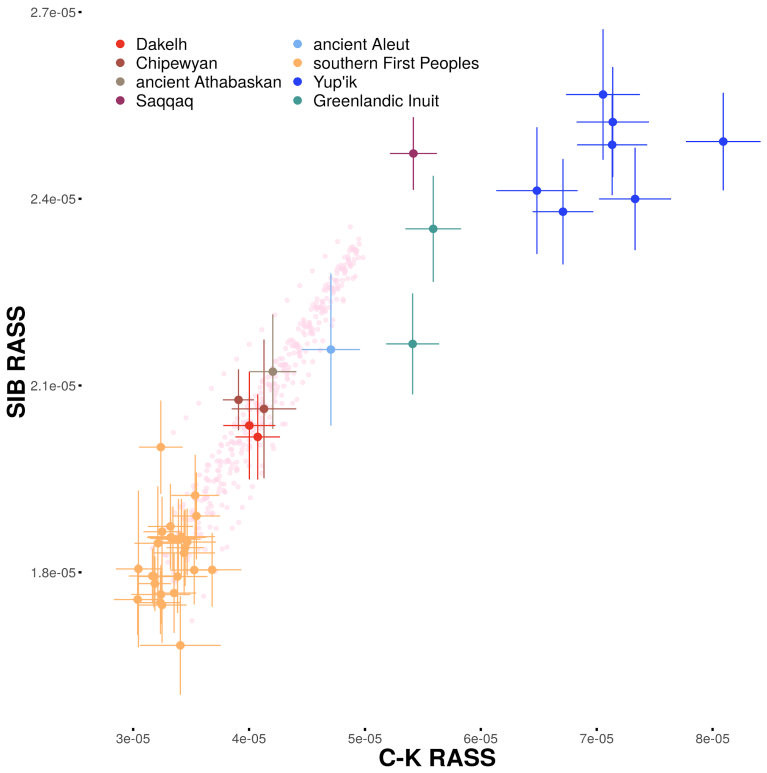

Fig. S8.2. Two-dimensional plot of Chukotko-Kamchatkan (C-K) and Siberian (SIB) rare allele sharing statistics (RASS). Rare alleles occurring from 2 to 5 times in the reference set of 238 haploid genomes (0.8-2.1% frequency) contributed to the statistics; the Chukchi individual was dropped from the C-K group, and the transversion-only dataset was used. The sample size for this analysis equals 238 + 2 haploid genomes in a target individual since individuals were analyzed separately. Standard deviations were calculated using a jackknife approach with chromosomes used as resampling blocks. Single standard error intervals and means are plotted. Populations and meta-populations are color-coded according to the legend. RASS for simulated mixtures of any present-day southern Native American individual and the Saqqaq individual (from 5% to 75% Saqqaq ancestry, with 5% increments) are plotted as semi-transparent pink circles.

E-A admixture found in all C-K populations (section 10), but especially high in Chukchi (Fig. 1a, Extended Data Figs. 2 and 8, section 5), influences RASS for the ancient Aleut individual. This effect is observed when the Chukchi individual is included into the C-K reference group (Fig. S8.3b,c), especially in the case of the 2 to 5 allele count range (Figs. S8.2 and S8.3c). The fact that E-A admixture in C-K influences results strongly when only the rarest alleles are considered is not surprising since the bidirectional E-A/C-K admixture has been

dated to 1,700-2,300 ya using *Rarecoal* (Table. S9.2), and it is expected to post-date the emergence of the first Neo-Eskimo archaeological culture on the Chukotkan side of Bering Strait ca. 2200 calBP (see the Discussion). In contrast, the P-E admixture events in E-A and Na-Dene have both been dated to roughly 4,400-4,900 ya using *Rarecoal* (Table S9.2) and to 2,700-4,900 ya using the *ALDER* method (Table S12.1). Therefore, the signal of the most recent event becomes stronger when the rarest alleles (reflecting recent mutations in most cases) are considered.

The C-K reference group can be replaced by the Saqqaq individual (SNP genotypes called as described above), see Fig. S8.4. This approach does not allow analysis of low-coverage ancient samples, but the signal of P-E admixture in Na-Dene speakers remains.

Using the same genomic dataset, we also calculated outgroup f_3-statistics:

$$f_3(x, y;\ O) = \frac{1}{L}\sum_i (o - x_i)(o - y_i)$$

where x_i is the allele frequency in the test population, y_i is the allele frequency in the reference population, and o_i is the allele frequency in the outgroup (the African meta-population). Again, L is the number of sites in the sum. This statistic takes into account all sites, not only rare ones. It is clear that the resolution provided by C-K, Saqqaq and Siberian RASS is much higher than that of outgroup statistics f_3(Africans; C-K, an American/E-A/P-E individual), f_3(Africans; Saqqaq, an American/E-A/P-E individual), and f_3(Africans; Siberians, an American/E-A/P-E individual) (Fig. S8.5). Chipewyans and Dakelh are not distinguishable from First Peoples using outgroup f_3-statistics, but are distinguishable using RASS.

RASS and outgroup f_3-statistics are correlated, especially if the rare allele count range from 2 to 10 is used (Fig. S8.6).

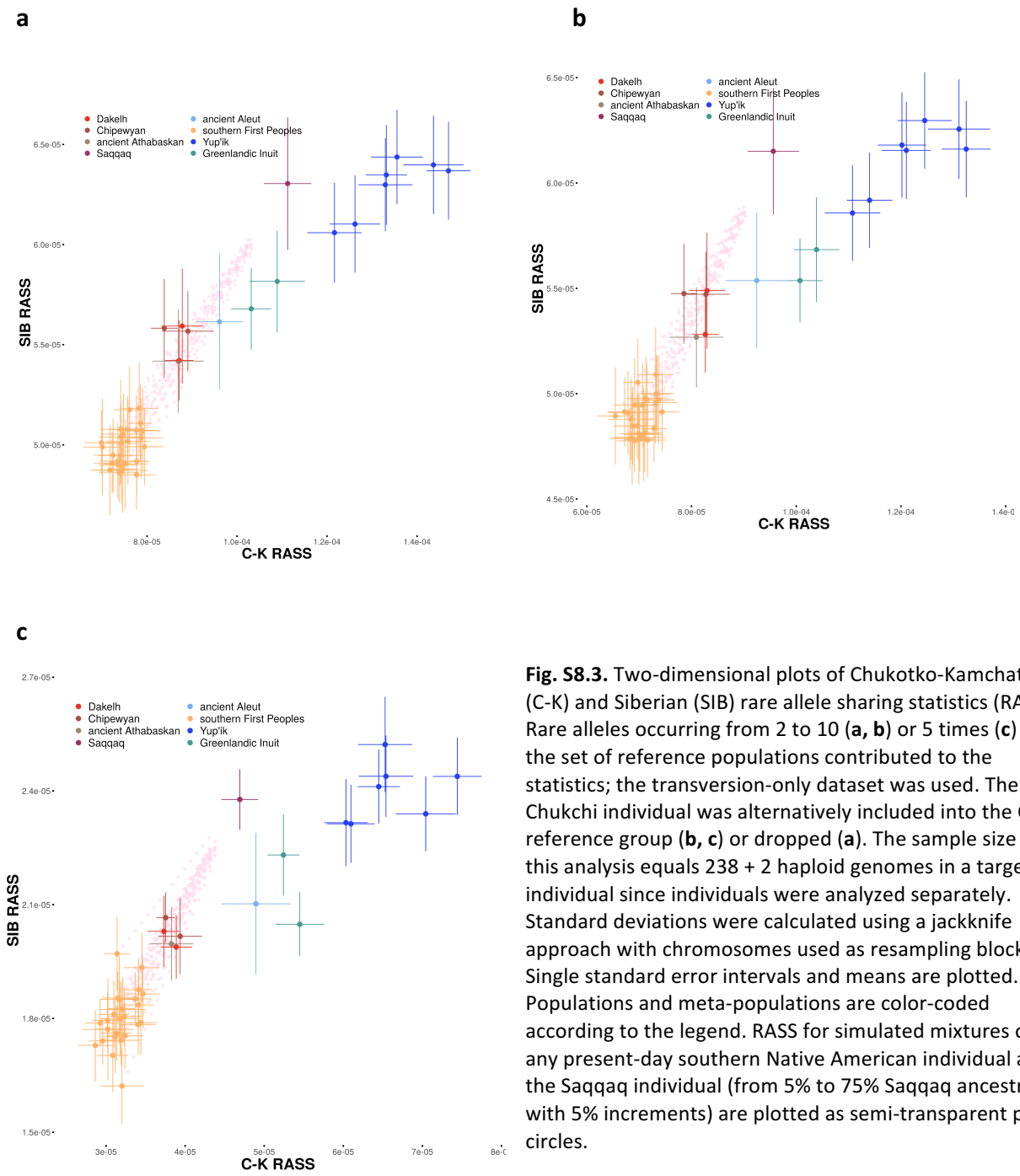

Fig. S8.3. Two-dimensional plots of Chukotko-Kamchatkan (C-K) and Siberian (SIB) rare allele sharing statistics (RASS). Rare alleles occurring from 2 to 10 (**a, b**) or 5 times (**c**) in the set of reference populations contributed to the statistics; the transversion-only dataset was used. The Chukchi individual was alternatively included into the C-K reference group (**b, c**) or dropped (**a**). The sample size for this analysis equals 238 + 2 haploid genomes in a target individual since individuals were analyzed separately. Standard deviations were calculated using a jackknife approach with chromosomes used as resampling blocks. Single standard error intervals and means are plotted. Populations and meta-populations are color-coded according to the legend. RASS for simulated mixtures of any present-day southern Native American individual and the Saqqaq individual (from 5% to 75% Saqqaq ancestry, with 5% increments) are plotted as semi-transparent pink circles.

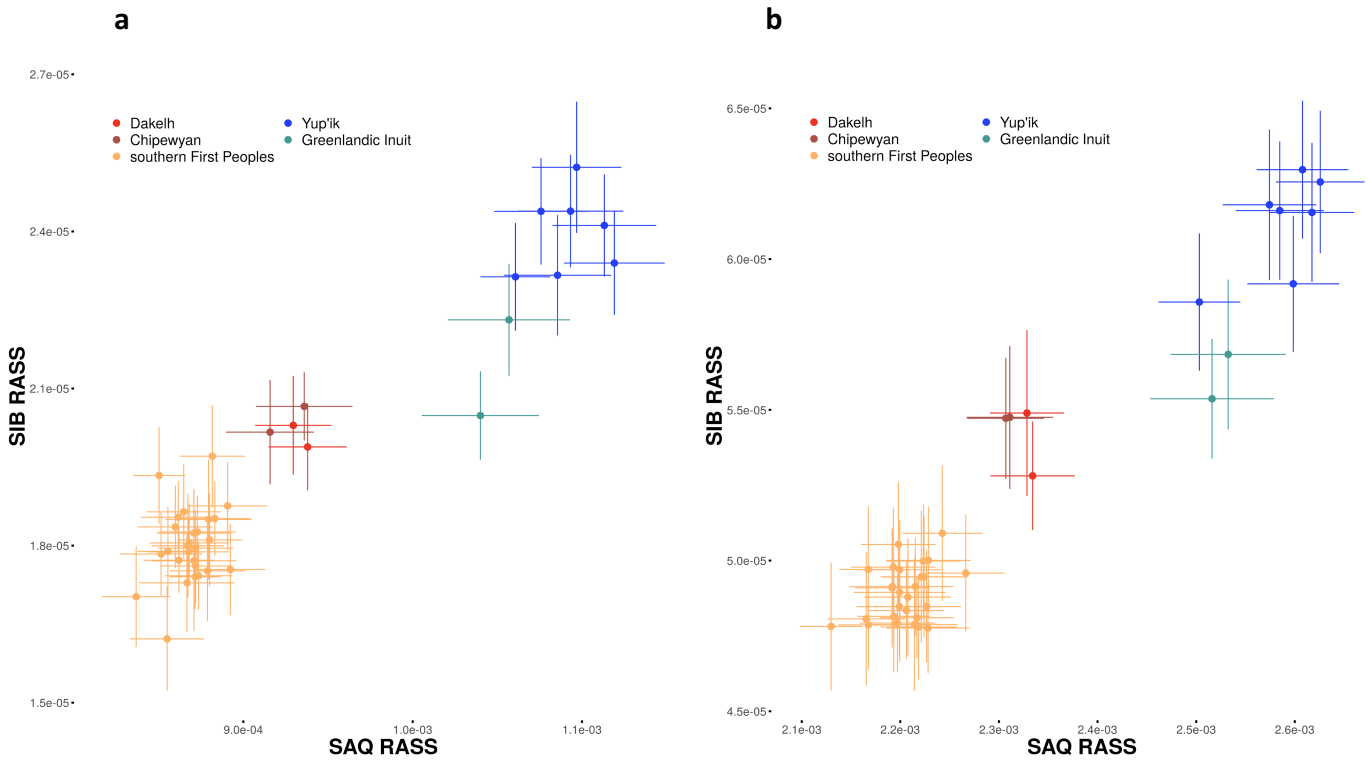

Fig. S8.4. Two-dimensional plots of Saqqaq (SAQ) and Siberian (SIB) rare allele sharing statistics (RASS). Rare alleles occurring from 2 to 5 (**a**) or 10 times (**b**) in the set of reference populations contributed to the statistics; the transversion-only dataset was used. The sample size for this analysis equals 238 + 2 haploid genomes in a target individual since individuals were analyzed separately. Standard deviations were calculated using a jackknife approach with chromosomes used as resampling blocks. Single standard error intervals and means are plotted. Populations and meta-populations are color-coded according to the legend.

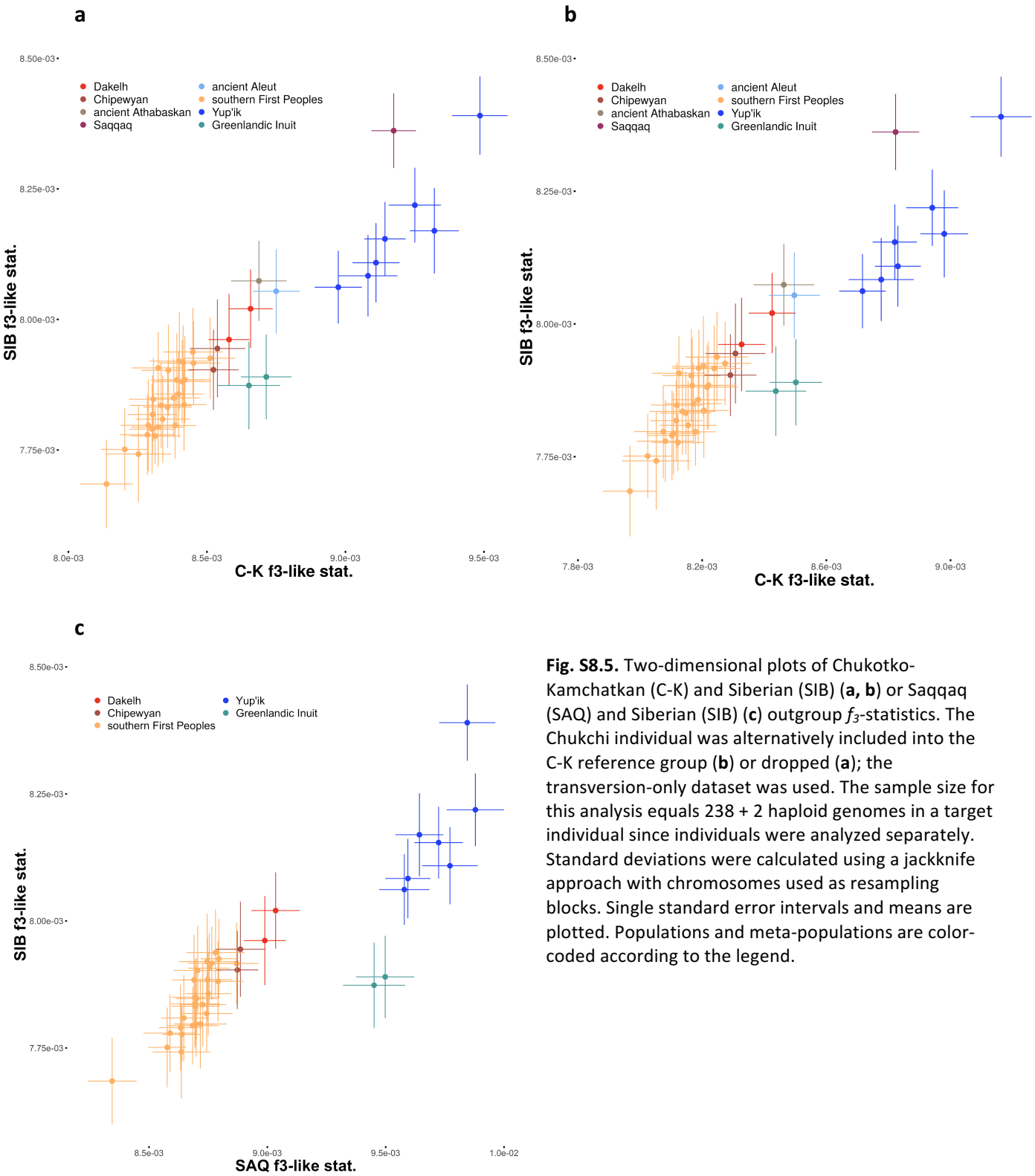

Fig. S8.5. Two-dimensional plots of Chukotko-Kamchatkan (C-K) and Siberian (SIB) (**a, b**) or Saqqaq (SAQ) and Siberian (SIB) (**c**) outgroup f_3-statistics. The Chukchi individual was alternatively included into the C-K reference group (**b**) or dropped (**a**); the transversion-only dataset was used. The sample size for this analysis equals 238 + 2 haploid genomes in a target individual since individuals were analyzed separately. Standard deviations were calculated using a jackknife approach with chromosomes used as resampling blocks. Single standard error intervals and means are plotted. Populations and meta-populations are color-coded according to the legend.

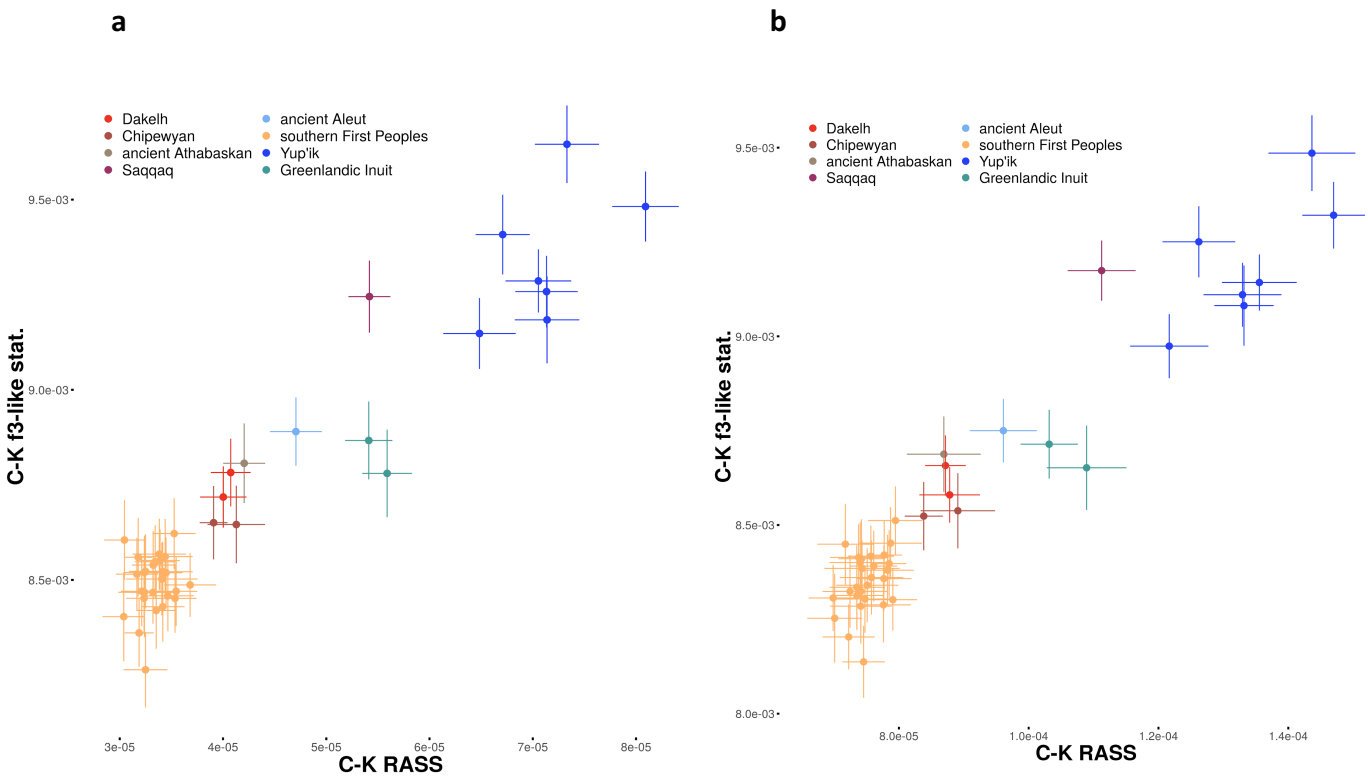

Fig. S8.6. Two-dimensional plots of Chukotko-Kamchatkan (C-K) rare allele sharing statistics vs. outgroup f_3-statistics. Rare alleles occurring from 2 to 5 (**a**) or 10 times (**b**) in the set of reference populations contributed to RASS; the transversion-only dataset was used. The Chukchi individual was not included into the C-K reference group. The sample size for this analysis equals 238 + 2 haploid genomes in a target individual since individuals were analyzed separately. Standard deviations were calculated using a jackknife approach with chromosomes used as resampling blocks. Single standard error intervals and means are plotted. Populations and meta-populations are color-coded according to the legend.

References (for this section)

Li, H. & Durbin, R. Inference of human population history from individual whole-genome sequences. *Nature* **475**, 493–496 (2011).

Mallick, S. *et al*. The Simons Genome Diversity Project: 300 genomes from 142 diverse populations. *Nature* **538**, 201–206 (2016).

Raghavan, M. *et al*. Genomic evidence for the Pleistocene and recent population history of Native Americans. *Science* **349**, 1–20 (2015).

Supplementary Information section 9

Demographic modeling with *Rarecoal*

Rarecoal

Rarecoal is a software that implements a fast algorithm to estimate the joint site frequency spectrum for rare alleles (Schiffels et al. 2016). Since the initial report in Schiffels et al. 2016, we have improved the software substantially: We have added pulse-like admixture events to be able to model admixture graphs, and we have significantly optimized crucial parts of the program. The updated mathematical derivations of the model are included as a PDF document in the repository: https://github.com/stschiff/rarecoal. We also built in a regularization for population size changes, which penalizes large changes of the population size and helps to avoid overfitting.

Data

In the following analysis, we will use the abbreviations for meta-populations shown in Table S9.1.

Abb.	Full Name	Populations	Nr of samples
EUR	Europeans	Basque, Bergamo, Bulgarian, Crete, Czech, English, Estonian, French, Greek, Hungarian, Norwegian, Orcadian, Polish, Sardinian, Spanish, Tuscan	33
SEA	Southeast Asians	Ami, Atayal, Burmese, Cambodian, Dai, Kinh, Lahu, Miao, She, Thai	21
SIB	Core Siberians	Nivkh, Altaian, Buryat, Even, Ket, Mansi, Tubalar, Ulchi, Yakut	22
C-K	Chukotko-Kamchatkan speakers	Itelmen, Koryak	3
ALE	Aleuts	Aleut	5
ESK	Eskimo speakers	Yup'ik from Chukotka, East and West Greenlandic Inuit	9
ATH	Northern Athabaskan speakers	Dakelh, Chipewyan	4
NAM	Northern First Peoples	Cree, Tsimshian	3
SAM	Southern First Peoples	Aymara, Mixe, Mixtec, Piapoco, Quechua, Yukpa, Zapotec	14
Total			**114**

Table S9.1: A table listing all modern samples and groups used in the *Rarecoal* analysis. Data is from the two sources: Raghavan et al. (2015) and the Simons Genome Diversity Project data set (Mallick et al. 2016), as indicated in Supplementary Table 4.

In the following model fits, we use “rarecoal maxl” to obtain maximum likelihood fits. For our final models, we also use “rarecoal mcmc” to obtain credibility intervals for parameters. We fit rare allele sharing histograms with maximum allele count of 4 in all modeled populations (corresponding to a maximum allele frequency of 1.7% in the full data set). This corresponds to 66% of all mutations in the full data set, i.e. much higher than the allele frequency due to the strong skew of the allele frequency spectrum towards rare alleles.

In order to check model fits, we use the Rare Allele Sharing statistics (RASS) as defined in the Methods section. RASS between two populations X and Y is defined as

$$RASS(X,Y) = \frac{1}{L}\sum_i x_i y_i,$$

where x_i and y_i are the derived allele frequencies in populations X and Y, respectively. The sum runs over all sites with total allele count less than or equal to 4 in the entire dataset considered in the fit, and L is the number of those sites. Note that RASS can be computed also with X=Y, in which case it describes rare allele sharing between individuals from the same population. In addition, we also consider the rate of singletons per population as a statistic to compare fits with data (see panels c in figures below).

Fitting a simple split model for Europeans and Southeast Asians

We started with only two populations, Europeans (EUR) and Southeast Asians (SEA), and fitted a simple model with 4 parameters (a single split time, two population sizes in the two extant branches, and one population size in the ancestral branch). The result yields – unsurprisingly – a very good fit with a split time of around 45,000 years ago (ya) (Fig. S9.1).

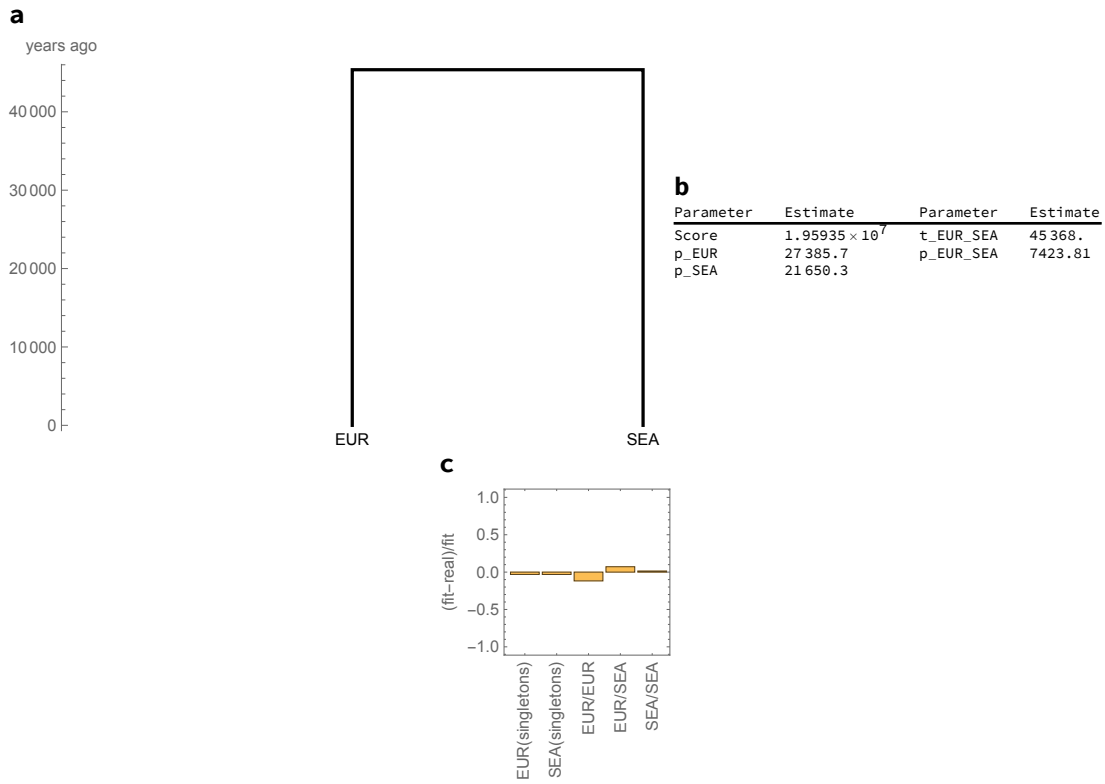

Fig. S9.1. A model connecting Europeans (EUR) and Southeast Asians (SEA). A schematic indicating the tree (**a**), the parameters (**b**) and the fit deviation between the model and the data (**c**).

As shown in Fig. S9.1, we summarize models using a schematic (a), a table with the parameters (b), and the relative deviation between the model and the data in terms of rare allele sharing statistics (RASS, see above and the Methods). Here, the statistics EUR(singletons) and SEA(singletons) indicate simply the deviation of the fit in terms of frequency of singletons in both populations. EUR/EUR and SEA/SEA indicate deviations between the data and the model for mutations shared within each group, and EUR/SEA indicates the fit deviation for allele sharing across groups.

Parameter names (Fig. S9.1b) starting with "p" denote population sizes, and those starting with "t" denote split times. By "Score" we denote the negative log-likelihood: the lower this number, the better the fit. The inferred population sizes and split times are scaled to real time and size using a mutation rate of 1.25×10^{-8} (Scally and Durbin 2012) and a generation time of 29 years (Fenner 2005, Scally and Durbin 2012).

Adding Native Americans

We next added Southern First Peoples (SAM) onto the tree. From our *qpGraph* analysis (see section 10), we know that First Peoples inherit a separate Eurasian lineage, which from previous publications is known as *Ancient North Eurasian* (ANE) (Patterson et al. 2012, Raghavan et al. 2014a). We model this lineage as a "ghost" population that split off from the EUR branch. The inferred model fits well (Fig. S9.2), although the inferred ANE contribution to Native Americans (here 8%) is far below the estimates in our *qpGraph* models, which are around 40% (Fig. S10.5). We believe this may be due to the lack of the Late Pleistocene Native American bottleneck, which we will add further below when adding other Native American populations. The EUR/ANE split time at 13.6 kya is also unrealistically late. Most likely this effect is observed because instead of ancient genomes we used high-coverage genomes of present-day Europeans having substantial ANE-related admixture (Haak et al. 2015).

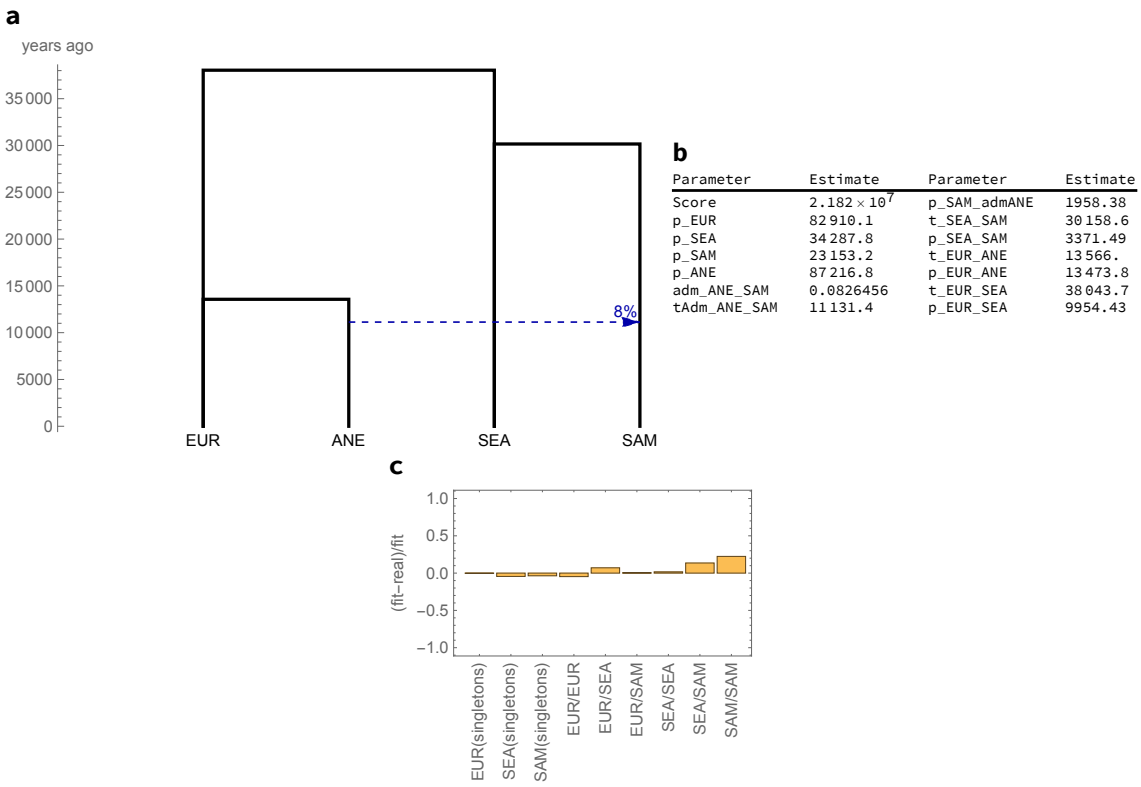

Parameter	Estimate	Parameter	Estimate
Score	2.182×10^7	p_SAM_admANE	1958.38
p_EUR	82910.1	t_SEA_SAM	30158.6
p_SEA	34287.8	p_SEA_SAM	3371.49
p_SAM	23153.2	t_EUR_ANE	13566.
p_ANE	87216.8	p_EUR_ANE	13473.8
adm_ANE_SAM	0.0826456	t_EUR_SEA	38043.7
tAdm_ANE_SAM	11131.4	p_EUR_SEA	9954.43

Fig. S9.2. Adding Southern First Peoples onto the EUR/SEA tree, with a ghost population ANE.

Adding Siberians

We then added Siberians (SIB) to the tree. According to our *qpGraph* models, they can be modeled as a sister clade to Native Americans, with extra European and East Asian contributions. We here omitted the East Asian contribution to check whether a simpler model with only European contribution also fits. Also, we now split the ANE contribution into two admixture events, one into the ancestral SIB/SAM branch, and one into the SAM branch (Fig. S9.3), as in the *qpGraph* models. The resulting fit shows substantial overestimation of SEA/SAM allele sharing, which is likely due to the lack of the American Pleistocene bottleneck, as well as the lack of additional Asian admixture in SIB, which "drags" the SEA split time close to SIB and SAM, leading to the overestimation. We therefore added SEA admixture in the next model with Chukotko-Kamchatkan speakers below.

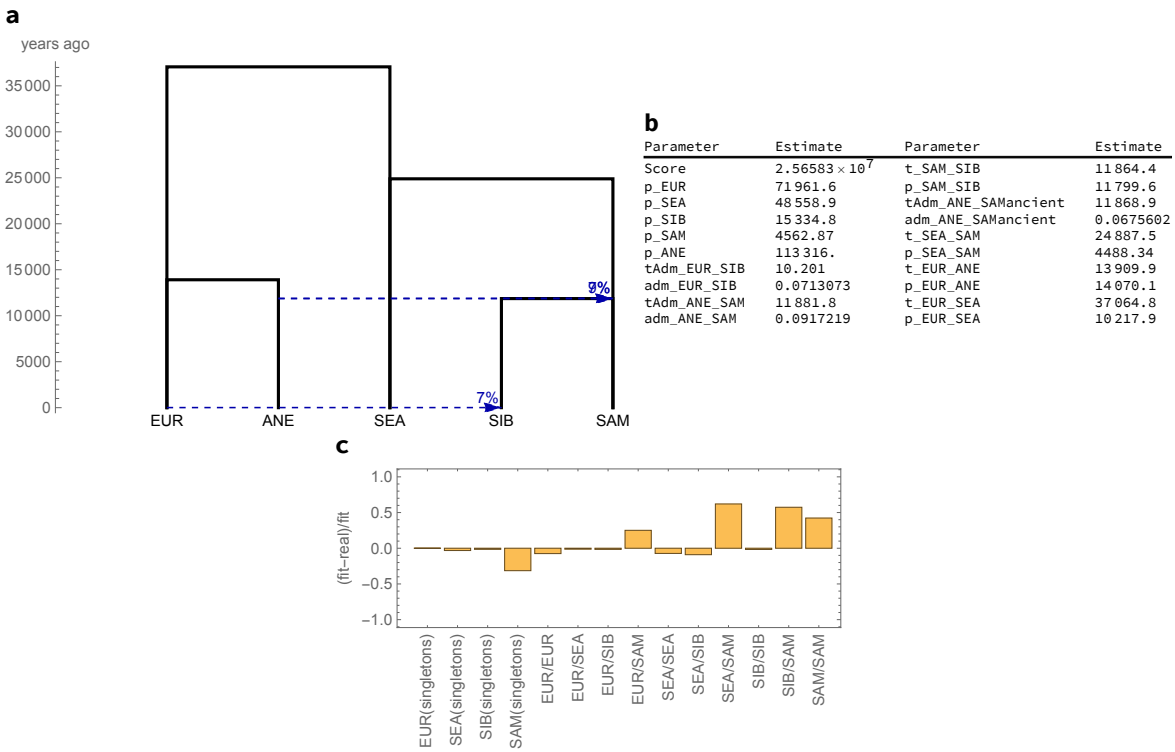

Fig. S9.3. Adding Siberians onto the EUR/SEA/SAM tree. As indicated in panel c, RASS between SEA and SAM is overestimated by 50% in this model.

Adding Kamchatkan populations

In addition to Siberians, we also added populations from the Russian Far East (Koryak and Itelmen) to the tree (Fig. S9.4). In contrast to the previous model, we now fix the time of the ancient ANE contribution into the SIB/SAM ancestral branch, in order to reduce the number of free parameters in the model, and since there is not much power to infer the times of these deep admixture events. We here also added an admixture edge from SEA into SIB, which improves the fit, but which apparently does not help much with the current overestimation of the SAM/SEA sharing.

Adding northern North Americans

We next added Northern First Peoples (NAM) to the tree, which should be a sister clade to the SAM, who – in contrast to Athabaskans – should not have any substantial Siberian ancestry according to the *qpGraph* analysis, although they are expected to have European colonial admixture. We therefore added NAM as a sister clade to SAM with additional EUR admixture, arbitrarily fixed at 250 years ago (Fig. S9.5). The resulting tree shows a large underestimation of the C-K/NAM allele sharing, which must be due to the small levels of First Peoples ancestry found in Chukotko-Kamchatkan speakers. As discussed in the *qpGraph* section (section 10), we believe this ancestry came into Kamchatka through bidirectional admixture with Yup'ik/Inuit branches, so we leave this underestimation for now and first add the Yup'ik/Inuit (ESK) group to the tree.

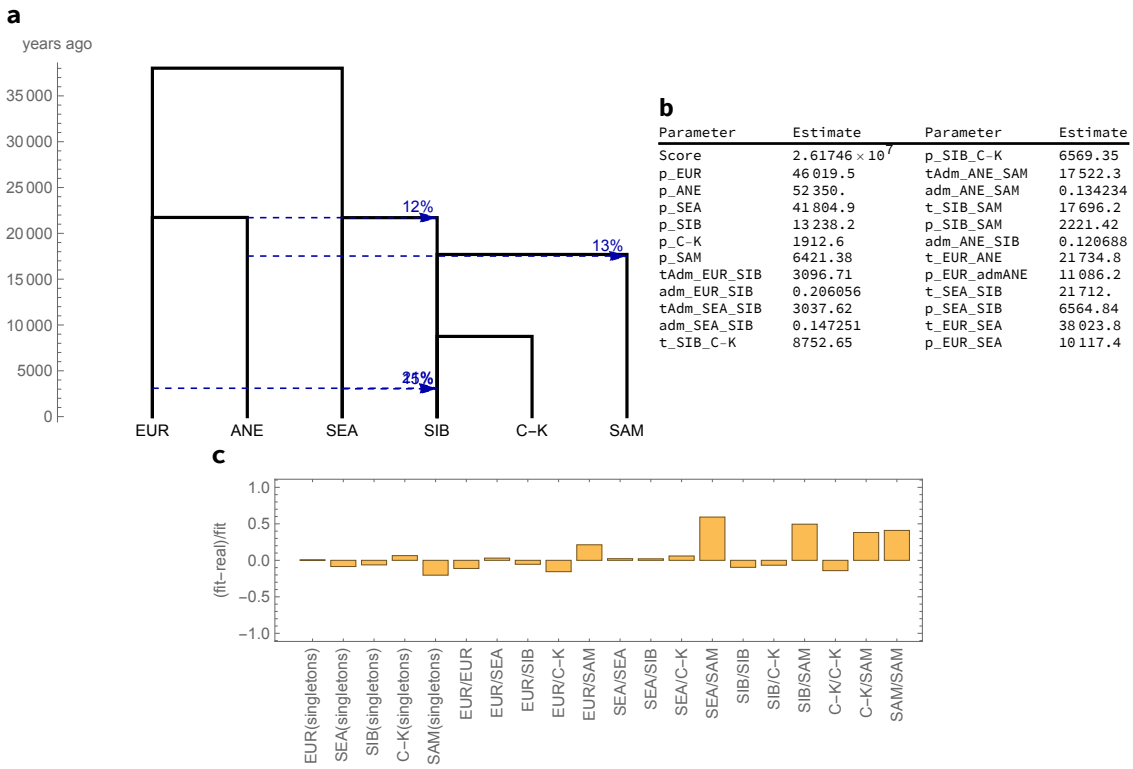

Parameter	Estimate	Parameter	Estimate
Score	2.61746×10^7	p_SIB_C–K	6569.35
p_EUR	46 019.5	tAdm_ANE_SAM	17 522.3
p_ANE	52 350.	adm_ANE_SAM	0.134234
p_SEA	41 804.9	t_SIB_SAM	17 696.2
p_SIB	13 238.2	p_SIB_SAM	2221.42
p_C–K	1912.6	adm_ANE_SIB	0.120688
p_SAM	6421.38	t_EUR_ANE	21 734.8
tAdm_EUR_SIB	3096.71	p_EUR_admANE	11 086.2
adm_EUR_SIB	0.206056	t_SEA_SIB	21 712.
tAdm_SEA_SIB	3037.62	p_SEA_SIB	6564.84
adm_SEA_SIB	0.147251	t_EUR_SEA	38 023.8
t_SIB_C–K	8752.65	p_EUR_SEA	10 117.4

Fig. S9.4. Adding Chukotko-Kamchatkan speakers (C-K) onto the EUR/SEA/SIB/SAM tree.

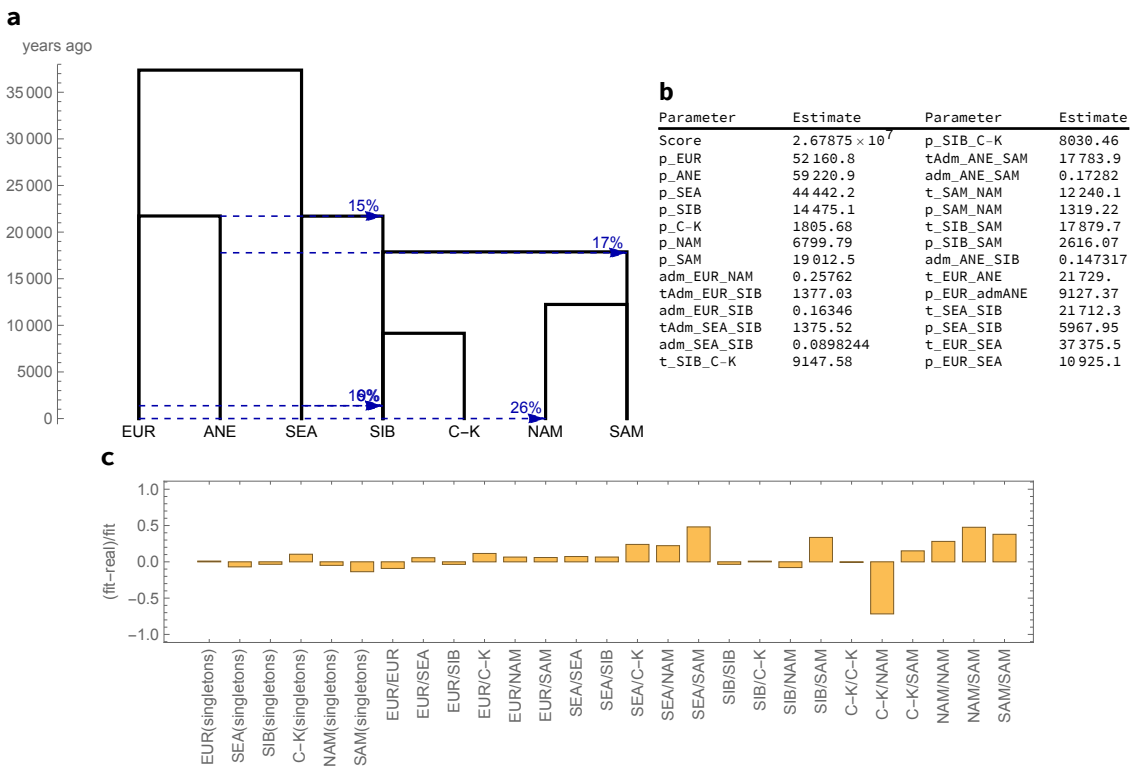

Parameter	Estimate	Parameter	Estimate
Score	2.67875×10^7	p_SIB_C–K	8030.46
p_EUR	52 160.8	tAdm_ANE_SAM	17 783.9
p_ANE	59 220.9	adm_ANE_SAM	0.17282
p_SEA	44 442.2	t_SAM_NAM	12 240.1
p_SIB	14 475.1	p_SAM_NAM	1319.22
p_C–K	1805.68	t_SIB_SAM	17 879.7
p_NAM	6799.79	p_SIB_SAM	2616.07
p_SAM	19 012.5	adm_ANE_SIB	0.147317
adm_EUR_NAM	0.25762	t_EUR_ANE	21 729.
tAdm_EUR_SIB	1377.03	p_EUR_admANE	9127.37
adm_EUR_SIB	0.16346	t_SEA_SIB	21 712.3
tAdm_SEA_SIB	1375.52	p_SEA_SIB	5967.95
adm_SEA_SIB	0.0898244	t_EUR_SEA	37 375.5
t_SIB_C–K	9147.58	p_EUR_SEA	10 925.1

Fig. S9.5. Adding Northern First Peoples (NAM) onto the EUR/SEA/SIB/C-K/SAM tree.

Adding Eskimo-Aleut-speaking populations to the tree

We next added several Eskimo-Aleut-speaking populations onto the tree, grouped into two populations: ALE (Aleuts) and ESK (Yup'ik from Chukotka and Greenlandic Inuit). We added them as a clade, which in turn is cladal with Chukotko-Kamchatkan speakers, with additional Native American ancestry from NAM. We also added the ESK/C-K bidirectional admixture event (Fig. S9.6). This model fits overall well, with one exception: The model largely underestimates

NAM/C-K sharing and to a much lesser extent SIB/NAM. This may suggest some Asian gene flow from C-K, ALE or ESK into NAM, potentially through Athabaskans (see below).

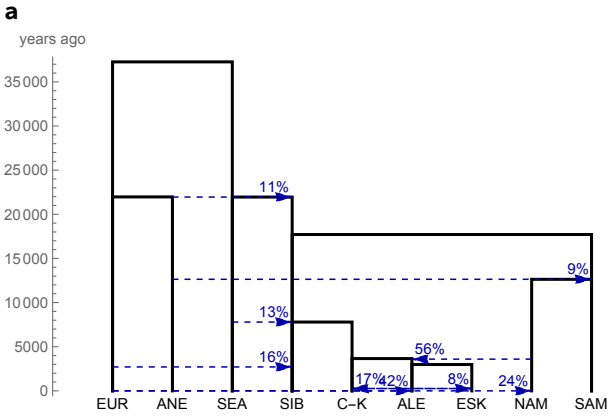

b

Parameter	Estimate	Parameter	Estimate
Score	2.8207×10^7	adm_NAM_ALE	0.556412
p_EUR	48 659.1	t_C-K_ALE	3658.98
p_ANE	83 666.5	p_C-K_ALE	4698.98
p_SEA	46 255.9	adm_SEA_SIB	0.134625
p_SIB	20 952.8	t_SIB_C-K	7794.64
p_C-K	890.702	p_SIB_C-K	6088.59
p_ALE	757.852	t_SAM_NAM	12 635.6
p_ESK	551.856	p_SAM_NAM	4630.45
p_NAM	8007.39	adm_ANE_SAM	0.0915951
p_SAM	34 170.6	tAdm_ANE_SAM	12 639.7
adm_EUR_NAM	0.242811	p_SAM_admANE	627.461
adm_EUR_ALE	0.423518	t_SIB_SAM	17 712.2
tAdm_EUR_SIB	2710.11	p_SIB_SAM	3496.46
adm_EUR_SIB	0.162805	adm_ANE_SIBanc	0.1088
adm_ESK_C-K	0.172704	t_EUR_ANE	21 971.4
tAdm_ESK_C-K	266.613	p_EUR_ANE	9474.75
adm_C-K_ESK	0.0849036	t_SEA_SIB	21 953.8
t_ALE_ESK	2984.25	p_SEA_SIB	6442.65
p_ALE_ESK	413.856	t_EUR_SEA	37 267.2
tAdm_NAM_ALE	3594.71	p_EUR_SEA	10 843.3

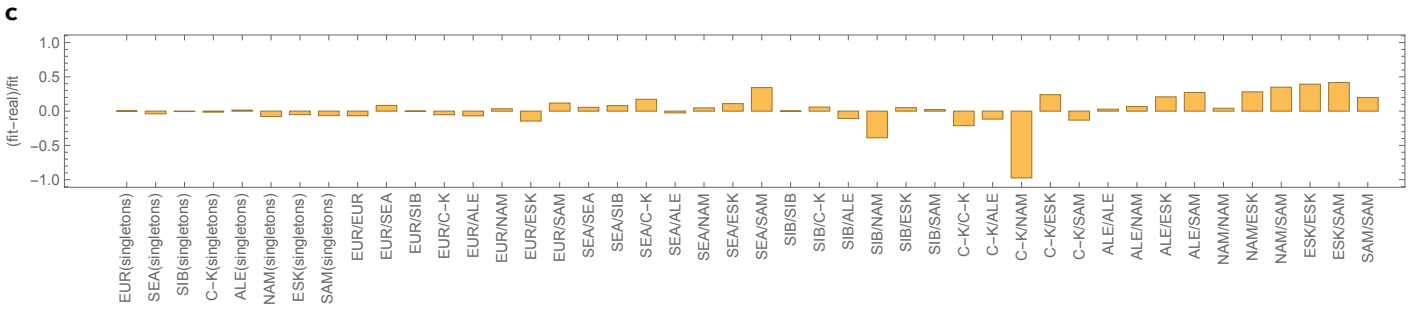

Fig. S9.6. Adding Eskimo-Aleut speakers (ALE and ESK) onto the EUR/SEA/SIB/C-K/NAM/SAM tree, as a sister group to C-K with additional Native American ancestry, and a bidirectional gene flow between C-K and ESK.

Adding Athabaskans

Finally, we added the Athabaskan meta-population to the tree (Dakelh and Chipewyans). We first modeled them as a sister clade to NAM (Fig. S9.7).

The model substantially underestimates the SIB/ATH allele sharing, suggesting some Asian gene flow into Athabaskans, as consistent with other analyses and previous publications (Reich et al. 2012, Raghavan et al. 2014b, 2015, Moreno-Mayar et al. 2018). We tested three different models with Asian gene flow into Athabaskans (distinguished by the topology on the Asian side) that emerged as best-fitting in our *qpGraph* analysis (Fig. S10.3):

Model_1 (C-K, (ATH, (ESK, ALE))): The source that contributed to Athabaskans split off the common ancestral branch of ESK and ALE after its split from the common ancestral branch with C-K.

Model_2 (ATH, (C-K, (ESK, ALE))): The source that contributed to Athabaskans split off the common ancestor of C-K, ESK and ALE and is therefore an outgroup to those three populations.

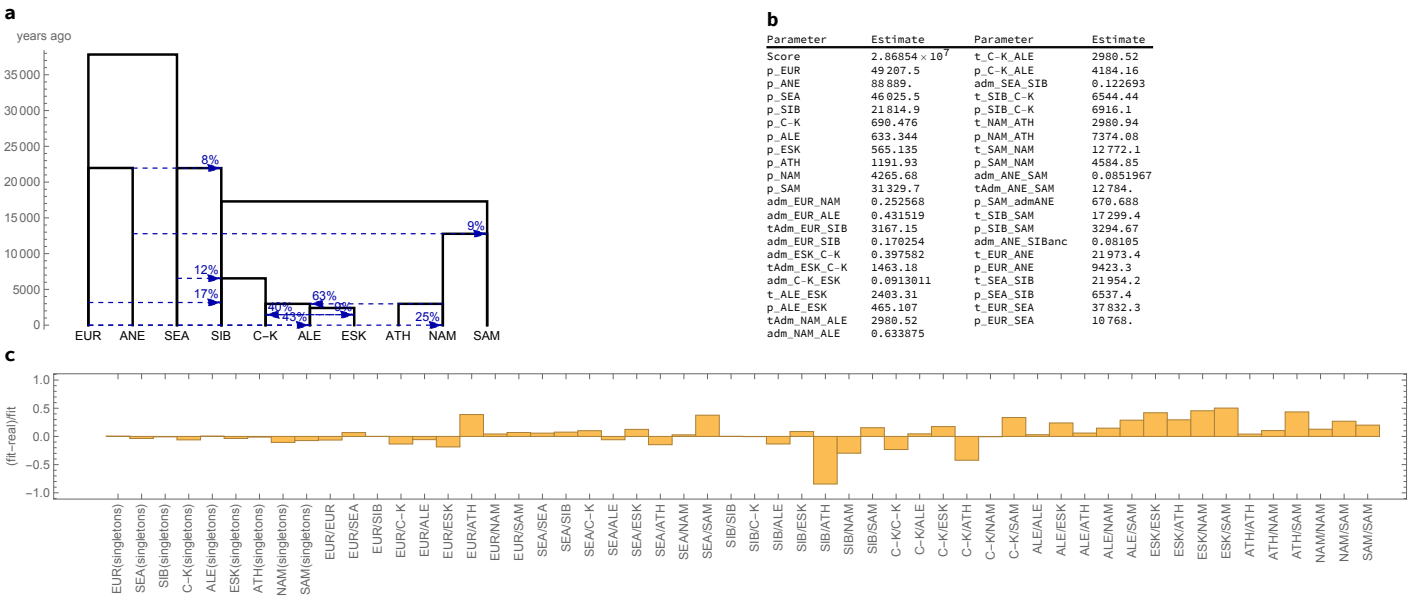

Parameter	Estimate	Parameter	Estimate
Score	2.86854×10^7	t_C-K_ALE	2980.52
p_EUR	49207.5	p_C-K_ALE	4184.16
p_ANE	88889.	adm_SEA_SIB	0.122693
p_SEA	46025.5	t_SIB_C-K	6544.44
p_SIB	21814.9	p_SIB_C-K	6916.1
p_C-K	690.476	t_NAM_ATH	2980.94
p_ALE	633.344	p_NAM_ATH	7374.08
p_ESK	565.135	t_SAM_NAM	12772.1
p_ATH	1191.93	p_SAM_NAM	4584.85
p_NAM	4265.68	adm_ANE_SAM	0.0851967
p_SAM	31329.7	tAdm_ANE_SAM	12784.
adm_EUR_NAM	0.252568	p_SAM_admANE	670.688
adm_EUR_ALE	0.431519	t_SIB_SAM	17299.4
tAdm_EUR_SIB	3167.15	p_SIB_SAM	3294.67
adm_EUR_SIB	0.170254	adm_ANE_SIBanc	0.08105
adm_ESK_C-K	0.397582	t_EUR_ANE	21973.4
tAdm_ESK_C-K	1463.18	p_EUR_ANE	9423.3
adm_C-K_ESK	0.0913011	t_SEA_SIB	21954.2
t_ALE_ESK	2403.31	p_SEA_SIB	6537.4
p_ALE_ESK	465.107	t_EUR_SEA	37832.3
tAdm_NAM_ALE	2980.52	p_EUR_SEA	10768.
adm_NAM_ALE	0.633875		

Fig. S9.7. Adding Athabaskans onto the EUR/SEA/SIB/C-K/ALE/ESK/NAM/SAM tree, as a sister group to NAM. The model underestimates SIB/ATH and C-K/ATH allele sharing.

Model_3 ((C-K, ATH), (ESK, ALE)): The Athabaskan source split off the branch leading to present-day C-K *after* its split from the common ancestor with ESK and ALE. This is the model proposed in (Moreno-Mayar et al. 2018).

We first used "rarecoal maxl" to numerically optimize each model, and then used "rarecoal mcmc" to refine the estimates, using Markov Chain Monte Carlo to search for a local optimum. This is computationally more costly, but ensures that the optimum has been reached. The composite likelihood of the three refined competing models are:

Model	Composite log-likelihood	Difference
Model_1	-28,682,166	0
Model_2	-28,682,227	-61
Model_3 (Moreno-Mayar et al. 2018)	-28,682,509	-343

The highest log-likelihood is achieved by Model_1 (C-K, (ATH, (ESK, ALE))) shown in Fig. S9.8. This model is consistent with the topology inferred by *qpGraph* (Fig. S10.5), but it underestimates allele sharing between NAM and SIB, suggesting some additional gene flow from ATH into NAM (consistent with *qpAdm* and PCA results, see Fig. 1, Extended Data Figs. 2-4, Tables S5.3, S5.4). To test this, we ran the three models proposed above with an additional ATH->NAM gene flow.

Model	Composite log-likelihood	Difference
Model_1_ATHadmNAM	-28,680,495	0
Model_2_ATHadmNAM	-28,680,861	-366
Model_3_ATHadmNAM	-28,681,925	-1,430

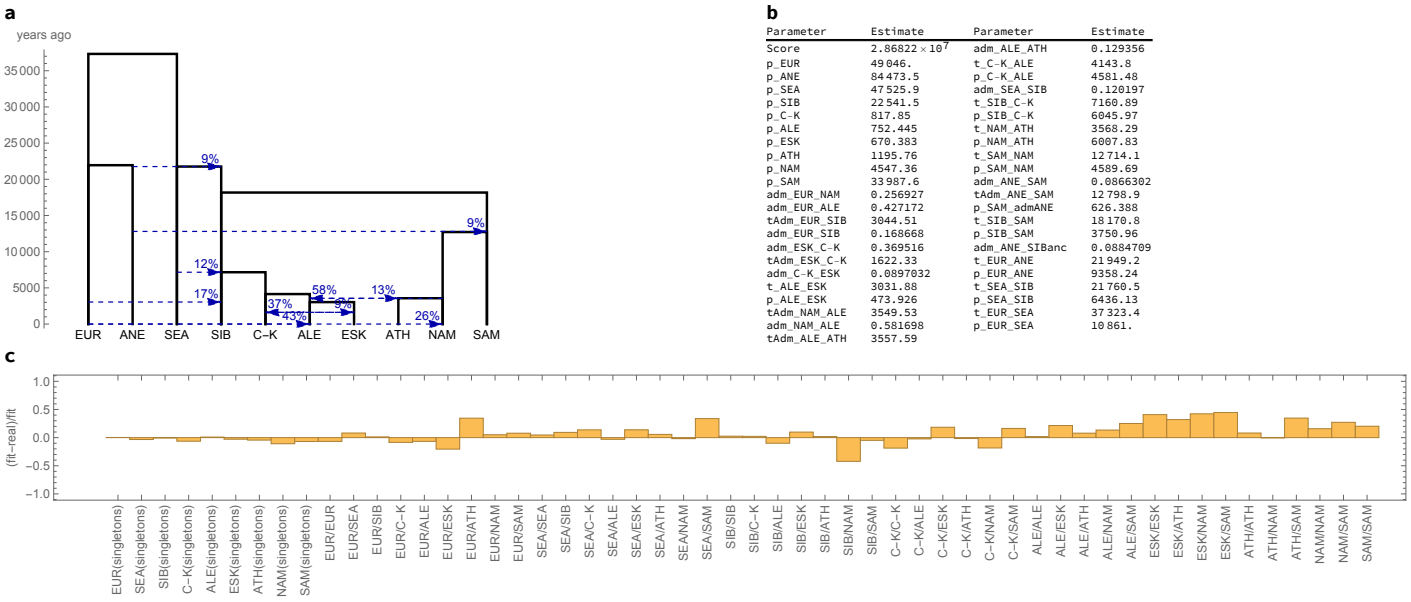

b

Parameter	Estimate	Parameter	Estimate
Score	2.86822×10^7	adm_ALE_ATH	0.129356
p_EUR	49046.	t_C-K_ALE	4143.8
p_ANE	84473.5	p_C-K_ALE	4581.48
p_SEA	47525.9	adm_SEA_SIB	0.120197
p_SIB	22541.5	t_SIB_C-K	7160.89
p_C-K	817.85	p_SIB_C-K	6045.97
p_ALE	752.445	t_NAM_ATH	3568.29
p_ESK	670.383	p_NAM_ATH	6007.83
p_ATH	1195.76	t_SAM_NAM	12714.1
p_NAM	4547.36	p_SAM_NAM	4589.69
p_SAM	33987.6	adm_ANE_SAM	0.0866302
adm_EUR_NAM	0.256927	tAdm_ANE_SAM	12798.9
adm_EUR_ALE	0.427172	p_SAM_admANE	626.388
tAdm_EUR_SIB	3044.51	t_SIB_SAM	18170.8
adm_EUR_SIB	0.168668	p_SIB_SAM	3750.96
adm_ESK_C-K	0.369516	adm_ANE_SIBanc	0.0884709
tAdm_ESK_C-K	1622.33	t_EUR_ANE	21949.2
adm_C-K_ESK	0.0897032	p_EUR_ANE	9358.24
t_ALE_ESK	3031.88	t_SEA_SIB	21760.5
p_ALE_ESK	473.926	p_SEA_SIB	6436.13
tAdm_NAM_ALE	3549.53	t_EUR_SEA	37323.4
adm_NAM_ALE	0.581698	p_EUR_SEA	10861.
tAdm_ALE_ATH	3557.59		

Fig. S9.8. Adding Athabaskans onto the EUR/SEA/SIB/C-K/ALE/ESK/NAM/SAM tree, as a sister group to NAM and with an additional gene flow from the ALE/ESK branch. The model underestimates SIB/NAM allele sharing.

The winning model is again Model_1, as above, and shown in Fig. S9.9. We note that while these log-likelihood differences establish Model_1 as the best-fitting model, they cannot be used naively to assess the statistical confidence of this comparison. We address this further below using a corrected likelihood approach. Indeed, the additional ATH->NAM gene flow improves the fit substantially, although the inferred admixture proportion is as high as 66%, and the time of admixture is very close to the ATH/NAM split point. We believe that alternative explanations might be direct gene flow into NAM from the same proto-Paleo-Eskimo source that contributed to ATH. We did not investigate these models further, since the complexity of the final model is already substantial even without the ATH->NAM gene flow. Despite the lack of fit of the SIB/NAM allele sharing (Fig. S9.8), we decided to use that simpler model as the final model, also since it is consistent with the final *qpGraph* model (Fig. S10.5).

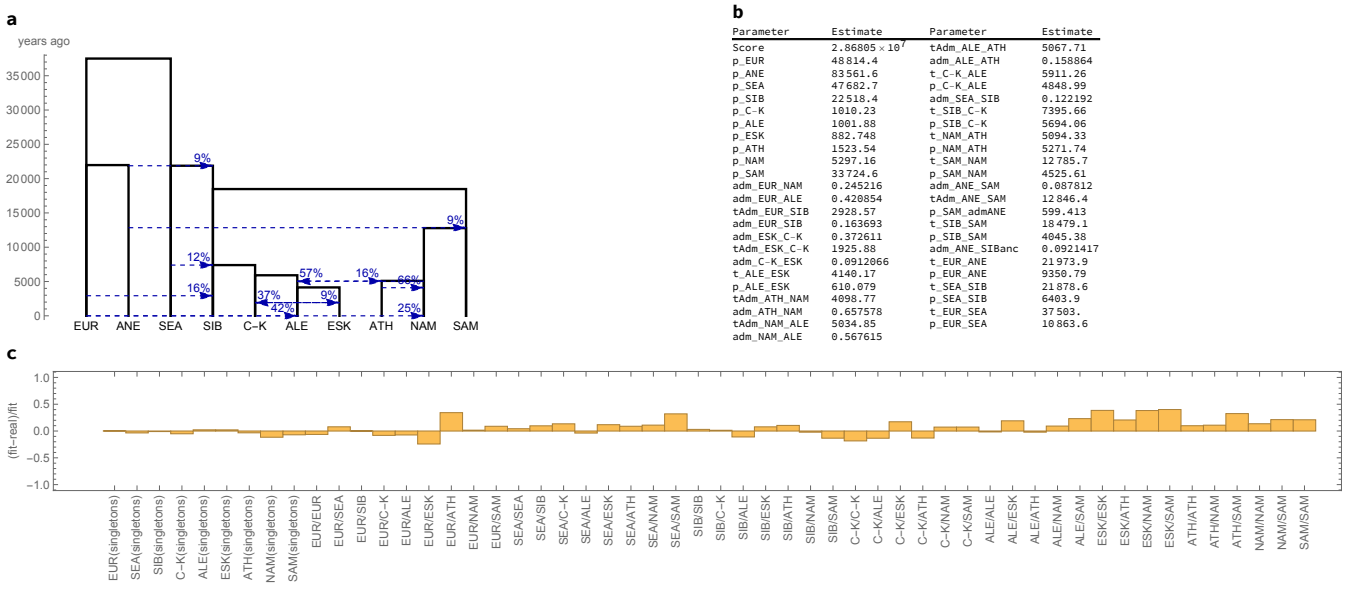

b

Parameter	Estimate	Parameter	Estimate
Score	2.86805×10^7	tAdm_ALE_ATH	5067.71
p_EUR	48814.4	adm_ALE_ATH	0.158864
p_ANE	83561.6	t_C-K_ALE	5911.26
p_SEA	47682.7	p_C-K_ALE	4848.99
p_SIB	22518.4	adm_SEA_SIB	0.122192
p_C-K	1010.23	t_SIB_C-K	7395.66
p_ALE	1001.88	p_SIB_C-K	5694.06
p_ESK	882.748	t_NAM_ATH	5094.33
p_ATH	1523.54	p_NAM_ATH	5271.74
p_NAM	5297.16	t_SAM_NAM	12785.7
p_SAM	33724.6	p_SAM_NAM	4525.61
adm_EUR_NAM	0.245216	adm_ANE_SAM	0.087812
adm_EUR_ALE	0.420854	tAdm_ANE_SAM	12846.4
tAdm_EUR_SIB	2928.57	p_SAM_admANE	599.413
adm_EUR_SIB	0.163693	t_SIB_SAM	18479.1
adm_ESK_C-K	0.372611	p_SIB_SAM	4045.38
tAdm_ESK_C-K	1925.88	adm_ANE_SIBanc	0.0921417
adm_C-K_ESK	0.0912066	t_EUR_ANE	21973.9
t_ALE_ESK	4140.17	p_EUR_ANE	9350.79
p_ALE_ESK	610.079	t_SEA_SIB	21878.6
tAdm_ATH_NAM	4098.77	p_SEA_SIB	6403.9
adm_ATH_NAM	0.657578	t_EUR_SEA	37503.
tAdm_NAM_ALE	5034.85	p_EUR_SEA	10863.6
adm_NAM_ALE	0.567615		

Fig. S9.9. Adding the ATH->NAM gene flow to the model.

Correcting the composite likelihood for linkage correlations

Rarecoal uses a composite likelihood approach, which simply computes the total likelihood of

the data given a model as the product of probabilities across all sites. This approach neglects linkage among sites, which does not affect the maximum likelihood parameter estimates. However, composite likelihoods cannot be used to compute posterior distributions or asses significance of model comparisons.

We can solve this issue by correcting the composite likelihood by a factor that reflects the *effective* number of independent sites, which is much smaller than the true number of sites analyzed. To estimate the reduction factor of the likelihood, we first use a simple Block-Jackknife procedure to estimate the sampling variance of the joint allele frequency spectrum (Busing et al. 1999). Jackknife error estimation is built into the program "freqSum2histogram" from the rarecoal-tools repository used here (https://github.com/stschiff/rarecoal-tools), using the flag "-j". This program generates a histogram of mutation patterns across the nine populations, which reports i) the number of times a given pattern is observed, ii) the frequency of that pattern, which is the number of observations divided by the total number of callable base pairs across the genome (here 1,068,434,478), and iii) a Jackknife error estimate of that frequency, computed by chromosome-wise block Jackknife. Fig. S9.10 summarizes the error estimates as a function of the frequency of each pattern (up to total allele count 4).

Under a true independent sites model without genetic linkage, the errors should follow a simple Poisson error model (the dashed line in Fig. S9.10), which predicts a square-root relationship between the error and the frequency of an observation. Specifically, the relationship between errors Δx and frequency x should be:

$$\Delta x = \sqrt{\frac{x}{N}}$$

where N is the number of callable sites.

As can be seen, the true error estimates are much higher than under the independent sites assumption, which naturally reflects genetic linkage. We fitted an "Effective sites" model to the observed errors (the solid line in Fig. S9.10), by simply reducing the total number of callable sites by a factor α. Specifically, we fit the function

$$\Delta x = \sqrt{\frac{x}{\alpha N}}$$

inferring the parameter α by a simple least-square fit. We estimate $\alpha = 0.055$, which means that the inferred effective number of sites is about 18 times smaller than the true number of sites. This effective sites correction is not used in the maximum likelihood estimates above, but only in MCMC runs below and in model comparisons where indicated.

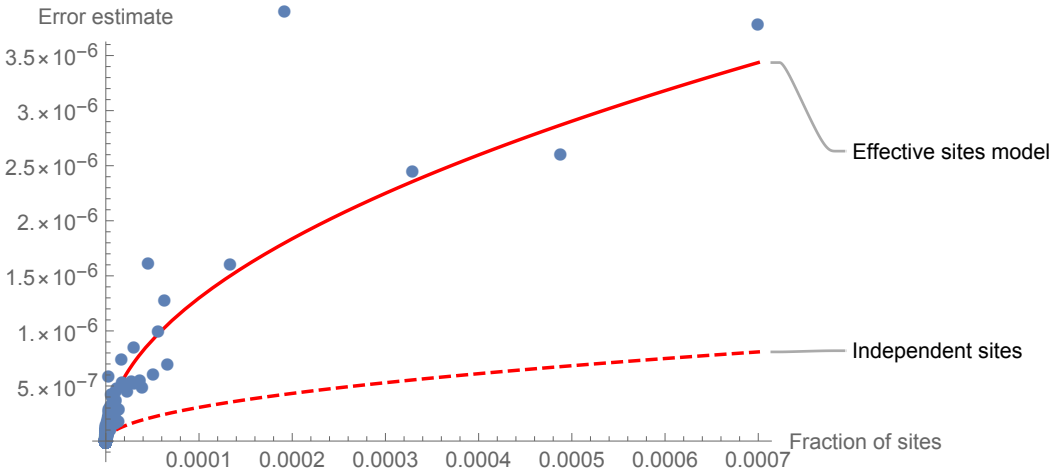

Fig. S9.10. Fitting an effective sites error model to the joint site frequency spectrum for 9 populations (EUR, SEA, SIB, C-K, ALE, ESK, ATH, NAM, SAM).

Since the composite log-likelihood is a sum across all sites, a model with reduced effective number of sites simply results in a log-likelihood that is reduced by the same factor. Hence, the log-likelihood differences are also reduced by that same factor. We can therefore correct the likelihood differences for the three competing models discussed above (here without the ATH->NAM gene flow):

Model	Composite log-likelihood difference	Corrected log-likelihood difference
Model_1	0	0
Model_2	-61	-3.3
Model_3 (Moreno-Mayar et al. 2018)	-343	-18.9

which shows that Model_2 is $e^{3.3} = 27.1$ times less likely than Model_1, and Model_3 is $e^{18.9} = 1.6{\times}10^{8}$ times less likely than Model_1, which gives significant support for Model_1, according to the arguments on significance in section 10.2.

We built into the program "rarecoal mcmc" an option implementing such an "effective sites" correction for reducing the total composite likelihood and hence widening the sampled posterior distribution. The resulting parameter estimates with and without that "effective sites" correction are shown in Fig. S9.11.

Overall, the parameter estimates with and without correction overlap as expected, with some exceptions in particular for split times estimates (first panel in Fig. S9.11), where the inference based on the corrected likelihood yields older estimates for the most recent split times among the ALE, ESK and C-K branches, as well as for admixture times within these branches. Specifically, parameter estimates for t_NAM_ATH, t_ C-K_ALE, t_ALE_ESK as well as admixture times tAdm_NAM_ALE and tAdm_ALE_ATH are about 1,000 years older with the corrected likelihood compared to the composite likelihood, while t_SIB_C-K is around 1,000 years younger compared to the composite likelihood estimate. We believe two factors might contribute to this discrepancy. First, the maximum likelihood estimate might represent a local optimum, whereas the broader parameter space exploration using the effective sites MCMC finds the global optimum which has older split times in this sub-tree. Second, these earlier split times might reflect differences in parameter space due to constraints imposed by the model topologies. In particular, the model topology itself imposes ordering constraints on split- and admixture time parameters. The joint posterior distribution therefore could have subtle topological features which might cause the MCMC to explore different regions of the parameter space despite slightly sub-optimal likelihoods but larger probability areas.

Overall, we believe the corrected likelihood Bayesian calculation yields realistic posterior credibility intervals for parameters, and we use the median estimates of those intervals for plotting our final model in Fig. 2. We summarize the maximum likelihood estimates, as well as the corrected likelihood marginal posterior percentiles in Table S9.2. The final model was calibrated using a mutation rate of 1.25×10^{-8} per basepair per generation, and a generation time of 29 years. The resulting model appears to be overall consistent with archaeology, with two small noteworthy issues. First, the ancient Anzick genome (12,600 calBP) (Rasmussen et al. 2014) has a substantially higher affinity to the SAM than to the NAM branch. To allow for this, the NAM/SAM split time needs to be sufficiently older than Anzick's age, which in our estimate is barely the case. We believe this can in principle be fixed by using the Anzick genome as a calibration point. A related issue poses our estimate of the ANE->SAM admixture edge, which is estimated to be too recent to allow for the older NAM/SAM split necessary to fit Anzick. We believe these discrepancies are tolerable, but acknowledge room for improvement by using directly dated ancient samples to further constrain the model fits, which however will also further increase the already substantial model complexity.

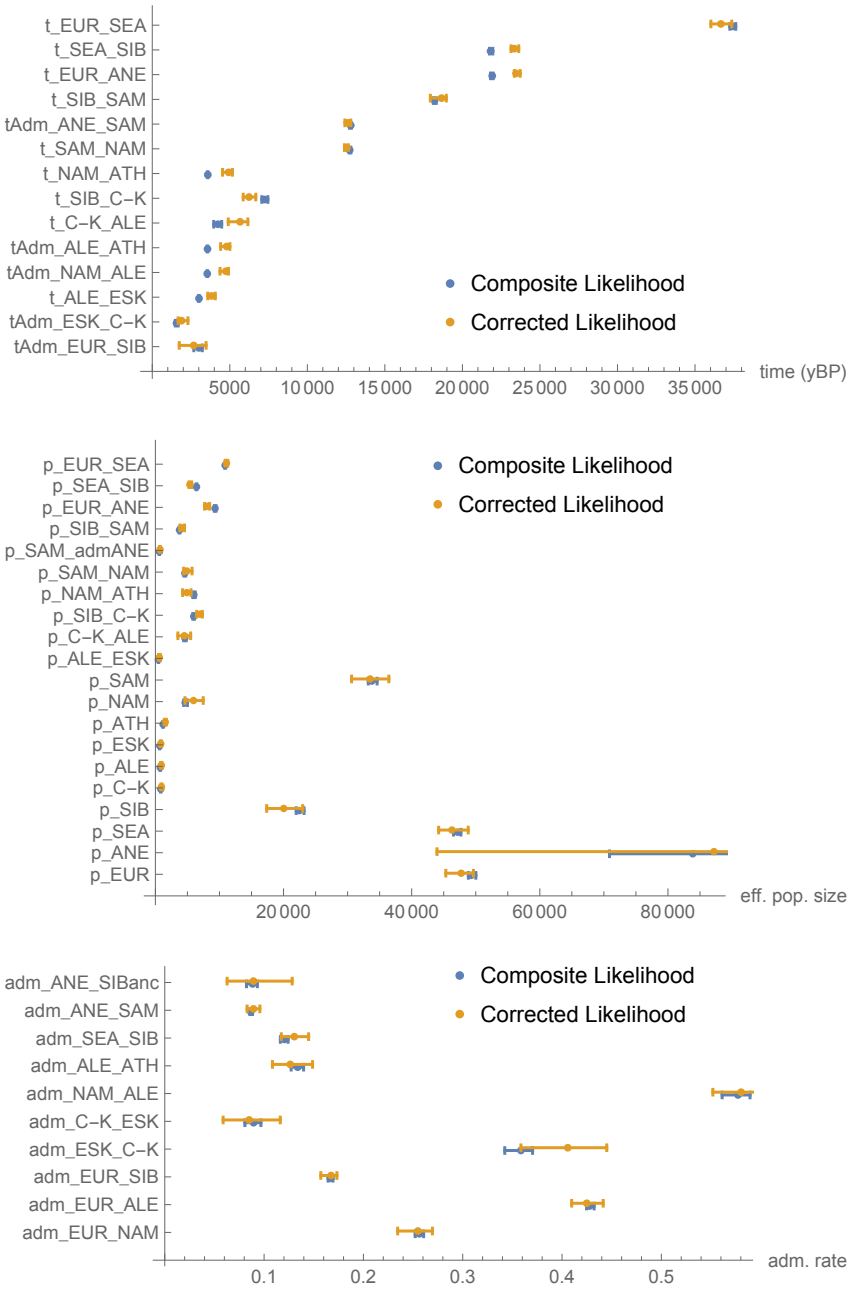

Fig. S9.11. Posterior credibility estimation for all parameters of the final model shown in Fig. S9.8 with and without the "effective sites" correction of the likelihood.

	Parameter	Maximum composite likelihood estimate	2.5% posterior percentile, corrected likelihood	50% posterior percentile, corrected likelihood	97.5% posterio percentile, corrected likelihood
Split Times (ya)	t_ALE_ESK	3,032	3,580	3,835	4,066
	t_C-K_ALE	4,144	4,901	5,662	6,165
	t_SIB_C-K	7,161	5,865	6,241	6,674
	t_NAM_ATH	3,568	4,533	4,924	5,168
	t_SAM_NAM	12,714	12,396	12,549	12,639
	t_SIB_SAM	18,171	17,935	18,654	18,962
	t_EUR_ANE	21,949	23,346	23,463	23,727
	t_SEA_SIB	21,760	23,136	23,349	23,633
	t_EUR_SEA	37,323	36,024	36,668	37,370
Admixture Times (ya)	tAdm_EUR_SIB	3,045	1,742	2,671	3,470
	tAdm_ESK_C-K	1,622	1,668	1,886	2,299
	tAdm_NAM_ALE	3,550	4,371	4,752	4,914
	tAdm_ALE_ATH	3,558	4,410	4,799	5,005
	tAdm_ANE_SAM	12,799	12,423	12,618	12,800
Admixture Rates (%)	adm_EUR_NAM	26%	23%	25%	27%
	adm_EUR_ALE	43%	41%	42%	44%
	adm_EUR_SIB	17%	16%	17%	17%
	adm_ESK_C-K	37%	36%	41%	45%
	adm_C-K_ESK	9%	6%	8%	12%
	adm_NAM_ALE	58%	55%	58%	62%
	adm_ALE_ATH	13%	11%	13%	15%
	adm_SEA_SIB	12%	12%	13%	14%
	adm_ANE_SAM	9%	8%	9%	10%
	adm_ANE_SIBanc	9%	6%	9%	13%
Population Sizes	p_EUR	49,046	45,330	47,722	49,648
	p_ANE	84,473	43,952	87,184	179,202
	p_SEA	47,526	44,208	46,288	48,824
	p_SIB	22,542	17,375	20,031	22,986
	p_C-K	818	863	936	1,042
	p_ALE	752	818	918	1,014
	p_ESK	670	759	841	937
	p_ATH	1,196	1,409	1,538	1,716
	p_NAM	4,547	4,631	5,944	7,464
	p_SAM	33,988	30,625	33,516	36,439
	p_ALE_ESK	474	499	613	770
	p_C-K_ALE	4,581	3,510	4,512	5,501
	p_SIB_C-K	6,046	6,441	6,975	7,326
	p_NAM_ATH	6,008	4,242	4,906	5,564
	p_SAM_NAM	4,590	4,403	4,899	5,715
	p_SAM_admANE	626	654	720	776
	p_SIB_SAM	3,751	3,830	4,118	4,546
	p_EUR_ANE	9,358	7,678	8,058	8,465
	p_SEA_SIB	6,436	5,254	5,380	5,664
	p_EUR_SEA	10,861	10,896	11,093	11,297

Table S9.2. Parameter estimates for the final model using default scaling with a mutation rate of 1.25×10^{-8} per generation per basepair, and a generation time of 29 years. Maximum likelihood estimates are based on the composite likelihood, while posterior distributions are computed for a corrected likelihood as described above.

Adding ancient genomes

Onto the final tree estimated from present-day sequences only, we added the genomes of three ancient individuals with whole-genome shotgun data: The ancient Saqqaq genome published in Rasmussen et al. 2010, an ancient Aleut individual, and an ancient Athabaskan individual, both sequenced within this study. For all three samples, we made a Majority call with a minimum coverage of 3 at all variable sites in our "SGDP/Raghavan et al." dataset (see details in section 8). Given previous results from *qpGraph* (see section 10), we tested a limited number of branching positions for these ancient individuals.

For the ancient Aleut, we tested a branching position onto the modern Aleut branch at 600 ya (the median C14 date for that sample) and before colonial admixture at 250 ya. For the ancient Athabaskan, we tested a branching position onto the modern Athabaskan branch at 780 ya (its median C14 date). In both cases we did not attempt to estimate a more precise split time between the ancient sample and its corresponding modern branch given the limited information available from a single ancient sample, in particular with pseudo-haploid genotyping calls, which provide no information on private drift within the ancient branch.

To evaluate those branching positions, we compared rare allele sharing statistics between the ancient individual and each of our modern populations with those estimated from a model with the ancient genome added to the final model (Fig. S9.12). Note that the Paleo-Eskimo admixture proportion in Athabaskans, as well as the Native American / PPE mixture proportions for Aleuts are taken from the final model estimates obtained without any ancient genomes (Table S9.2).

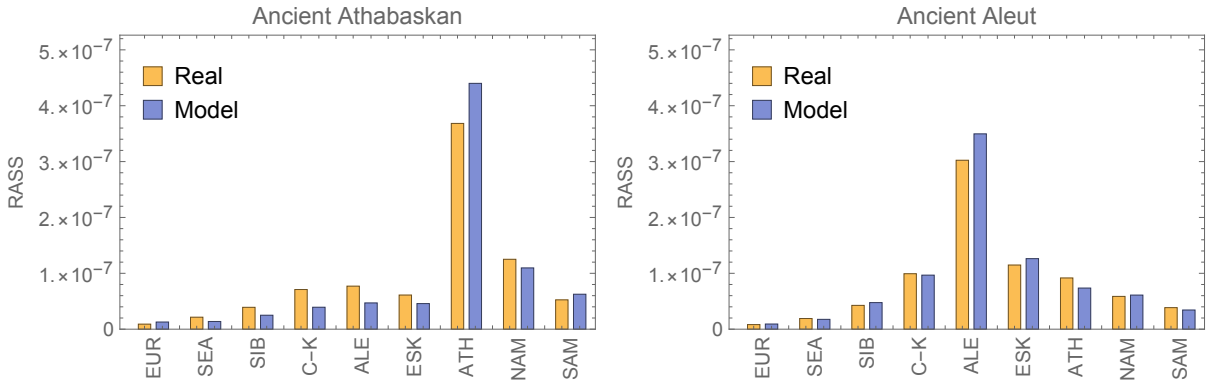

Fig. S9.12. Mapping the ancient Athabaskan and ancient Aleut samples onto the tree.

In both cases, the model and real data agree very well. By far the highest allele sharing between ancient and modern populations is seen with the modern Athabaskan and the modern Aleut branch, respectively, strongly suggesting that these ancient samples are direct ancestors of the respective modern populations. However, in the case of the ancient Athabaskan, the allele sharing with C-K and ALE is higher than predicted under our model, suggesting that the ancient Athabaskan has even higher proportions of Paleo-Eskimo ancestry than does modern Athabaskans, which may be due to population structure within the Athabaskan population, or a dilution through subsequent admixture of non-Athabaskan First Peoples into the present-day Athabaskan population. This result is supported by our extensive admixture modeling using the *qpAdm* approach and by PCA (Fig. 1, Extended Data Figs. 2-4).

In the case of the 3,900-year-old ancient Saqqaq genome (Rasmussen et al. 2010), we tested four different locations on the tree to merge its branch with the best-fitting modern

phylogeny (Fig. S9.8). The first position, called ALE_beforeATHadm, is a position on the ancestral branch leading to present-day Eskimo-Aleuts, but *before* admixture from that branch into Athabaskans. The next position, called ALE_afterATHadm, is also on the ancestral branch leading to Eskimo-Aleuts, but *after* admixture from that branch into Athabaskans. The third position, called C-K_beforeALEsplit, is a position on the ancestral branch leading to ALE, ESK and C-K. The final position, called C-K_afterALEsplit, is a position on the branch leading to present-day C-K, after its split from the Eskimo-Aleut branch. The four positions correspond to four different topologies within the PPE clade, as indicated in Table S9.3:

Saqqaq branch point	PPE clade topology	Split time	Log-likelihood	Log-likelihood difference	Corrected log-likelihood difference
ALE_beforeATHadm	(C-K, (P-E, (ATH, E-A)))	5,104 ya	-93,800	-277	-15
ALE_afterATHadm	(C-K, (ATH, (P-E, E-A)))	4,756 ya	-93,523	0	0
C-K_beforeALEsplit	(P-E, (C-K, (ATH, E-A)))	5,800 ya	-94,559	-1,036	-57
C-K_afterALEsplit	((C-K, P-E), (ATH, E-A)))	5,220 ya	-94,375	-852	-47

Table S9.3. Tested models for Saqqaq to branch onto the final maximum likelihood tree of 9 populations.

The winning position is the position on the branch leading to Eskimo-Aleuts, but after the admixture into Athabaskans, corresponding to the topology (C-K, (ATH, (P-E, E-A))), which is also the most likely topology obtained using the *qpGraph* method (section 10). All model comparisons are significant, since the corrected log-likelihood differences are above 3 (see arguments from section 10.2).

The comparison of RASS between the model and data for the winning topology is shown in Fig. S9.13. The model captures the salient feature of the RASS statistics, which is the high level of rare allele sharing between C-K and the ancient Saqqaq individual. However, the model also underestimates RASS between Saqqaq and each population in the PPE clade, i.e. Eskimo-Aleuts and Chukotko-Kamchatkans, which is difficult to explain, but could be due to additional gene flow between Saqqaq descendants and ancestors of extant populations that we currently do not model.

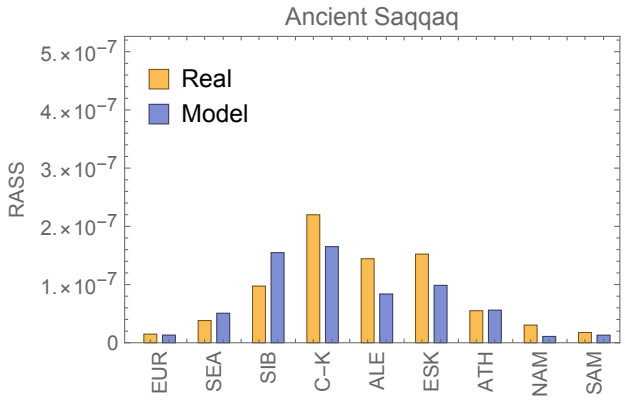

Fig. S9.13. Mapping the ancient Saqqaq individual onto the 9 population tree.

References (for this section)

Busing, F. M. T. A., Meijer, E. & Van Der Leeden, R. Delete-M Jackknife for Unequal M. *Statistics and Computing* **9**, 3–8 (1999).

Fenner, J. N. Cross-cultural estimation of the human generation interval for use in genetics-based population divergence studies. *Am. J. Phys. Anthropol*. **128**, 415–423 (2005).

Haak, W. *et al*. Massive migration from the steppe was a source for Indo-European languages in Europe. *Nature*

522, 207–211 (2015).
Mallick, S. *et al*. The Simons Genome Diversity Project: 300 genomes from 142 diverse populations. *Nature* **538**, 201–206 (2016).
Moreno-Mayar, J. V. *et al*. Terminal Pleistocene Alaskan genome reveals first founding population of Native Americans. *Nature* **553**, 203–207 (2018).
Patterson, N. *et al*. Ancient admixture in human history. *Genetics* **192**, 1065–1093 (2012).
Raghavan, M. *et al*. Upper Palaeolithic Siberian genome reveals dual ancestry of Native Americans. *Nature* **505**, 87–91 (2014a).
Raghavan, M. *et al*. The genetic prehistory of the New World Arctic. *Science* **345**, 1255832 (2014b).
Raghavan, M. *et al*. Genomic evidence for the Pleistocene and recent population history of Native Americans. *Science* **349**, 1–20 (2015).
Rasmussen, M. *et al*. Ancient human genome sequence of an extinct Palaeo-Eskimo. *Nature* **463**, 757–762 (2010).
Rasmussen, M. *et al*. The genome of a Late Pleistocene human from a Clovis burial site in western Montana. *Nature* **506**, 225–229 (2014).
Reich, D. *et al*. Reconstructing Native American population history. *Nature* **488**, 370–374 (2012).
Scally, A. & Durbin, R. Revising the human mutation rate: implications for understanding human evolution. *Nat. Rev. Genet*. **13**, 745–753 (2012).
Schiffels, S. *et al*. Iron Age and Anglo-Saxon genomes from East England reveal British migration history. *Nat. Commun*. **7**, 10408 (2016).

Supplementary Information section 10

Admixture graph modeling using *qpGraph*

10.1 Generating a basic model for present-day populations

dataset: *transitions and transversions*;

populations: *selected present-day populations.*

To investigate the phylogenetic relationship between relevant populations for this study, we tested models which fit observed f_4-statistics using autosomal markers present in the 1240K capture panel[1]. The f_4-statistic measures correlations between allele frequency differences of two pairs of groups[2]. Given a graph topology with population splits, genetic drift and admixture edges, the algorithm implemented in the *qpGraph* program infers branch lengths and mixture proportions that minimize the difference between the observed and expected f_4-statistics.

For the analysis, we used whole genome sequence data from the Simons Genome Diversity Project[3] and added additional 35 genomes published by Raghavan et al.[4]. Genotype calls for the autosomal part of the 1240K panel were extracted, and SNPs with >10% missing rate were removed, leaving 1,062,979 SNPs for the analysis (Supplementary Table 5). *qpGraph* analyses were performed in the "useallsnps: NO" mode. We first performed a comprehensive search for tree topologies fitting the data. For this, we selected the following populations: Mbuti, French, Ami, Mixe, Even, Yup'ik Naukan, Koryak, and Chipewyan to represent each of the 7 relevant meta-populations (AFR, EUR, SEA, SAM, SIB, E-A, C-K, and ATH, see Table S10.1). To perform an extensive search for possible population relationships, we began with a simple tree of three populations (Mbuti, (French, Ami)) and iteratively added one population to the tree in the following order: Mixe, Even, Koryak, Chipewyan, Yup'ik Naukan. More specifically, the added population was modeled either as a sister branch of an existing one or as a mixture of two branches. We tested all branches and branch pairs and kept all fitting models (having absolute Z-scores of the worst-fitting f_4-statistic < 3) at each step. A total of 2,932 models were tested this way, and at the end of our search, we found 108 graphs that fit all observed f_4-statistics within three standard error intervals (|Z-score| < 3) and 14 graphs that fit all observed f_4-statistics within two standard error intervals (|Z-score| < 2). Six best-fitting graphs are shown in Fig. S10.1.

The fitting graphs share several key features. The most important feature is that Mixe, Even, Koryak, Chipewyan and Yup'ik Naukan are all modeled as a mixture of western and eastern Eurasian branches, and none of them forms a sister branch with each other: i.e. at least one additional gene flow is required to add each population to the graph (Fig. S10.1). For example, Koryak cannot be a sister group to Even because of its excessive affinity to Mixe. Also, Chipewyan cannot be modeled as a sister group of Mixe and requires a gene flow from a Siberian source, e.g. either Koryak- or Even-related branch. Finally, Yup'ik Naukan is well modeled as a mixture of Koryak- and Chipewyan-related branches, or as a mixture of Koryak- and Mixe-related ones (Fig. S10.1). All possible topologies within the proto-Paleo-Eskimo (PPE) clade appear among the best-fitting models shown in Fig. S10.1: (PPE_{ATH}, ($PPE_{C\text{-}K}$, $PPE_{E\text{-}A}$)) (Fig. S10.1a,b); ($PPE_{C\text{-}K}$, (PPE_{ATH}, $PPE_{E\text{-}A}$)) (Fig. S10.1c,f); ($PPE_{E\text{-}A}$, (PPE_{ATH}, $PPE_{C\text{-}K}$)) (Fig. S10.1d,e). The abbreviations PPE_{ATH}, $PPE_{C\text{-}K}$, and $PPE_{E\text{-}A}$ denote the sources of proto-Paleo-Eskimo-related ancestry in Chukotko-Kamchatkan (C-K), Athabaskan (ATH), and Eskimo-Aleut speakers (E-A), respectively. However, the latter two graphs (Fig. S10.1d,e) contain 0-length branches within the PPE clade, i.e. there is a trifurcation. Notably, to account for excessive affinity between Koryak and Mixe, the former population is in all cases modelled as having admixture from a source related to Native Americans, but prior to the West Eurasian gene flow into them. For

convenience, we term this source “proto-American”. We also tested whether the models generated here fit the data for composite meta-populations (Table S10.1) used for *Rarecoal* modeling (section 9). All topologies shown in Fig. S10.1 fit the data (|Z-scores| < 3) for the AFR, EUR, SEA, SAM, C-K, E-A, and ATH meta-populations.

Abb.	Full Name	Populations	Nr. of samples
AFR	Africans	Bantu Herero, Bantu Kenya, Bantu Tswana, Biaka, Dinka, Esan, Gambian, Ju|'hoan North, Khomani San, Luhya, Luo, Mandenka, Masai, Mbuti, Mende, Somali, Yoruba	45
EUR	Europeans	Basque, Bergamo, Bulgarian, Crete, Czech, English, Estonian, French, Greek, Hungarian, Orcadian, Polish, Sardinian, Spanish, Tuscan	32
ANE	Paleolithic Siberian hunter-gatherers	Mal’ta (MA1) (Raghavan et al. 2014)	1
WHG	West European hunter-gatherers	Loschbour (Lazaridis et al. 2014)	1
SEA	Southeast Asians	Ami, Atayal, Dai, Kinh, Lahu, Miao, She	15
SIB	Core Siberians	Altaian, Buryat, Ket, Nivkh, Even, Mansi, Tubalar, Ulchi, Yakut	22
C-K	Chukotko-Kamchatkan speakers	Itelmen, Koryak	3
E-A	Eskimo-Aleut speakers	East and West Greenlandic Inuit, Yup'ik	7
E-A anc.	ancient Aleuts and Neo-Eskimos	Aleuts (this study)	6
		Ekven (this study)	16
		Uelen (this study)	3
ATH	Northern Athabaskan speakers	Dakelh, Chipewyan	4
ATH anc.	ancient Athabaskans	Tochak McGrath (this study)	2
USR	ancient Beringian	Upward Sun River 1 (USR1) (Moreno-Mayar et al. 2018)	1
NAM	Northern First Peoples (in some figures, “northern First Americans”)	Cree, Tsimshian	3
SAM	Southern First Peoples (in some figures, “southern First Americans”)	Aymara, Mixe, Mixtec, Piapoco, Quechua, Yukpa, Zapotec	13

Table S10.1. A table listing all present-day and ancient (grey shading) individuals and groups used in the *qpGraph* analysis. The present-day data is from the two sources: Raghavan *et al.*[4] and the Simons Genome Diversity Project data set[3] as indicated in Supplementary Table 4. The sources of ancient data are indicated in the table.

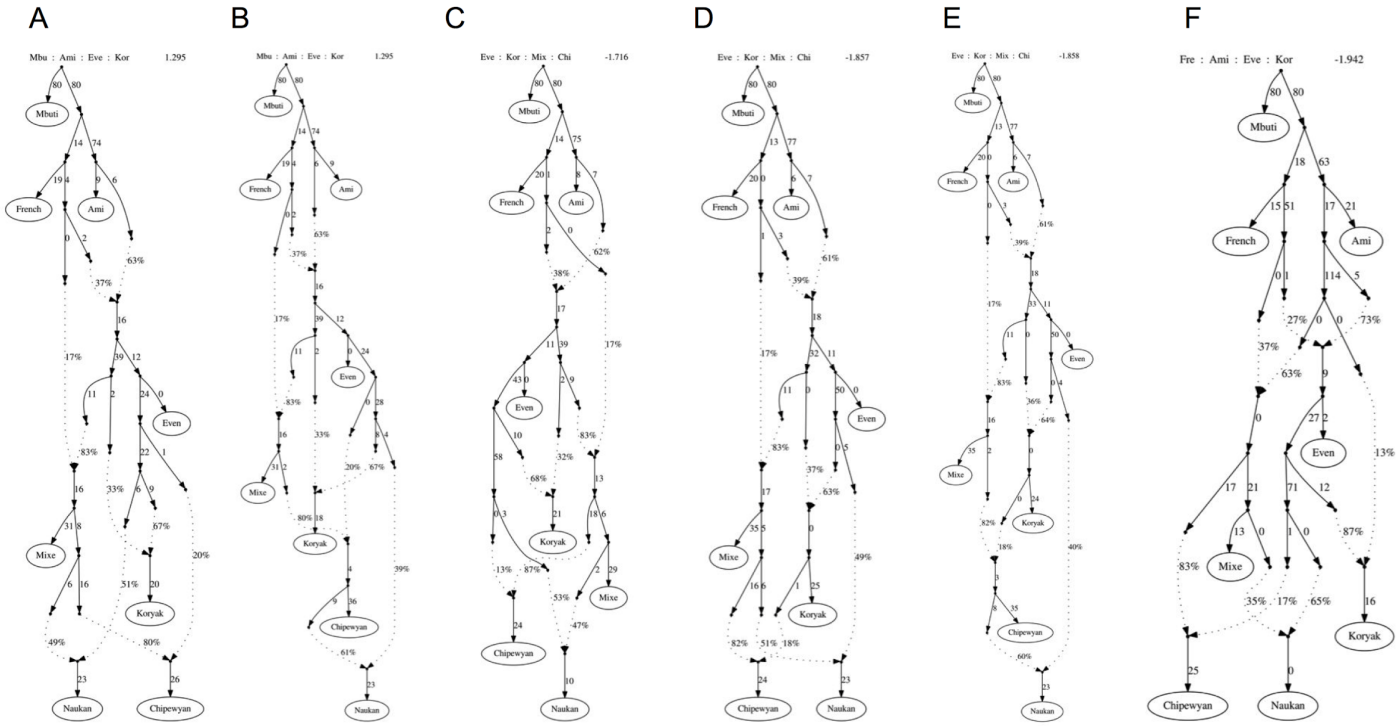

Fig. S10.1. Best-fitting models from an extensive search of population graphs. In most cases, Mixe receives two gene flows from a French-related branch (interpreted as ancient North Eurasians, ANE). Yup'ik Naukan is modeled as a mixture of proto-Paleo-Eskimos (PPE) and a Chipewyan-related branch, either before (**a**, **c**, **d**, **f**) or after (**b**, **e**) the PPE gene flow into Chipewyan. Chipewyan is modeled as a mixture of a Native American lineage and either PPE (**a-c**, **f**) or a Koryak-related lineage (**d**, **e**).

10.2 Testing all possible topologies within the proto-Paleo-Eskimo clade

dataset: *transversions only*;

populations: *present-day meta-populations*; *pseudo-haploid Saqqaq, ancient Aleuts, ancient Neo-Eskimos or present-day Yup'ik or Inuit, present-day or ancient Athabaskans.*

We added ancient populations (the Saqqaq Paleo-Eskimo, Aleutian Islanders, Old Bering Sea population from the Ekven and Uelen burial grounds) onto the backbone meta-population graph created in the previous section. To mitigate ancient DNA biases, all transition polymorphisms were removed from the dataset, with 208,649 sites remaining. We found that ancient Aleuts can be modelled as a roughly one to one mixture of First Peoples and a Saqqaq-related lineage, but the Ekven, Uelen and present-day Yup'ik populations require an additional pulse of admixture from a lineage related to C-K. This reflects the fact that all these groups were/are located in Chukotka, where they could interact with local C-K groups. We then constructed a series of more complex models including both ancient Aleuts and present-day Yup'ik or the ancient Ekven/Uelen populations (E-A). Using this set of populations, we tested all possible topologies within the PPE clade. We varied the following parameters: the branching order of real/hypothetical populations (18 topologies, including models with E-A admixture in ATH) and the lineages receiving the "proto-American" and Native American gene flows. In total, 56 models were tested for each ancient/modern E-A population (see model statistics in Table S10.2). Only the following 8 topologies of the PPE clade fit the data: 1/ ((ATH, *C-K), (E-A, P-E)); 2/ (*(ATH, C-K), (E-A, P-E)); 3/ ((ATH, C-K), (E-A, P-E)); 4/ (*C-K, (ATH, (E-A, P-E))); 5/ (C-K, (ATH, (E-A, P-E))); 6/ (ATH, (*C-K, (E-A, P-E))); 7/ (ATH, *(C-K, (E-A, P-E))); 8/ (ATH, (C-K, (E-A, P-E))), where an asterisk denotes the entry point of the "proto-American" gene flow. Note that here and in the following, topology notations involving ATH, C-K, E-A and P-E denote the PPE component in those populations (unless explicitly specified), not the First Peoples component

nor the sum of admixed ancestries. In summary, E-A and P-E (Saqqaq) are always the closest sister-groups, and the branching order of the PPE source populations that contributed to Athabaskans and C-K remains ambiguous. Another observation is that models either lacking the "proto-American" gene flow into C-K, or with this admixture not exclusive to C-K, are not among the best-fitting ones (compare Z-scores for models 1, 2, 4, and 6 and for models 3, 5, 7, and 8 above, Table S10.2). Two fitting models of this type are shown in Fig. S10.2 (topologies 2 and 5 listed above).

We suspected that the affinity between C-K and First Peoples, which resulted in the "proto-American" gene flow emerging as an outcome of the unsupervised branch-adding procedure, can be explained in a much simpler way, if we suppose that the C-K/E-A admixture was bidirectional allowing us to remove the "proto-American" gene flow. Out of 18 topologies of this kind, 15 do not fit at all (|Z-scores| > 4 or > 5), while 3 fit with exactly the same Z-scores around 2 and the same log-likelihood values: ((ATH, C-K), (E-A, P-E)); (ATH, (C-K, (E-A, P-E))); (C-K, (ATH, (E-A, P-E))) (see model statistics in Table S10.3). Present-day Inuit can also be incorporated into the graph instead of Yup'ik, Ekven or Uelen, but cannot be modelled without an additional pulse of European gene flow which plausibly reflects colonial admixture (Table S10.3).

Finally, we replaced present-day Athabaskans (4 individuals) with ancient Athabaskans (2 individuals), and the impasse was resolved: only one among 6 fitting topologies has no trifurcations and has the lowest Z-score and the best log-likelihood value, and that is the topology (C-K, (ATH, (E-A, P-E))). The log-likelihood difference between this topology and the second-best topologies ((ATH, C-K), (E-A, P-E)) and (ATH, (C-K, (E-A, P-E))) ranges from 2 to 2.7, depending on the E-A population. Thus, the best-fitting model is from 7.2 to 15.5 times more likely than the second-best models, however these likelihood differences are non-significant in the case of the transversion-only dataset. See model statistics in Table S10.4 and 3 best-fitting graphs with absolute Z-scores <2 in Fig. S10.3.

Here and in the following, we generally consider likelihood ratios between competing models of 20 and higher (corresponding to log-likelihood differences of 3 and higher) to be "significant", provided the two competing models have the same number of parameters and are applied to the same data. This can be derived using the Bayesian Information Criterion (BIC) for model comparisons, which is defined as $BIC = -2 \log L + \mathrm{C}$, where C is a constant factor depending on sample size and number of model parameters, and L is the likelihood. A feature of BIC is the fact that it can be used to approximately compute the posterior probability of the model given the data, via $p(M|\mathrm{data}) \sim \exp\left(-\frac{BIC}{2}\right) p(M) = L\, p(M)$, where $p(M)$ is the prior probability of the model. Using this, and using flat priors, it follows that deciding between two models $M1$ and $M2$ with the same number of parameters and applied to the same data, we can use the likelihood ratio directly as an estimate of the ratio of posterior probabilities. It follows that a likelihood ratio of 20 or higher corresponds to one model being 20 times more likely (or higher) than the other model, which renders the posterior probability for one model being below 0.05 and the other above 0.95, which we consider to be significant support for one model over the other.

A similar pattern as seen above for the transversion-only dataset is observed for the full dataset including transitions, but with generally poorer fits: the lowest absolute Z-score equals 2.87 (Table S10.5). In this case, however, the model (C-K, (ATH, (E-A, P-E))) is from 39 to 202 times more likely than second-best models ((ATH, C-K), (E-A, P-E)) and (ATH, (C-K, (E-A, P-E))), which according to the arguments above can be considered significant. According to the best models, a low-level C-K admixture of up to 15-20% is characteristic for all Old Bering Sea, Yup'ik and Inuit groups studied here, but not for Aleuts. E-A admixture is inferred in all C-K

groups: low levels up to 10% in Koryak and Itelmen, and a higher level (Fig. 1a, Extended Data Figs. 2-4 and 8, section 5) in Chukchi, omitted from the C-K meta-population here. The topology favored by this analysis is not only a significantly better fit than the other two including the ((ATH, C-K), (E-A, P-E)) topology favored by Moreno-Mayar et al. (2018), but is also the "simplest" one from the archaeological point of view, as detailed in the Discussion. The topology favored by Moreno-Mayar et al. (2018) - ((ATH, C-K), (E-A, P-E)) - is among the best supported, however it results in a trifurcation (ATH, C-K, (E-A, P-E)) and has a significantly worse log-likelihood (Tables S10.4, S10.5).

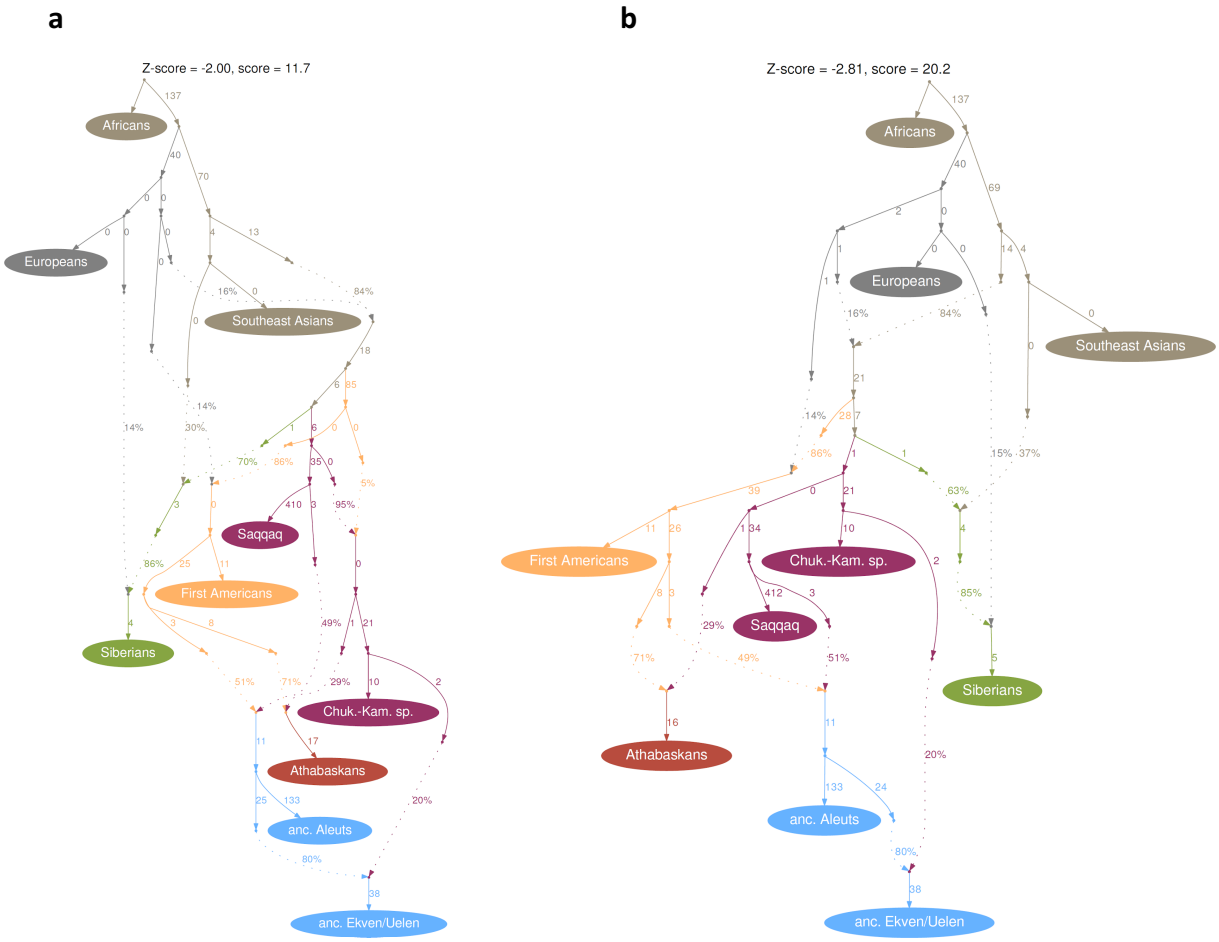

Fig. S10.2. Two fitting admixture graphs (based on the transition-free dataset) with unidirectional C-K to E-A gene flow, for other fitting topologies see Table S10.2. **a**, topology (*(ATH, C-K), (E-A, P-E)); **b**, topology (C-K, (ATH, (E-A, P-E))). The asterisk in the topology notation stands for the entry point of the "proto-American" gene flow.

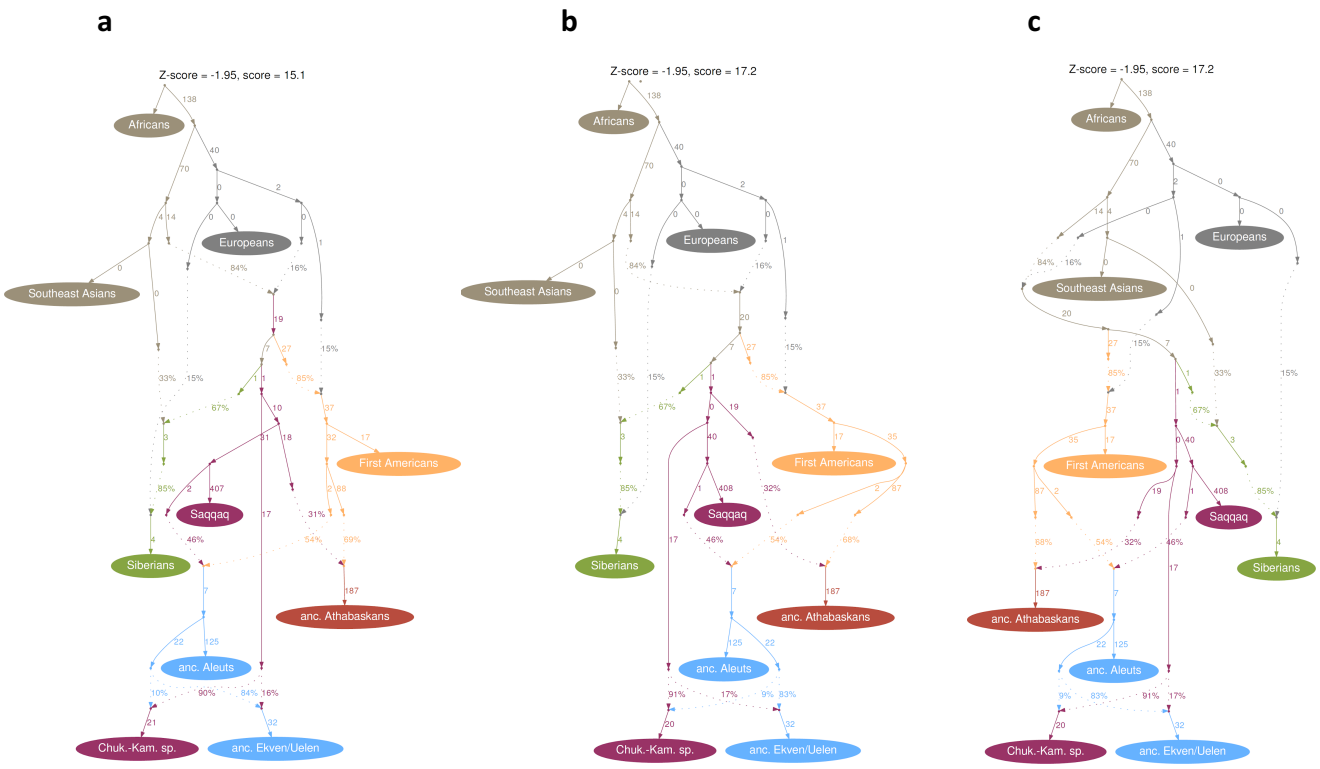

Fig. S10.3. Three best-fitting admixture graphs (based on the transition-free dataset) including ancient Athabaskans and a bidirectional C-K to E-A gene flow, for other fitting topologies see Table S10.4. **a**, topology (C-K, (ATH, (E-A, P-E))) having the highest likelihood and, the only fitting topology with no 0-length edges at key positions in the PPE clade; **b**, topology (ATH, (C-K, (E-A, P-E))); **c**, topology ((ATH, C-K), (E-A, P-E)). While the likelihood differences of these models are not significant, they are significant when using the full dataset including transitions, although all models fit worse in that case (see text).

10.3 Improving the West Eurasian and Native American sub-graphs

dataset: *transversions only*;

populations: *present-day meta-populations including Northern First Peoples*; *pseudo-haploid Saqqaq, ancient Aleuts, ancient Neo-Eskimos (Ekven+Uelen), ancient Athabaskans, Mal'ta (MA1), Loschbour, and the ancient Upward Sun River 1 individual.*

Next, we attempted to construct a more realistic model and added further ancient individuals onto the best-fitting graph including the merged Ekven+Uelen Old Bering Sea population and ancient Athabaskans. First, we tested all 5 possible placements of the Upward Sun River 1 individual (USR1, Moreno-Mayar et al. 2018) as an unadmixed branch within the First Peoples clade (Table S10.6). As demonstrated by Moreno-Mayar et al. (2018), USR1 occupies the most basal position within the clade, and this topology is by far the most supported. In parallel, we attempted constructing a more realistic model for present-day Europeans as a mixture of three sources (Lazaridis et al. 2014): western hunter-gatherers (WHG, represented by the Loschbour individual, Lazaridis et al. 2014); Siberian Paleolithic hunter-gatherers of European origin, also known as ancient North Eurasians (the Mal'ta 1 individual a.k.a. MA1, Raghavan et al. 2014); and early European farmers (EEF) with substantial basal Eurasian ancestry (Haak et al. 2015, Lazaridis et al. 2016), here represented by a ghost basal Eurasian branch. The Mal'ta-related gene flow was mediated by Yamnaya steppe pastoralists and followed the initial WHG-EEF admixture event (Allentoft et al. 2015, Haak et al. 2015). We constructed our models accordingly: first, a group related to WHG admixed with the basal Eurasian branch; second, a

Mal'ta-related West Eurasian lineage contributed to First Peoples, Siberians/PPE, and Europeans.

Initially we tested simpler models, where Europeans = a West Eurasian lineage + a basal Eurasian lineage. On this graph we tested all possible split points of MA1 within the West Eurasian clade (Table S10.7). Although all Z-scores were the same, the topology ((EUR, SIB), (MA1, (NEA, SAM))) was the single most plausible one from the perspective that it resulted in the smallest number of 0-length edges at key positions within the West Eurasian clade, and at the same time the basal Eurasian contribution in present-day Europeans was not overestimated (Fig. S10.4a). SIB here stands for the recent European admixture source in present-day Siberians, NEA and SAM - for Mal'ta-related admixture sources in northeast Asians (a group uniting Siberians, PPE, and Native Americans) and in Native Americans, respectively. Then we added WHG (Loschbour) onto the best graph from the previous step, switched to the 3-component model for Europeans described above, and tried to derive the gene flow into Europeans from all possible branches within the Mal'ta clade (Table S10.7). The topology ((WHG, (EUR<, SIB)), <(MA1, (NEA, SAM))) was probably the best one: it resulted in the smallest number of 0-length edges at key positions within the West Eurasian clade, and at the same time the basal Eurasian contribution in present-day Europeans was not overestimated (Fig. S10.4b). The "<" signs here show the direction of the Mal'ta-related gene flow in Europeans: from the (MA1, (NEA, SAM)) clade into EUR. We acknowledge that the model for Europeans should be even more complex and include Early European farmers and Yamnaya pastoralists or related herder groups explicitly. The latter population can be modelled as a roughly 50%-50% mixture of Mal'ta-related eastern hunter-gatherers (EHG) and Iranian farmers or related Caucasian hunter-gatherers (CHG) (Lazaridis et al. 2016). But in order to keep the number of groups in our final model (presented below) reasonably small, we preferred the simplified version that is anyway much more complex than the initial version including unadmixed Europeans (Fig. S10.3).

Next, we combined in the same model the updated West Eurasian clade with the updated Native American clade including the USR1 individual (associated with a major basal Native American population, termed Ancient Beringians (Moreno-Mayar et al 2018)), and again tried to derive the gene flow into Europeans from all possible branches within the Mal'ta clade (Table S10.8). The same best topology was recovered as in the previous search: ((WHG, (EUR<, SIB)), <(MA1, (NEA, SAM))). We further tested whether any USR1-related gene flow into Athabaskans improves the model fit. USR1 is associated with the Denali complex (Potter et al. 2014), which was replaced by the Northern Archaic tradition ca. 6000 calBP (Potter 2010). The Northern Archaic tradition likely includes ancestors of Na-Dene speakers given its geographic distribution and continuity with the recent past (Workman 1978). We tested various entry points for the USR1-related gene flow: into the common ancestor of ATH and the Native American source population of E-A, into ATH only, and into E-A ancestors only, and combined these topologies with 5 possible topologies of the Mal'ta-related gene flow into EUR. All models had 0-length edges at key positions in the Native American clade, or 0% admixture from the USR1 lineage in other lineages, or the model-fitting process failed (Table S10.8). Hence, we conclude that the gene flow from the USR1 branch into the Northern North American clade is unlikely to improve the model fit. This suggests Ancient Beringians were replaced by Northern Native Americans (including Na-Dene) around 6000 calBP in interior Alaska.

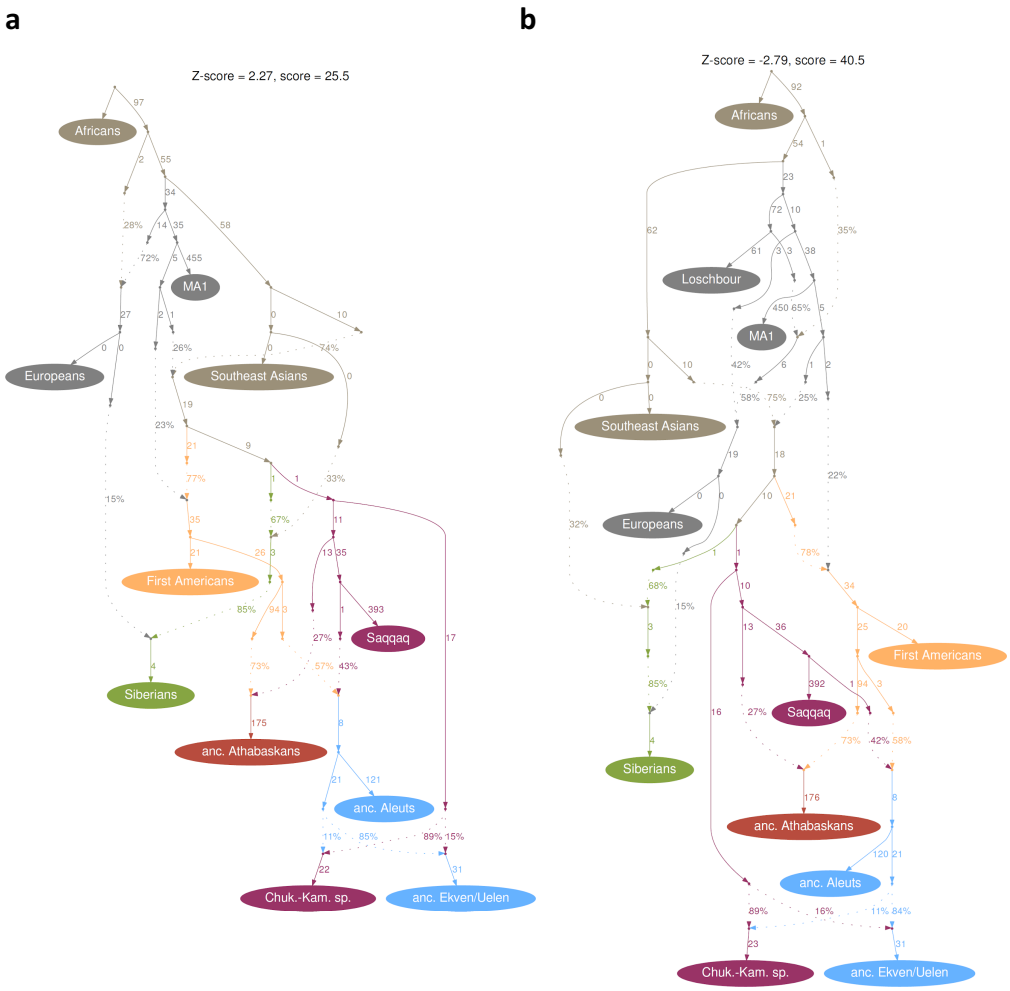

Fig. S10.4. Best-fitting admixture graphs (based on the transition-free dataset) including a two-component (**a**) or a three-component (**b**) model for Europeans.

We next included into the model other representatives of the Northern North American clade (a.k.a. Northern First Peoples or NAM) (Raghavan et al. 2015, Lindo et al. 2017, Scheib et al. 2018) besides Athabaskans: two Cree and one Tsimshian individual. This NAM branch required a recent European admixture and was placed at all possible positions within the Native American clade. Each topology was combined initially with the best 2-component model for Europeans, and also with three best-fitting 3-component models tested previously (Table S10.9). The best-fitting model of the latter class has a |Z-score| of 3.12, has no 0-length edges at key positions within the Native American, West Eurasian, and PPE clades, and the basal Eurasian contribution into Europeans stands at 34% (Fig. S10.5). Thus, the main part of the modeling process was finished. We believe that the Z-score of 3.12, although being higher than the commonly accepted threshold of 3, is a reasonably low score for such a complex model composed of 14 groups: present-day composite meta-populations and ancient individuals. The best model fits the data with only two outlying f_4-statistics with |Z-scores| > 3 (Table S10.10):

a) f_4(Southern First Peoples, USR1; ancient Aleuts, MA1), with the observed value larger than the expected value, Z-score = 3.123;

b) f_4(Southern First Peoples, USR1; Ekven+Uelen, MA1), with the observed value larger than the expected value, Z-score = 3.034.

These deviations might reflect elevated Mal'ta-related ancestry in the USR1 individual as compared to Southern First Peoples. To keep this complex graph as simple as possible, we avoided modeling separate Mal'ta-related gene flows into all relevant groups since that would

add 7 admixture events on top of 11 modelled currently.

Finally, we re-tested three by far best-fitting alternative topologies in the PPE clade (Table S10.4, Fig. S10.3) on the background of this complex model (Table S10.11). The topology (ATH, (C-K, (E-A, P-E))) (here again referring to the PPE components in those groups) resulted in a 0-length edge (a trifurcation), and the other two topologies showed no 0-length edges. The topology (C-K, (ATH, (E-A, P-E))) as compared to the topology ((ATH, C-K), (E-A, P-E)) published by Moreno-Mayar et al. (2018) had a 5.7 times higher likelihood and a slightly lower number of outlying f_4-statistics with absolute Z-scores > 2, 137 vs. 138 statistics (Table S10.11). A similar result was observed for the full dataset with transitions included: the topology (C-K, (ATH, (E-A, P-E))) as compared to the topology ((ATH, C-K), (E-A, P-E)) had a 9.4 times higher likelihood and a lower number of outlying f_4-statistics with absolute Z-scores > 2, 322 vs. 340 statistics (Table S10.11). The likelihood differences observed are suggestive, but not significant, and thus do not allow us to confidently pick one model. However, significant likelihood differences were observed for the simpler graph and the full dataset including transitions (see section 10.2). *Rarecoal*, another demographic modeling method we used, also provides better resolution (see section 9).

10.4 Testing all possible combinations of populations at key branches

dataset: *transversions only*;

populations: *separate present-day populations*; *pseudo-haploid Saqqaq, ancient Aleuts, ancient Neo-Eskimos (Ekven, Uelen), ancient Athabaskans, Mal'ta (MA1), Loschbour, ancient Upward Sun River 1 individual.*

To explore the best model further, instead of meta-populations we tested all possible combinations of separate populations. First, we returned to a simple model without the MA1, Loschbour, USR1, and NAM clades (Z-score = 1.95, Table S10.4, Fig. S10.3a) and tested separate populations in the merged SGDP+Raghavan et al.+ancient dataset (Supplementary Table 4) composed of two or more individuals at the following five branches in the graph : E-A (3 populations: Ekven, Uelen, Yup'ik; present-day Inuit cannot be simply integrated into this model since they require an additional pulse of recent European admixture); EUR (16 populations); SAM (7 populations, excluding Mayans and Mixtec having low-level European and/or African admixture); SEA (8 populations); SIB (10 populations, including an Ust'-Belaya Angara individual I7760 having the West Siberian genetic profile (section 4), abbreviated as UBS). To replace populations that were removed due to the minimum size requirement of 2 individuals, we considered some additional populations (Table S10.12) that were not included into the original meta-populations as defined in Table S10.1. Among 26,880 models tested, just 7% were non-fitting (|Z-score| > 3), and for one model the algorithm failed. Absolute Z-scores down to 0.91 were observed (2.19 on average among all models), and in 7 graphs no 0-length edges were found (4.9 on average among all models). See Table S10.12 for a full list of tested models and summary statistics. Since the simple topology is fitting for almost all combinations of populations, it is unlikely that the observed result depends on the composition of meta-populations.

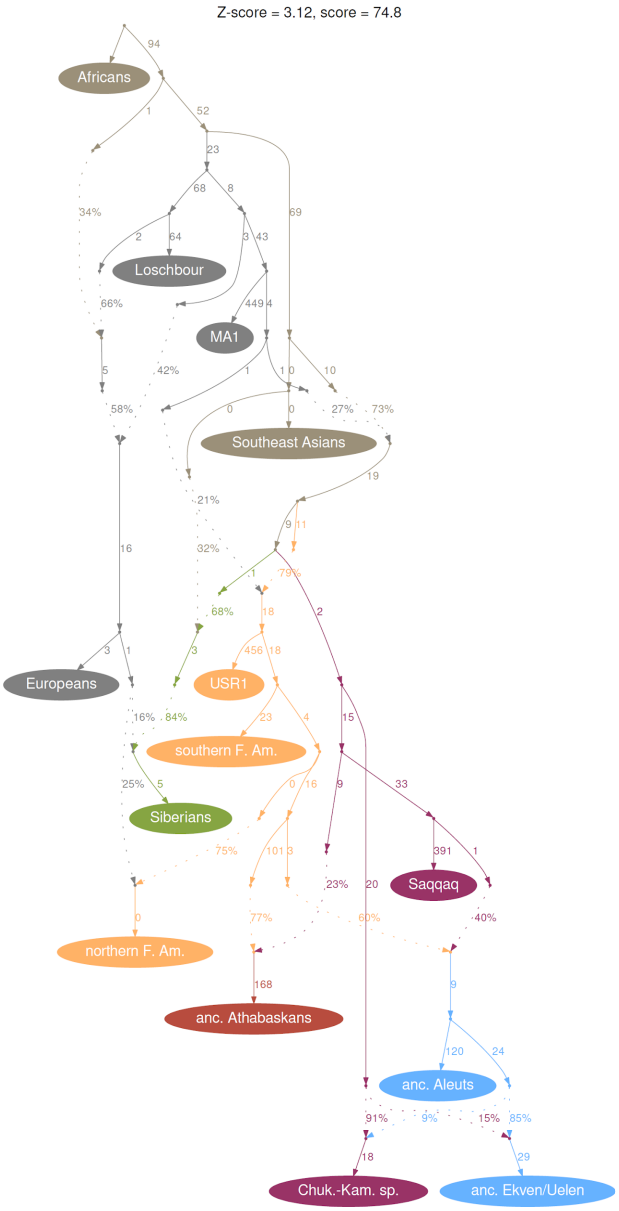

Fig. S10.5. The best-fitting admixture graph (based on the transition-free dataset) featuring a three-component model for Europeans and a complex American clade including the ancient USR1 individual and present-day Northern First Peoples (NAM).

Second, we attempted an even more exhaustive testing of population combinations at 6 branches for the most complex model (Z-score = 3.12, Fig. S10.5). We relaxed the population size requirement of 2 or more individuals and took the following populations (Table S10.13): E-A (3 populations: Ekven, Uelen, Yup'ik); EUR (19 populations); SAM (13 populations, including the Clovis ancient individual); NAM (2 populations); SEA (9 populations); SIB (10 populations, including the Ust'-Belaya Angara ancient individual I7760). Among 133,380 models tested, 12% had a |Z-score| < 4. Absolute Z-scores down to 2.98 were observed, and 4.8% of graphs had no 0-length edges at key positions within the EUR, PPE, and Native American clades.

We also re-tested three by far best-fitting alternative topologies in the PPE clade (Table S10.4, Fig. S10.3) on the background of this complex model with separate populations. First, we took 1,831 population combinations that yielded absolute Z-scores < 3.5 for the (C-K, (ATH, (E-A, P-E))) topology (Table S10.13) and tested the three topologies (Table S10.11). The topology (ATH, (C-K, (E-A, P-E))) was the worst one according to all metrics, and it also had the lowest likelihood among the three best meta-population-based models (Table S10.11),

therefore we excluded it from further testing. Then we tested 133,380 population combinations for the topologies (C-K, (ATH, (E-A, P-E))) and ((ATH, C-K), (E-A, P-E))). We find that both topologies are favored by some combinations of populations, with the topology (C-K, (ATH, (E-A, P-E))) winning more often in terms of absolute Z-scores and higher likelihoods than the topology ((ATH, C-K), (E-A, P-E)) (Table S10.14). Although the distributions of likelihoods over 133,380 population combinations are largely overlapping (Table S10.14), median likelihood of the topology (C-K, (ATH, (E-A, P-E))) is 58.5 higher than that of the topology ((ATH, C-K), (E-A, P-E)), a significant difference according to our arguments from section 10.2. On average, the topology ((ATH, C-K), (E-A, P-E)) also yields more 0-length edges within the PPE clade (2.3 vs. 1.5 edges), which in particular includes many cases with a trifurcation of the form (ATH, C-K, (E-A, P-E)), and also yields a larger number of outlying f_4-statistics with absolute Z-scores > 2 (409 vs. 379 statistics).

Overall, the outcome of the model testing with separate populations is the same as that of the meta-population approach, which arguably has a higher resolution due to larger number of individuals per populations, and may be less prone to overfitting. Thus, we favor the topology (C-K, (ATH, (E-A, P-E))) over the alternative ((C-K, ATH), (E-A, P-E)), although the difficulty of distinguishing between the two topologies may also reflect the possibility of a near-trifurcation of the three groups C-K, ATH, and (E-A, P-E).

To obtain an independent hypothesis test for the PPE topology, we performed demographic modeling with *Rarecoal* (section 9), as well as exhaustive testing of population triplets and quadruplets using *qpWave* and *qpAdm* with various outgroup sets (section 5).

References (for this section)

Allentoft, M. E. *et al*. Population genomics of Bronze Age Eurasia. *Nature* **522**, 167–172.

Haak, W. *et al*. Massive migration from the steppe was a source for Indo-European languages in Europe. *Nature* **522**, 207–211 (2015).

Lazaridis, I. *et al*. Ancient human genomes suggest three ancestral populations for present-day Europeans. *Nature* **513**, 409–413 (2014).

Lazaridis, I. *et al*. Genomic Insights into the Origin of Farming in the Ancient Near East. *Nature* **536**, 419–424 (2016).

Lindo, J. *et al*. Ancient individuals from the North American Northwest Coast reveal 10,000 years of regional genetic continuity. *Proc. Natl. Acad. Sci. U. S. A*. **114**, 4093–4098 (2017).

Moreno-Mayar, J. V. *et al*. Terminal Pleistocene Alaskan genome reveals first founding population of Native Americans. *Nature* **553**, 203–207 (2018).

Potter, B. A. Archaeological patterning in Northeast Asia and Northwest North America: an examination of the Dene-Yeniseian hypothesis. *The Dene-Yeniseian Connection*, ed. Kari, J., Potter, B. A. *Anthropological Papers of the University of Alaska: New Series* **5**, 138–167 (2010).

Potter, B. A. *et al*. New insights into Eastern Beringian mortuary behavior: a terminal Pleistocene double infant burial at Upward Sun River. *Proc. Natl. Acad. Sci. U. S. A.* **111**, :17060–17065 (2014).

Raghavan, M. *et al*. Upper Palaeolithic Siberian genome reveals dual ancestry of Native Americans. *Nature* **505**, 87–91 (2014).

Raghavan, M. *et al*. Genomic evidence for the Pleistocene and recent population history of Native Americans. *Science* **349**, 1–20 (2015).

Scheib, C. L. *et al*. Ancient human parallel lineages within North America contributed to a coastal expansion. *Science* **360**, 1024–1027 (2018).

Workman, W. B. The Prehistory of the Aishihik-Kluane area, southwest Yukon Territory. *National Museum of Man, Mercury Series* No. 74 (1978).

Supplementary Information section 11

Additional results on Aleutian population history

A controversial chapter of American Arctic prehistory concerns Aleuts (Balter 2012). The Aleutian Islands were settled much earlier than the American Arctic, about 9,000 calBP (Hatfield 2010), and discontinuities in the Aleutian archaeological record were observed at ~4,500 calBP (Knecht and Davis 2001, Hatfield 2010, Davis et al. 2016) and at ~800 – 900 calBP (Brenner Coltrain et al. 2006, Hatfield 2010). The first discontinuity was associated with Paleo-Eskimo influence, which is consistent with the final model presented in this study, and the latter with Neo-Eskimo influence, although the extent of technological interactions, and the role of genetic continuity vs. population replacement is debated (Brenner Coltrain et al. 2006, Smith et al. 2009, Misarti and Maschner et al. 2015). Three burial sites in the eastern Aleutian Islands received most attention so far: the Chaluka midden site on the Umnak Island was associated with an early population (3,600 – 300 calBP) with a dolichocranic morphology, inhumation burials (Hrdlička 1945, Brenner Coltrain et al. 2006) and a predominance of mtDNA haplogroup A2a (Smith et al. 2009). Other sites, at the Kagamil and Ship Rock Islands, were associated with a later population (800 – 900 calBP and later), a brachycranic morphology, mummification burials (Hrdlička 1945, Brenner Coltrain et al. 2006) and a predominance of mtDNA haplogroup D2a (Smith et al. 2009). The former population has been historically termed Paleo-Aleut, and the latter Neo-Aleut.

We carried out a small-scale sampling of ancient genomes from all three sites (Extended Data Table 1). Radiocarbon dates obtained for these individuals in a previous study (Brenner Coltrain et al. 2006) were recalibrated using a more appropriate marine reservoir correction (Misarti and Maschner 2015) resulting in the following median dates: 2,050 – 530 calBP for Paleo-Aleuts and 580 – 280 calBP for Neo-Aleuts (Supplementary Table 2, Supplementary Information section 2). Among 11 ancient Aleuts subjected to in-solution target enrichment of more than 1.2 million SNPs using a protocol by Fu *et al.* (2015), 4 Neo-Aleuts and 2 Paleo-Aleuts passed the 70% missing rate cut-offs that we applied in order to permit high-density SNP analyses and were incorporated into both the HumanOrigins and Illumina SNP array datasets (Supplementary Table 4). In addition, one Paleo-Aleut individual dated to 700 – 310 calBP (IDs I0719 and 378620, the latter used by Brenner Coltrain et al. 2006) was sequenced with the shotgun approach at 2.3x coverage (with filtered reads). Due to low coverage of both the enrichment and shotgun data, only pseudo-haploid SNP calls were generated for ancient Aleuts, hence these samples were used for *qpWave*/*qpAdm*, PCA, *ADMIXTURE*, *ALDER*, and rare allele sharing analyses only.

Analyzing these data, we found that four Neo-Aleut samples with median dates between 580 – 340 calBP and two Paleo-Aleut samples dated to 1260 – 870 and 700 – 310 calBP are indistinguishable. In particular, in both the HumanOrigins and Illumina datasets, the Paleo- and Neo-Aleuts were indistinguishable according to PCA (Fig. 1a, Extended Data Fig. 2, section 4) and *ADMIXTURE* patterns (Extended Data Fig. 8), showing that the Neo-Aleuts arose directly form the Paleo-Aleuts and contradicting suggestions – based on morphology (Hrdlička 1945) and mitochondrial DNA haplogroup frequency changes (Smith et al. 2009) – that the transition between Paleo- and Neo-Aleuts was driven by a new migration into the islands from the outside. Pooling the six ancient Aleuts together for *qpWave*/*qpAdm* and *qpGraph* analyses (sections 5 and 10), we find that both groups have a strong Neo-Eskimo genetic affiliation, and in this respect are similar to present-day Aleuts. In addition, the single Paleo-Aleut genome (I0719) that we generated was placed into the Aleut branch with high certainty using *Rarecoal* (Fig. 2b, section 9).

We also used this first data from the Aleutian Islands prior to European colonization to test a claim by Raghavan *et al*. (2015) of a genetic affinity between Papuans and Aleuts. The original study attempted to account for the substantial amounts of recent European ancestry in the

present-day Aleutian individuals analyzed by identifying and excluding segments of the genomes that could be reliably called as European in ancestry. However, this procedure could in principle have introduced bias that affected the original reported signal that had a significance level of Z=2 to Z=3 (because the ancestry inference is not perfect and may selectively exclude segments of non-colonial ancestry with greater or lesser affinity to Papuans). We thus used *D*-statistics to test whether there was evidence of an excess affinity to Papuans in the ancient Aleuts, using a variety of subsets of the data, but find no evidence of an excess affinity to Papuans (Z<2) (Table S11.1). These results suggest that an excess affinity to Australo-Melanesians is exclusively found in South America and primarily observed in Amazonian populations (Skoglund et al. 2015).

Table S11.1. Aleutian ancient DNA shows no evidence of Papuan-related gene flow hypothesized by Raghavan *et al*. (2015) on the basis of present-day European-admixed Aleuts. The following *D*-statistics were calculated: *D*(A, B; X, Y), where A=Yoruba or Dai; B=Papuans, Australians, or Onge; X=Mixe; Y=Neo-Aleuts, Paleo-Aleuts, Ancient Aleuts combined, or Surui. Z-scores are color-coded: Z > 3 in red, and 2 < Z < 3 in yellow.

				pop Y							
				Neo-Aleut	Paleo-Aleut	ancient Aleuts combined	Surui	Neo-Aleut	Paleo-Aleut	ancient Aleuts combined	Surui
dataset	treatment	pop A, pop B	pop X	Z-scores				informative SNPs			
HumanOrigins (Lazaridis et al. 2014)	normal	Yoruba, Australian	Mixe	0.7	1.63	1.43	1.67	272,013	275,100	306,158	314,186
		Yoruba, Papuan		0.65	1.46	1.31	2.88	274,210	277,200	308,606	316,685
		Yoruba, Onge		0.85	1.32	1.41	3.87	273,679	276,757	308,026	316,118
		Dai, Australian		-1.34	-0.91	-1.21	1.08	262,660	265,765	295,150	302,843
		Dai, Papuan		-1.51	-1.28	-1.52	2.29	267,002	270,010	300,081	307,977
		Dai, Onge		-1.54	-1.78	-1.79	3.26	265,435	268,527	298,351	306,289
	no transitions	Yoruba, Australian		-0.18	0.76	0.06	0.85	50,109	51,071	56,733	58,428
		Yoruba, Papuan		-0.34	1.18	-0.03	2.11	50,487	51,441	57,158	58,866
		Yoruba, Onge		0.15	1.29	0.83	3	50,415	51,366	57,073	58,770
		Dai, Australian		-1.53	-1.29	-1.69	0.72	48,383	49,290	54,706	56,306
		Dai, Papuan		-1.74	-1.03	-1.93	2.05	49,161	50,067	55,601	57,250
		Dai, Onge		-1.43	-1.11	-1.24	3.08	48,864	49,762	55,263	56,918
genomes (Mallick et al. 2016)	normal	Yoruba.DG, Australian.DG		2.01	2.68	2.37	3.65	433,909	405,920	494,182	506,885
		Yoruba.DG, Papuan.DG		1.56	1.9	1.86	4.06	459,513	428,834	523,154	536,078
		Yoruba.DG, Onge.DG		2	2.01	2.25	3.27	432,997	405,045	493,166	506,158
		Dai.DG, Australian.DG		-1.28	-0.92	-1.24	2.13	442,560	413,584	503,073	516,854
		Dai.DG, Papuan.DG		-1.96	-2.02	-2.09	2.68	460,213	429,322	523,311	536,979
		Dai.DG, Onge.DG		-1.35	-1.65	-1.45	1.59	441,305	412,384	501,610	515,733
	no transitions	Yoruba.DG, Australian.DG		0.8	1.3	0.95	1.62	84,512	79,527	97,011	101,213
		Yoruba.DG, Papuan.DG		0.76	1.58	1.05	2.66	89,441	83,985	102,642	107,037
		Yoruba.DG, Onge.DG		1.65	2.81	2.59	2.05	84,355	79,368	96,826	101,115
		Dai.DG, Australian.DG		-1.75	-2.11	-2.2	1.06	86,131	80,979	98,740	103,131
		Dai.DG, Papuan.DG		-1.94	-2.13	-2.36	2.18	89,599	84,130	102,768	107,298
		Dai.DG, Onge.DG		-0.88	-0.56	-0.6	1.38	85,861	80,703	98,441	102,861

References (for this section)

Balter, M. The peopling of the Aleutians. *Science* **335**, 158–161 (2012).

Brenner Coltrain, J. B., Hayes, M.G. & O'Rourke D.H. Hrdlička's Aleutian population-replacement hypothesis. A radiometric evaluation. *Curr. Anthropol.* **47**, 537–548 (2006).

Davis, R., Knecht, R. & Rogers, J. First Maritime Cultures of the Aleutians. *The Oxford Handbook of the Prehistoric Arctic*, ed. Friesen, T. M., Mason, O. K. New York: Oxford University Press. 279–302 (2016).

Fu, Q. *et al*. An early modern human from Romania with a recent Neanderthal ancestor. *Nature* **524**, 216–219 (2015).

Hatfield, V. L. Material culture across the Aleutian archipelago. *Hum. Biol*. **82**, 525–556 (2010).

Hrdlička, A. *The Aleutian and Commander Islands and their inhabitants*. Philadelphia: Wistar Institute of Anatomy and Biology (1945).

Knecht, R. A. & Davis, R. S. A prehistoric sequence for the eastern Aleutians. *Archaeology in the Aleut zone of Alaska: Some recent research*, ed. Dumond, D. *University of Oregon Anthropological Papers* **58**, 269–288 (2001).

Misarti, N. & Maschner, H. D. G. The Paleo-Aleut to Neo-Aleut transition revisited. *J. Anthropol. Archaeol*. **37**, 67–84 (2015).

Raghavan, M. *et al*. Genomic evidence for the Pleistocene and recent population history of Native Americans. *Science* **349**, 1–20 (2015).

Skoglund, P. *et al*. Genetic evidence for two founding populations of the Americas. *Nature* **525**, 104–108 (2015).

Smith, S. *et al*. Inferring population continuity versus replacement with aDNA: A cautionary tale from the Aleutian Islands. *Hum. Biol.* **81**, 19–38 (2009).

Supplementary Information section 12

Dating admixture events using *ALDER*

We have dated the Paleo-Eskimo admixture event in Na-Dene speakers using the *GLOBETROTTER* method (section 7). In addition, we applied a different linkage disequilibrium (LD)-based method, *ALDER*, that relies on allele frequency data at SNP sites and can accommodate pseudo-haploid ancient data (Loh et al. 2013). Although a single-pulse admixture model implemented in *ALDER* is likely to be an oversimplification, it can still provide a reasonable time frame for the admixture events. *ALDER v.1.03* works in the following way (Loh et al. 2013): 1/ builds a weighted LD-decay curve given a test population and a pair of reference populations related to the admixture partners; 2/ estimates a jackknife-based *p*-value and Z-score by leaving out each chromosome in turn and refitting the decay curve; 3/ determines the distance to which LD in the test population is significantly correlated with LD in either reference A or reference B; 4/ to minimize signal from shared demographic history, data from SNP pairs at distances smaller than this correlation threshold are ignored; 4/ computes additional LD curves and associated *p*-values and Z-scores, substituting either reference A or B by the test population. If the test population is admixed between populations related to references A and B, the one-reference curves are expected to pick up the same LD decay signal. If the test population is not admixed but has experienced a shared bottleneck with one of the reference groups, an LD decay curve is unlikely to emerge. Thus, if the two-reference test and both one-reference tests yield Z-scores > 2, the *ALDER* test is considered successful. This test procedure is intended to be conservative (Loh et al. 2013).

In Table S12.1 *ALDER* results for present-day and ancient E-A groups are summarized. Outcomes of two-reference tests that yielded *p*-values < 0.05 (Z-scores > 2) are shown. Target groups composed of 4 or more individuals were suitable for this analysis. Various First Peoples (SAM or NAM) and Saqqaq were used as surrogates for the admixture partners. Given the strong support we have obtained for the *qpGraph* and *qpAdm* models "E-A = FAM + P-E" (sections 5 and 10), we expected similar models to be supported by *ALDER*. On the other hand, the additional pulse of C-K admixture in Yup'ik and Inuit ancestors is expected to compromise the *ALDER* results: populations with complicated histories (e.g., multiple waves of admixture) often have different estimates of admixture dates with one- and two-reference LD-decay curves (Loh et al. 2013).

Here we consider the *ALDER* results population by population (HumanOrigins dataset, Table S12.1). First, for Iñupiat, a relatively large present-day population of 15 individuals without noticeable colonial European admixture and having a low level of C-K admixture (judging by the overall PPE ancestry proportion, see section 5), most *ALDER* admixture tests were successful (16 of 22 tests with different FAM references), and a further 5 tests were nearly successful (Z-scores for a one-reference test with a FAM group > 1.84). Upper and lower boundaries of the SD interval around the admixture date were averaged across all FAM surrogates, and thus the admixture date probably falls between 2,700 and 4,400 years ago (ya, values rounded to the nearest century, see Table S12.1). This is a broad range, but it fits two important archaeological constraints: the arrival of P-E to Alaska ca. 5,000 calBP and the emergence of Chukotkan Neo-Eskimos in the archaeological record ca. 2,200 calBP in the form of the Old Bering Sea culture (Mason et al. 2016). We expect that the formative admixture event that gave rise to Eskimo-Aleut speakers happened at least few centuries before the back-migration of Yup'ik and Inuit ancestors to Chukotka, thus the estimate of 2,700 ya and earlier seems realistic.

Ancient Aleuts are expected to yield “cleaner” results because of the absence of the C-K gene flow (section 10), however this group is composed of just 6 pseudo-haploid non-contemporaneous samples (Supplementary Table 2). Although 8 FAM surrogates resulted in two-reference *p*-values < 0.05, all one-reference pre-tests (ancient Aleuts + FAM as references) failed (Table S12.1), probably due to lack of power. Reassuringly, admixture dates averaged across these 8 tests are similar to those obtained for Iñupiat: 2,700 ya to 4,900 ya. For calculating these dates, we introduced an offset of 600 ya by averaging the calibrated radiocarbon dates obtained for the 6 ancient Aleut individuals analyzed here (Supplementary Table 2) and rounding to the nearest hundredth. The admixture dates estimated for the ancient Ekven population (16 ind.) were roughly 400 years older (Table S12.1). For this population, we introduced an offset of 1000 ya by averaging the calibrated radiocarbon dates obtained for the 16 ancient individuals buried at Ekven and analyzed here (Supplementary Table 2) and rounding to the nearest hundredth. The admixture dates estimated for two present-day Yup'ik groups (9 and 15 ind.) were even older than those for Ekven (Table S12.1). The results for the Yup'ik and Ekven groups were most probably confounded by a high proportion of PPE ancestry contributed by the second (C-K) gene flow (Extended Data Fig. 8, sections 5, 8, and 10).

References (for this section)

Loh, P. R. *et al*. Inferring admixture histories of human populations using linkage disequilibrium. *Genetics* **193**, 1233–1254 (2013).

Mason, O. K. The Old Bering Sea florescence about Bering Strait. *The Oxford Handbook of the Prehistoric Arctic*, ed. Friesen, T. M., Mason, O. K. New York: Oxford University Press. 417–442 (2016).

Supplementary Information section 13

Overview of the Dene-Yeniseian linguistic hypothesis

by Edward J. Vajda

The Dene-Yeniseian language hypothesis is considered here in light of the demonstrated Paleo-Eskimo genetic contribution to modern Tlingit, Eyak and Athabaskan speakers dated to ~4,400-5,000 ya and shared more distantly with Siberians at a time depth of ~6,200 ya (Table S9.2). The timing of this genetic link and plausible archaeological patterning described below provide the first evidence apart from linguistics that realistically supports the Dene-Yeniseian language hypothesis. Given that Paleo-Eskimo-related ancestry is likewise found in populations speaking Eskimo-Aleut and Chukotko-Kamchatkan languages, the Paleo-Eskimo linguistic legacy could instead be associated with the origins of either of these families rather than with Dene-Yeniseian. However, because the accumulated Dene-Yeniseian and internal Na-Dene comparative linguistic evidence correlates so plausibly with the coalescence dates of the Paleo-Eskimo genetic loci shared by populations speaking precisely these languages, it is useful to elaborate further on the potential significance of these results for situating the Dene-Yeniseian language family in space and time – questions left without clear answers in Kari and Potter (2010) and the genetic results of this paper.

The Dene-Yeniseian hypothesis posits that the Ket language spoken near the Yenisei River in Central Siberia is related to the widespread Na-Dene language family in North America. Na-Dene comprises Tlingit and the recently extinct Eyak in Alaska along with over thirty Athabaskan languages spoken from the western North American Subarctic to pockets in California (Hupa), Oregon (Tolowa) and the American Southwest (Navajo, Apache) (Krauss 1976). The severely endangered Ket is the sole survivor of Siberia's once widespread Yeniseian language family, whose ancient presence in the region predates the expansion of reindeer breeders and other pastoralists in North and Inner Asia (Dul'zon 1959, 1962, Vajda 2001, 2009, Werner 2005). Dene-Yeniseian as a linguistic hypothesis dates back to at least 1923, when Italian linguist Alfredo Trombetti linked Athabaskan and Tlingit with Ket on the basis of a few similar-sounding words (Trombetti 1923). In the past two decades new evidence supporting the connection has been published in the form of shared morphological systems and lexical cognates showing interlocking sound correspondences (Ruhlen 1998, Vajda 2001, Werner 2004, Vajda 2010a, 2010b). However, Dene-Yeniseian cannot be accepted as a proven language family until the evidence of lexical and morphological correspondences between Yeniseian and Na-Dene is significantly expanded and tested by further critical analysis. It will also be essential to determine the potential relationship between Yeniseian and Old World languages and families such as Sino-Tibetan, North Caucasian, and the Burushaski isolate of northern Pakistan – all of which have been proposed at various times in the past as relatives of Yeniseian, and sometimes also of Na-Dene (G. Starostin 2010). While parallel research from genetics, archaeology and folklore studies cannot prove a language connection (only comparative linguistic analysis can accomplish that), interdisciplinary archaeological and genetic studies can demonstrate in important ways the plausibility or implausibility of such a connection, as well as situating populations in space and time.

The timing of the Dene-Yeniseian language split could shed important light on Native American as well as North Asian prehistory. In attempting to reconcile the apparent closeness of Yeniseian and Na-Dene grammatical homologies with what at the time was assumed to be a much greater genetic distance between Ket and Na-Dene speakers, Potter (2010) discussed a number of possible scenarios for the Dene-Yeniseian connection, including: 1) a Late

Pleistocene separation connected with the Paleo-Indian migrations into the Americas, with an extraordinary slow rate of linguistic change; 2) a separation involving a back migration of Yeniseians from Beringia; and 3) an Early to Mid-Holocene separation connected with the entrance into Alaska around 5,000 calBP by the population associated with the Arctic Small Tool tradition (ASTt) (see also Dumond 2010). The first two scenarios are unlikely based on results from this paper, while the third becomes more plausible (see below).

In contrast to the ability of archaeologists to radiocarbon-date their finds, or geneticists to calibrate the time separating two related populations, there is no universally accepted method to reliably and precisely compute the time of separation of languages known to be genealogically related. All proposed methods of dating prehistoric language splits have been criticized (Campbell 2013:447-492). McMahon & McMahon (2005: 177-204) distinguish between methods of establishing relatedness or degrees of relatedness between languages (lexicostatistics) from the use of such data to assign precise dates for prehistoric language splits based on an assumed regular rate of linguistic change (glottochronology), which in fact does not exist across languages or even in a single language over time. While rejecting glottochronology, McMahon & McMahon (2005:204) support the value of gathering and comparing lexicostatistic data, which then can sometimes be useful for purposes of dating when combined with facts from other disciplines such as archaeology and genetics. Several types of evidence can potentially be combined with evidence of shared vocabulary and grammatical homologies to help narrow the range of plausible separation dates between related languages. For Dene-Yeniseian, all of them suggest a split roughly between 9,000 and 7,000±500 ya. The shallower end is favored by the detailed morphological homologies shared by the two families (Nichols 2010). The deeper end, which is suggested by the more meager number of shared lexical cognates, would still be far too shallow to match a connection with the earliest Paleo-Indian migrations during the Late Pleistocene. However, this range does provide a realistic temporal parallel for the migration of ASTt ancestors from North Asia into the Americas about 5,000 calBP. If this population consisted of Pre-Proto-Na-Dene speakers, then the split with their Yeniseian-speaking cousins in south-central Siberia would necessarily have been earlier.

Most previous calculations by historical linguists place the timeline for the internal diversification of Na-Dene languages between 6,000 and 3,500 ya. All Athabaskan languages, whether spoken in Alaska, Canada, California, or Arizona, share over 70% cognates in basic vocabulary, the number becoming higher if the list includes words associated with northern boreal forest lifeways, such as ‘birch’, ‘wolverine’, etc. Krauss (1976:330) showed that all Athabaskan languages share 33% of basic vocabulary from the 100-word Swadesh List with Eyak. Athabaskan-Eyak, in turn, is clearly more distantly related to the Tlingit dialect cluster spoken in the southeast Alaskan coast and parts of interior Yukon Territory (Heggarty & Renfrew 2014:1236). Using a variety of lexicostatistic methods and reliable data, Krauss (1976:333) estimated a time depth for Proto-Athabaskan of 2,400±500 years and for Athabaskan-Eyak of 3,400±500 years. Estimates for the earlier breakup of Tlingit and Athabaskan-Eyak range from 6,000 (Mülenbernd & Rama 2017) or 5,000 years (Swadesh 1958) to as shallow as 3,500 years (Kaufman & Golla 2000), with an estimate of 4,500 years by Krauss (1980:11-13). The deeper dates would be favored by the known conservatism of Na-Dene languages and also by the fact that the phylogenetic relationship between Athabaskan-Eyak-Tlingit (Na-Dene) was universally accepted only in the past decade, despite being suspected for over a century (Campbell 2011). The late acceptance date derives mainly from the fact that before Leer (2010), the evidence for Athabaskan-Eyak-Tlingit in the form of shared finite verb structure significantly outweighed the expected parallel lexical evidence, making it unclear whether language mixing rather than genetic inheritance was involved in the historical

similarities between these languages.

The relatedness between Athabaskan languages, despite their far-flung geography, is close enough that it has never been in doubt (Campbell 1997). This suggests a rapid spread from a common source, most likely somewhere in Northwestern Canada near the current border between British Columbia and Alaska or in adjacent parts of Interior Alaska. Another support for a recent dispersal is the high rate of mutual intelligibility between geographically distant Athabaskan languages (Krauss 1976). Some scholars posit a time depth for Proto-Athabaskan as shallow as 2,000 ya (Kaufman & Golla 2000), though a date closer to 3,000 is more likely given the resistance to borrowing observed with all of these languages. A time depth of at least 2,500 years for Athabaskan, following the estimate in Krauss (1976), would concur with the westward spread of the Taltheilei Culture beginning 2,750 calBP, which has been previously linked with the spread of Athabaskan speakers (Potter 2010, Kari 2010).

The interior Alaskan and northwestern Canadian portions of the Athabaskan range show no clear archaeological evidence of prehistoric population replacement during the past ~6000 years (Potter 2010, Kari 2010). For this reason, Kari (2010) posits that the Athabaskans have lived in interior northwestern North America for at least that span of time. Kari cites the near complete absence of substrate place names in the Northern Athabaskan areas as evidence for their ancient occupation of these areas. However, the Navajo and Apache areas of the American Southwest likewise have virtually no toponymic substrate from the languages previously spoken there, yet the Athabaskan presence in this area dates no farther back than 1,200 calBP. This reflects a strong Athabaskan avoidance of borrowing place names rather than ancient occupancy. In any event, such a degree of linguistic conservatism, whereby geographically distant languages maintain mutual intelligibility over a span of ~6000 years, would be unique and unprecedented. After adjusting for the conservatism of Na-Dene languages, retention rates for vocabulary and grammatical structures would appear to support a time depth of 5,000±500 years for the ancestral Athabaskan-Eyak-Tlingit language (i.e., Proto-Na-Dene). This coheres well with the possibility that the language ancestral to Na-Dene could have been introduced around 5,000 ya into Alaska by North Asian immigrants associated with the later development and spread of the ASTt. Also probably connected with these "Paleo-Eskimos" is the spread of other elements of North Asian material culture and folklore (Alekseenko 1995; Berezkin 2015) to the Na-Dene.

Like the Athabaskan family, Yeniseian languages are obviously related genealogically. Ket and its now extinct relatives (Yugh, Kott, Assan, Arin, and Pumpokol) were recognized as closely related more than 150 years ago (Vajda 2001). Studies of substrate toponyms (Vajda 2018b) show that the known Yeniseian daughter branches (except the Ket-Yugh sub-branch) had already diversified by 2,000 ya, when Turkic and Uralic-speaking pastoralists started displacing them in most of their southern and western territory, acquiring Ket-related river names and other substrate linguistic elements in the process. If the main sub-branching existed 2,000 years ago, the family is clearly older. The high rate of shared cognates in basic vocabulary (over 70%) between Ket and Kott, which belong to different primary branches of the family, suggest that Proto-Yeniseian must be at least 2,500 to 3,000 years, if not older, which would roughly match the more plausible estimates of time depth for Athabaskan. It is possible to reconstruct Proto-Yeniseian vocabulary (Starostin 1995) and many aspects of grammatical structure (Vajda 2013; Vajda 2017) with a high degree of confidence. If Para-Yeniseian linguistic relatives once existed in other parts of North Asia, the influx of pastoral tribes from the south must have obliterated them during the past 3,000 years, leaving no observable traces. Taking into account the probability of language extinction, the breakup of the earliest Proto-Yeniseian language, one predating the form reconstructable on the basis of Ket and Kott, could conceivably have begun earlier than 3,000 ya.

All Na-Dene languages share innovations demonstrating their equidistance from Yeniseian, whose split from the language ancestral to Na-Dene must be older than Proto-Na-Dene itself. To cite one particularly vivid example, Pre-Proto-Na-Dene restructured three of its inherited Dene-Yeniseian verb prefixes into the so-called classifier complex, for which the family is well known. All three component prefixes have cognates in Yeniseian but did not develop the characteristic function of transitivity increase and decrease found in all Na-Dene languages (Vajda 2016, 2017, 2018a). Contrary to Holton and Sicoli (2014), there is no linguistic evidence indicating a back migration into Asia of Yeniseian speakers from Beringia after Na-Dene had already begun to diversify.

The evidence supporting Dene-Yeniseian so far appears asymmetrically stronger in the realm of shared morphology than in the lexicon (Nichols 2010). The number and specificity of homologies in verb structure on their own would seem to preclude a separation earlier than the Mid-Holocene. Given the low number of lexical cognates, the time depth of Dene-Yeniseian may be twice that of Na-Dene. So far, the number of proposed Dene-Yeniseian cognates, even if all of them are valid, is less than half the number shared between Tlingit and Athabaskan-Eyak. If the Dene-Yeniseian linguistic link is fully demonstrable, however, substantially more abundant evidence of lexical cognates should be expected to emerge as the sound correspondences shared between the two families are fully worked out, favoring a shallower time depth range in line with the morphological evidence. This would repeat the historiography of Athabaskan-Eyak-Tlingit comparative linguistic studies, whereby the family's striking parallels in verb morphology were successfully identified well in advance of the accumulation of a large enough body of cognates in basic vocabulary to support a full range of systematic sound correspondences between Tlingit and Athabaskan-Eyak and fully demonstrate the Na-Dene family.

Though linguistic science can only rarely offer precise dates for prehistoric language splits, few linguists would claim it is not possible to distinguish a split that occurred two or three thousand years ago from one that is at least six or seven thousand years old. The evidence that can be brought to bear on the possible time depth of the lexical and grammatical homologies shared by Yeniseian and Na-Dene all point roughly to an Early to Mid-Holocene date of 9,000 to 7,000 ya as a plausible time depth for the breakup of Dene-Yeniseian. A separation date significantly earlier than 9,000 ya would be incompatible with generally accepted facts about language change, while a date significantly more recent than 7,000 ya is contradicted by the fact that Na-Dene itself shows evidence of internal diversification that likely began at least 4,500 ya (Krauss 1976). Both the grammatical and lexical comparative data indicate that the Dene-Yeniseian connection is significantly deeper than Proto-Na-Dene but still detectable using the Comparative Method. The accumulated linguistic and genetic evidence preclude the possibility that the Dene-Yeniseian connection dates back to the original peopling of the Americas from a common Beringian population, or that the Yeniseians derive from a recent back migration from Alaska across Bering Strait. Rather, the connection of Dene-Yeniseian with the ASTt migration, first suggested explicitly by Dumond (2010) and Potter (2010), appears increasingly plausible. These early suggestions assumed a congruence between language, material culture, and genetics, and did not consider more complex admixture models.

However, the language(s) of a prehistoric population can never be identified based on DNA studies alone, and pairing genetic and linguistic data to hypothesize about the language of the founding ASTt population yields at least four additional possibilities. The ASTt / Paleo-Eskimo people could have spoken a language that disappeared leaving no living descendants. A second possibility is that the material culture known as ASTt, along with related Siberian Neolithic groups, could reflect multiple populations speaking different languages, including

Proto-Eskimo-Aleut, Proto-Na-Dene, Proto-Chukotko-Kamchatkan, and perhaps others. It is also possible that the Paleo-Eskimos spoke only Proto-Eskimo-Aleut and were responsible for introducing that family into the Americas five millennia ago. Eskimo-Aleut consists of a branch containing the closely related Eskimoan languages (Yup'ik, Iñiupiaq, etc.), probably separated at a depth of less than 2,500 years, and a more divergent Aleut branch. Krauss (1980:7) roughly estimates the split between Eskimoan and Aleut at about 4,000 ya, which, even with the inexactness of linguistic time depth estimations, would still roughly fit the scenario that the original Paleo-Eskimo founding population may have in fact spoken Proto-Eskimo-Aleut (Fortescue 2017). The Eskimo-Aleut family is less likely to descend from a language brought into North America during the Pleistocene than from a language brought from Asia after 5,000 ya, given the many typological, areal, and possibly deep genetic affinities it shares with Uralic, Yukaghir and other North Asian families that have long been noted by linguists (Fortescue 1998, 2017). The fourth possibility is that the ASTt population, which also shows a close genetic link to present-day Chukchi and Koryak peoples in the Russian Far East, could have spoken a language belonging to the Chukotko-Kamchatkan family, but which subsequently disappeared in North America, leaving living relatives only on the Asian side of Bering Strait. Within Chukotko-Kamchatkan, the Itelmen branch is quite divergent from the family's other branch, which contains Chukchi and Koryak – languages so similar that they could almost be regarded as dialects of a single language (Comrie 1981: 240). Estimating the age of this family as a whole, however, is hindered by the probability that the Itelmen and Chukchi-Koryak sub-branches mixed with different neighbor languages (Fortescue 1998: 210-213). The same could be argued for estimating the Aleut split with Eskimoan, as Aleut also shows possible signs of substrate admixture or at least of rapid phonological and morphological change (Fortescue 1998: 35-37), which could make the split appear older than it actually is. Chukotko-Kamchatkan and Eskimo-Aleut are both regarded as first-order families, not relatable to one another using the Comparative Method. A fully convincing demonstration of the Dene-Yeniseian linguistic hypothesis, however, would favor the scenario whereby Paleo-Eskimos brought a language directly ancestral to Proto-Na-Dene into Alaska, whether or not this was the only language spoken by bearers of the culture known as ASTt. The genetic link through Paleo-Eskimos between present-day Siberians (including Kets) and the population ancestral to Na-Dene speaking peoples appears to be the only physical connection between the two groups that falls within a time depth known to be recoverable by the Comparative Method.

Table S14.1 below summarizes a plausible prehistoric scenario for the existence of a Dene-Yeniseian language link involving the Paleo-Eskimo arrival into Alaska 5,000 calBP from an earlier source in the Syalakh Culture (6,500 to 5,200 calBP) spreading eastward from Siberia.

Table S14.1. Chronology of Dene-Yeniseian linguistic diversification

~5,900-6,700 ya – breakup of the Dene-Yeniseian proto-language in central-eastern Siberia (based on the coalescence date of Paleo-Eskimo ancestry shared between contemporary Siberians and Na-Dene-speaking populations, see Table S9.2); speakers of the language ancestral to Proto-Yeniseian remained in Siberia, where diversification of the known Yeniseian daughter languages is unlikely to predate 4,000 ya (based on lexicostatistic estimates).

~5,000 ya – language ancestral to Proto-Na-Dene, and possibly also the language ancestral to Eskimo-Aleut, brought into Alaska by Paleo-Eskimos (indexed by archaeological data).

after 5,000 ya – split between Tlingit and Athabaskan-Eyak (indexed by the coalescence date of Paleo-Eskimo genetic ancestry shared by contemporary Na-Dene peoples, see Table S9.2).

~3,400 to 3,000 ya – split between Eyak and Athabaskan (based on lexicostatistic estimates).

~2,700 to 2,200 ya – beginning of diversification and spread of Athabaskan languages (based on lexicostatistic estimates).

Despite the shared Paleo-Eskimo genetic component in their speaker populations, the Dene-Yeniseian, Eskimo-Aleut, and Chukotko-Kamchatkan language families are not relatable to one another using the Comparative Method. Various deep connections have been proposed between Eskimo-Aleut, Uralic, and sometimes Yukaghiric and other Eurasian families (Fortescue 1998; see Campbell and Poser 2008 for a critique); however, even if any of these hypotheses are valid, the linguistic unity in question would greatly predate the spread of Middle Holocene cultures as well as the coalescence dates of the Paleo-Eskimo genetic ancestry shared by their speakers.

References (for this section)

Alekseenko, E. A. K izucheniju mifologicheskikh parallelej medvezh'emu kul'tu ketov [Mythological parallels to the Ket Bear Cult]. *Sistemnye Issledovanija Vzaimosvjazi Drevnikh Kul'turr Sibiri i Severnoj Ameriki. Vypusk 2: Dukhovnaja Kul'tura*. St. Petersburg: RAN, 22-46. (1995).

Berezkin, Y. Sibirskij fol'klor i proiskhozhdenie na-dene [Siberian folklore and Na-Dene origins]. *Arkheologija, Ètnografija i Antropologija Evrazii* **43**.1: 122-134. (2015)

Campbell, L. *American Indian Languages: The Historical Linguistics of Native America*. Oxford: Oxford University Press (1997).

Campbell, L. Review of "The Dene-Yeniseian Connection". *International Journal of American Linguistics* **77**.3, 445-451 (2011).

Campbell, L. *Historical Linguistics: An Introduction* (3rd edition). Cambridge, Mass.: MIT Press (2013).

Campbell, L, & Poser, W. *Language Classification: History and Method*. Cambridge: Cambridge University Press. (2008).

Comrie, B. *The Languages of the Soviet Union*. Cambridge: Cambridge University Press. (1981).

Dul'zon, A. P. Ketskie toponimy Zapadnoy Sibiri [Ket toponyms of Western Siberia]. *Uchenye Zapisky Tomskogo Gosudarstvennogo Pedagogicheskogo Instituta* [*Scholarly Proceedings of Tomsk State Pedagogical Institute*] **18**, 91–111 (1959).

Dul'zon, A. P. Byloe rasselenie ketov po dannym toponimiki [The former settlement of the Kets according to the facts of toponymy]. *Voprosy Geografii* **68**, 50–84 (1962).

Dumond, D. The Dene arrival in Alaska. *The Dene-Yeniseian Connection*, ed. Kari, J., Potter, B. *Anthropological Papers of the University of Alaska: New Series* **5**, 335-346 (2010).

Fortescue, M. *Language Relations Across Bering Strait: Reappraising the Archaeological and Linguistic Evidence*. London & New York: Cassell (1998).

Fortescue, M. The relationship of Nivkh to Chukotko-Kamchatkan revisited. *Lingua* **121**: 1359-1376 (2011)

Fortescue, M. Correlating Palaeo-Siberian language populations: Recent advances in the Uralo-Siberian Hypothesis. *Man in India*: **97**.1, 47-68 (2017).

Golla, V. *California Indian Languages*. Berkeley, Los Angeles, London: University of California Press (2011).

Heggarty, P, & Renfrew, C. The Americas: languages. *Cambridge World Prehistory*. Cambridge: Cambridge University Press, 1326-1353 (2014).

Holton G, & Sicoli, M. 2014. Linguistic phylogenies support back-migration from Beringia to Asia. *PLoS ONE* **9**.3: e91722. doi:10.1371/journal.pone.0091722

Kari, J. The concept of geolinguistic conservatism in Na-Dene prehistory. *The Dene-Yeniseian Connection*, ed. Kari, J., Potter, B. *Anthropological Papers of the University of Alaska: New Series* **5**, 194-222. (2010).

Kari, J, & Potter, B. (Eds.). *The Dene-Yeniseian Connection*. *Anthropological Papers of the University of Alaska: New Series* **5**. Fairbanks, AK: ANLC (2010).

Kaufman, T., & Golla, V. Language groupings in the New World: their reliability and usability in cross-disciplinary

studies. *America Past, America Present: Genes and Languages in the Americas and Beyond*, ed. Renfrew, C. Cambridge: Macdonald Institute for Archaeological Research, 47-57 (2000).
Krauss, M. Na-Dene. *Native Languages of the Americas*, vol. 1, ed. Sebeok, T. A. New York & London: Plenum Press, 283-358 (1976).
Krauss, M. *Alaska Native Languages: Past, Present and Future.* Fairbanks, AK: ANLC (1980).
Krauss, M. Athabaskan tone. *Athabaskan Prosody, ed.* Hargus, S., Rice, K, Amsterdam & New York: John Benjamins, 55-136 (2005).
Leer, J. *Comparative Athabaskan Lexicon*: www.uaf.edu/anla/collections/ca/cal/ (2006).
Leer, J. The palatal series in Athabascan-Eyak-Tlingit with an overview of the basic sound correspondences. *The Dene-Yeniseian Connection*, ed. Kari, J., Potter, B. *Anthropological Papers of the University of Alaska: New Series* **5**, 168-193 (2010).
McMahon, A, & McMahon, R. *Language Classification by Numbers*. Oxford: Oxford University Press (2005).
Mühlenbernd, R., & Rama, T. What phoneme networks tell us about the age of language families. *Journal of Language Evolution* **2**, 67-76. (2017).
Nichols, J. Proving Dene-Yeniseian genealogical relatedness. *The Dene-Yeniseian Connection*, ed. Kari, J., Potter, B. *Anthropological Papers of the University of Alaska: New Series* **5**, 299-309 (2010).
Pevnov, A. M. The problem of the localization of the Tungus-Manchu homeland. *Recent advances in Tungusic linguistics*, ed. A. Malchukov, Whaley, L. Wiesbaden: Harrassowitz, 17-40. (2012).
Potter, B. Archaeological patterning in northeast Asia and northwest North America: an examination of the Dene-Yeniseian Hypothesis. *The Dene-Yeniseian Connection*, ed. Kari, J., Potter, B. *Anthropological Papers of the University of Alaska: New Series* **5**, 138-167 (2010).
Ruhlen, M. The origin of the Na-Dene. *Proc. Natl. Acad. Sci. USA* **95**, 13994–13996 (1998).
Starostin, G. Dene-Yeniseian and Dene-Caucasian: pronouns and other thoughts. *Working Papers in Athabaskan Languages* 8. Fairbanks, AK: ANLC, 107-117 (2010).
Starostin, S. A. Sravnitel'nyj slovar' enisejskikh jazykov [A comparative vocabulary of Yenisseian languages]. *Ketskij Sbornik* vol. 4, Moscow: Vostochnaja Literatura, 176-315 (1995).
Swadesh, M. Some new glottochronological dates for Amerindian linguistic groupings. *Proceedings of the 32nd International Congress of Americanists* 670-674 (1958).
Trombetti, A. *Elementi di Glottologia*. Bologna: Nicola Zanichelli. pp. 486, 511 (1923).
Vajda, E. *Yeniseian Peoples and Languages: A History of their Study with an Annotated Bibliography and a Source Guide*. Surrey, England: Curzon Press (2001).
Vajda, E. Loanwords in Ket. *The Typology of Loanwords*, ed. Haspelmath, M., Tadmoor, U. Oxford: Oxford University Press, 125–139 (2009).
Vajda, E. Siberian link with Na-Dene languages. *The Dene-Yeniseian Connection*, ed. Kari, J., Potter, B. *Anthropological Papers of the University of Alaska: New Series* **5**, 33–99 (2010a).
Vajda E. Yeniseian, Na-Dene, and historical linguistics. *The Dene-Yeniseian Connection*, ed. Kari, J., Potter, B. *Anthropological Papers of the University of Alaska: New Series* **5**, 100–118 (2010b).
Vajda, E. Vestigial possessive morphology in Na-Dene and Yeniseian. *Working Papers in Athabaskan (Dene) Languages 2012.* (Alaska Native Language Center Working Papers No. 11). Fairbanks: ANLC, 79-91 (2013).
Vajda, E. Dene-Yeniseian. *Oxford Research Encyclopedia of Linguistics*. Oxford Online (2016).
Vajda, E. Patterns of innovation and retention in templatic polysynthesis. *Handbook of Polysynthesis*, ed. Fortescue, M, Mithun, M., Evans, N. Oxford: Oxford University Press, 363-391 (2017).
Vajda, E. Dene-Yeniseian: progress and unanswered questions. *Diachronica* 35.2: 277-295 (2018a).
Vajda, E. Yeniseian and Athapaskan toponyms. *Language and Toponomy in Alaska and Beyond*. (2018b).
Werner, H. *Zur jenissejisch-indianischen Urverwandtschaft [Yeniseian and Native American Relatedness]*. Wiesbaden: Harrassowitz (2004).
Werner, H. *Die Jenissej-Sprachen des 18. Jahrhunderts [Yeniseian Languages of the 18th Century]*. Wiesbaden: Harrassowitz (2005).

Supplementary Discussion

The time and place of the Eskimo-Aleut founder admixture event remains uncertain. Under our demographic model, the admixture event that is shared by all members of this lineage was dated by two independent methods, *ALDER* and *Rarecoal*, at 2,700-4,900 ya and 4,400-4,900 ya, respectively (Fig. 2b, Supplementary Information section 12), and involved a substantial (~55-62%) genetic contribution from a Northern First Peoples population distantly related to Athabaskans (Fig. 2). There is no clear archaeological evidence for a Native American back-migration to Chukotka[1,2], increasing the weight of evidence that this admixture event occurred in Alaska. Indeed, the Alaskan Peninsula and Kodiak Archipelago have long been suggested as a source of influences shaping the Neo-Eskimo material culture[3,4] (Fig. 3b). Some of the earliest maritime adaptations in Beringia and America are encountered in this region associated with the Ocean Bay tradition (~6,800 – 4,500 calBP)[5,6]. Around 4,000 calBP, the Ocean Bay tradition was succeeded by the Early Kachemak tradition, which is seen as a dramatic departure from the preceding phase, with some archaeological evidence for contacts with the Paleo-Eskimo Arctic Small Tool tradition[6]. Given the new genetic results, it seems possible that this cultural discontinuity is associated with the emergence of the ancestral Eskimo-Aleut population. Early Paleo-Eskimo people used marine resources on a seasonal basis only, depended for the most part on hunting caribou and muskox, and lacked sophisticated hunting gear that allowed the later Inuit to become specialized in whaling[7]. It is conceivable that a transfer of cultural traits and gene flow between Paleo-Eskimos and First Peoples happened simultaneously.

An important further clue is given by our finding that the ancestors of Inuit/Yup'ik experienced bidirectional gene flow with Chukotko-Kamchatkan ancestors, while Aleuts did not. This is consistent with a scenario of PPE/First Peoples admixture in Alaska, and a subsequent migration of Aleut ancestors into the Aleutian Islands (Fig. 3b), which might have occurred around 4,000 calBP according to known discontinuities in the Aleutian archaeological record (the onset of the Margaret Bay phase, which saw an influx of ASTt and Kodiak elements[8]). Conversely, ancestors of Inuit and Yup'ik migrated back to Chukotka, where around 2,200 calBP they established the earliest culture securely assigned archaeologically and genetically to Neo-Eskimos[9], i.e. the Old Bering Sea culture[10,11], admixed with local populations, most likely in interior Chukotka, and re-expanded from there to Alaska and later throughout the American Arctic. The Thule expansion was likely driven by innovations in hunting and the food surplus created by whaling. The oldest Old Bering Sea individual in this study was dated to ~1,500-1,900 calBP, which also overlaps our estimated time of the bidirectional admixture between Inuit/Yup'ik ancestors and Chukotko-Kamchatkan-speaking groups (~1,700-2,300 ya).

A succession of western Alaskan cultures, namely the Old Whaling, Choris, Norton, and Ipiutak (with the earliest dates around 3,100, 2,700, 2,500, and 1,700 calBP, respectively), combined cultural influences from earlier local Paleo-Eskimo sources as well as sources in Chukotka and southwestern Alaska[3,12]. Parallels between these cultures and subsequent Neo-Eskimos are notable[3], and they might represent partial links between the founding population at 4,800 ya and the Old Bering Sea culture at 2,200 calBP (Fig. 3b). The location and source populations for early Eskimo-Aleuts will likely be resolved if future analyses can include samples from these western Alaskan traditions, as well from the Ocean Bay and Kachemak traditions in southwestern Alaska.

The descendants of the proto-Paleo-Eskimo lineage speak widely different languages, belonging to the Chukotko-Kamchatkan, Eskimo-Aleut, and Na-Dene families. Based on lexicostatistical studies of languages surviving in the 20th century, the time depth of the former two families is likely shallow, and the Na-Dene family is probably much older, on the order of

5,000 years (Supplementary Information section 13). Thus, while the linguistic affiliation of Paleo-Eskimos is impossible to determine from genetic data, the finding that the most diverse linguistic group whose speakers carry large proportions of PPE ancestry is Na-Dene and that Na-Dene linguistic variation may reach back to the Paleo-Eskimo period suggests that proto-Na-Dene may have been spoken by a Paleo-Eskimo population. A Siberian linguistic connection was proposed for the Na-Dene family under the Dene-Yeniseian hypothesis[13,14]. This hypothetical language macrofamily unites Na-Dene languages and Ket, the only surviving remnant of the Yeniseian family, once widespread in South and Central Siberia[15,16]. Although the Dene-Yeniseian family is not universally accepted among historical linguists[17,18], and correlations between linguistic and genetic histories are far from perfect, evidence of a genetic connection between Siberian and Na-Dene populations mediated by Paleo-Eskimos suggests that future research should further explore Dene-Yeniseian as a genealogical family[14] or as part of a wider clade[18].

References (for this section)

1. Potter, B. A. Archaeological patterning in Northeast Asia and Northwest North America: an examination of the Dene-Yeniseian hypothesis. *The Dene-Yeniseian Connection*, ed. Kari, J., Potter, B. A. *Anthropological Papers of the University of Alaska: New Series* **5**, 138–167 (2010).
2. Hoffecker, J. F. & Elias, S. A. *Human Ecology of Beringia.* New York: Columbia University Press (2007).
3. Dumond, D. E. Norton hunters and fisherfolk. *The Oxford Handbook of the Prehistoric Arctic*, ed. Friesen, T. M., Mason, O. K. New York: Oxford University Press. 395–416 (2016).
4. Ackerman, R. E. Early maritime traditions in the Bering, Chukchi, and East Siberian seas. *Arctic Anthropol*. **35**, 247–262 (1998).
5. Fitzhugh, B. The origins and development of Arctic maritime adaptations in the Subarctic and Arctic Pacific. *The Oxford Handbook of the Prehistoric Arctic*, ed. Friesen, T. M., Mason, O. K. New York: Oxford University Press. 253–278 (2016).
6. Steffian, A., Saltonstall, P. & Yarborough, L. F. Maritime economies of the central Gulf of Alaska after 4000 B.P. *The Oxford Handbook of the Prehistoric Arctic*, ed. Friesen, T. M., Mason, O. K. New York: Oxford University Press. 303–322 (2016).
7. Hoffecker J. F. *A Prehistory of the North: human settlement of the higher latitudes*. Rutgers University Press (2004).
8. Davis, R., Knecht, R. & Rogers, J. First Maritime Cultures of the Aleutians. *The Oxford Handbook of the Prehistoric Arctic*, ed. Friesen, T. M., Mason, O. K. New York: Oxford University Press. 279–302 (2016).
9. Raghavan, M. *et al*. The genetic prehistory of the New World Arctic. *Science* **345**, 1255832 (2014).
10. Mason, O. K. The Old Bering Sea florescence about Bering Strait. *The Oxford Handbook of the Prehistoric Arctic*, ed. Friesen, T. M., Mason, O. K. New York: Oxford University Press. 417–442 (2016).
11. Bronshtein, M. M., Dneprovsky, K. A. & Savintesky, A. B. Ancient Eskimo cultures of Chukotka. *The Oxford Handbook of the Prehistoric Arctic*, ed. Friesen, T. M., Mason, O. K. New York: Oxford University Press. 469–488 (2016).
12. Darwent, C. M. & Darwent, J. The enigmatic Choris and Old Whaling cultures of the Western Arctic. *The Oxford Handbook of the Prehistoric Arctic*, ed. Friesen, T. M., Mason, O. K. New York: Oxford University Press. 371–394 (2016).
13. Ruhlen, M. The origin of the Na-Dene. *Proc. Natl. Acad. Sci. USA* **95**, 13994–13996 (1998).
14. Vajda, E. J. Siberian link with Na-Dene languages. *The Dene-Yeniseian Connection*, ed. Kari, J., Potter, B. A. *Anthropological Papers of the University of Alaska: New Series* **5**, 33–99 (2010).
15. Dul'zon, A. P. Byloe rasselenie Ketov po dannym toponimiki [The former settlement of the Kets according to the facts of toponymy]. *Voprosy Geografii* **68**, 50–84 (1962).
16. Vajda, E. J. Loanwords in Ket. *The Typology of Loanwords*, ed. Haspelmath, M., Tadmoor, U. Oxford: Oxford University Press, 125–139 (2009).
17. Campbell, L. Review of 'The Dene-Yeniseian Connection', ed. by James Kari and Ben A. Potter. *Int. J. Am. Linguistics* **77**, 445–451 (2011).
18. Starostin, G. Dene-Yeniseian: a critical assessment. *J. Language Relationship* **8**, 117–138 (2012).